6-2015

Phylogeographic Study of Ctenosaura similis

Hasret Ozturk
hxo1948@rit.edu

R·I·T

Phylogeographic Study of *Ctenosaura similis*

by Hasret Ozturk

A Thesis Submitted in Partial Fulfillment of the Requirements
for the Degree of Master of Science in Bioinformatics

Thomas H. Gosnell School of Life Sciences

College of Science

Rochester Institute of Technology

Rochester, NY

June, 2015

Rochester Institute of Technology

Thomas H. Gosnell School of Life Sciences

Bioinformatics Program

To: Head, Thomas H. Gosnell School of Life Sciences

The undersigned state that Hasret Ozturk, a candidate for the Master of Science degree in Bioinformatics, has submitted his thesis and has satisfactorily defended it.

This completes the requirements for the Master of Science degree in Bioinformatics at Rochester Institute of Technology.

Thesis committee members:

Name Date

_____ _____

Larry J. Buckley, Ph.D.

Thesis Advisor

_____ _____

Michael V. Osier, Ph.D.

_____ _____

David Lawlor, Ph.D.

Table of Contents

List of Figures

List of Tables

Acknowledgements:

I would like to express my great appreciation, deepest gratitude to my adviser, Dr. Larry J. Buckley. I thank him for his valuable and excellent guidance, patience for doing my research work. It has been an honor to be his MSc student.

I would also like to thank Dr. Michael Osier who was always willing to help, give his suggestions and helped to develop my background for my research in his classes. His willingness to give his time so generously has been very much appreciated.

I would like to thank Dr. David Lawlor for his kindness and great contributions of time, ideas, and great suggestions. His continuous support always encouraged me to finish this thesis.

I thank my family; Umut K. Ozturk, Sehriban Ozturk, Dogan Ozturk, and Zekiye Pur for their extraordinary support. They were always supporting me and encouraging me with their best wishes. I thank my fiance Jean-Paul B. Pala for his love and patience. He was always there cheering me up. I thank Alex Berken , Elif Subasi, Berivan Subasi, Berken Subasi for being my family in Rochester. I thank my precious friend Michael Noble for his support and trust in me.

Lastly, I offer my regards to all of those who supported me in any respect during the completion of the research.

This thesis would have been impossible to complete without you.

A picture of *Ctenasaura similis*

Source:https://en.wikipedia.org/wiki/Ctenosaurasimilis

Abstract

The genus *Ctenosaura* (spiny-tailed iguanas) represents the most diverse group of iguanas with 18 currently recognized species. *Ctenosaura similis* has the most widespread ranges of all the *Ctenosaura* species, and extends from southern Mexico to Panama including many coastal islands. The purpose of this study is to explore the genetic diversity within *C. similis* and look for correlations between genetic relationships and biogeographic patterns related to the spread of the species. This study sequenced and aligned 1140 bp from the cytochrome *b (*cytb) locus for 159 individuals and 847-878 bp from the rhodopsin locus for 127 individuals. A total of 71 mtDNA and 40 nuclear haplotypes were detected.

C.similis has successfully occupied and dispersed in Central America and Southern Mexico with at least 2-3 million-year history. Costa Rica and Panama region can be the origin of this species due to high haplotype diversity, and deeper splits between existing haplotypes are visible on both gene trees and networks. Less haplotype diversity is observed on the Pacific Coast. In most cases, there is still ongoing gene flow, migration on both coasts from South (Costa Rica-Panama) to North (The Isthmus of Mexico) especially on the Atlantic coast. There is no clear separation based on geographical distribution except recent dispersal for small clades in certain areas. Gene trees and networks are consistent to each other for each locus. However, the general pattern of the rod and *cytb* gene trees/networks does not exactly match each other. There is a consistency between the genetic distance and number of haplotypes (*cytb:* 3.7%, 71 haplotypes; rhodopsin: 1.85%, 40 haplotypes).

The geographic distribution of *C. similis* has provided valuable information about the spread of iguanas in Central America. These two molecular markers offered important

information about the evolutionary historical expansion of *C.similis* individuals in Central America. Monitoring *Ctenosaura similis* is necessary for (1) conservation in existing habitats, and (2) invasive potential in new habitats (e.g.Florida and Northern SA).

Keywords: *Ctenosaura similis*, Phylogeography, cytochrome *b*, Rhodopsin, Phylogenetic trees and networks.

Introduction

The existence of the reptiles dates back to Carboniferous period (Laurin and Reisz, 1995). After approximately 310-320 million years of evolutionary history, reptiles diverged, dispersed to the world and became one of the most dominant animals on this planet. The ability of surviving in several habitats, having of different ecological niches, and physical strength of this animals led to reptiles having a highly diverse evolutionary history (Vitt and Pianka 2005). In particular, the order Squamata, which includes lizards and snakes, has significantly dispersed in all major continents. Therefore, this order is ideal to study phylogenetic patterns (Vitt and Pianka, 2005).

Iguanidae is a family of Squamata that contains iguanas and related species. One of the important genera of Iguanidae is spiny-tailed iguanas, *Ctenosaura* (Wiegmann, 1828). According to Buckley (1997), this genus has approximately 15 million years history starting from late-Miocene and mid-Pliocene in Central America based on mitochondrial DNA (Figure.1). Some recent studies also show that it has at least 8 million year evolutionary history based on nuclear DNA data (Townsend *et al.,* 2011; MacLeod et al*.,* 2015).

Ctenosaura is species-rich with 18 recognized currently known species. *Ctenosaura similis* (Gray, 1831), the black spiny-tailed iguana, is an important species of this genus. It appears that this species is the sister group to all other species within the genus (Buckley, 1997). Moreover, it has approximately 2.5 million year history in Central America based on a mitochondrial DNA substitution rate of 1-2% per million years.

Ctenosaura species have a broad distribution in Central America and according to Buckley (1997); this group is a very informative genus to understand the biogeography of the

Caribbean region. *C. similis* has the broadest range of all the *Ctenosaura* species and is the largest member of the genus (Krysko*et al.,* 2003). Individuals are dispersed along the Isthmus of Tehuantepec in Mexico down through Panama (Bailey, 1928). It is also reported in the southern Florida, Columbia, and Venezuela (Townsend *et al.*, 2003; Pasachnik and McCranie, 2010; Avery et al, 2014).

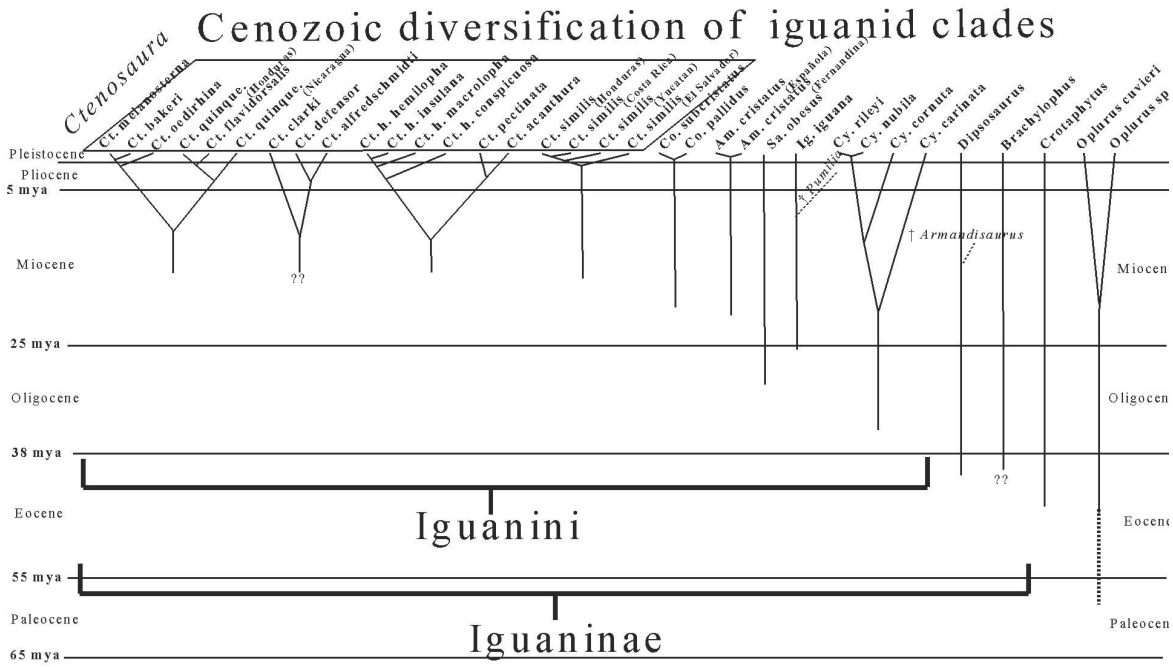

Figure.1. From "Age of iguanine genera species groups of Ctenosaura" by Buckley L. J. Phylogeny and Evolution of the Genus Ctenosaura (Squamata: Iguanidae). Doctor of Philosophy Dissertation. Southern Illinois University at Carbondale. 1997. Reprinted with permission.

Central America has long and high mountainous areas, valleys between mountains, volcanoes, plateaus, coastal areas. It is also characterized by a broad variety of climate types (Berglee, 2012). Because of its varied climate and geographical features it is a valuable area to study evolutionary history of species and phylogeography in animals (Fortunato, 2008).

Scientists have not done many evolutionary studies for *C. similis* until recently. The purpose of this study is to explore the genetic diversity within *C. similis* range from Southern Mexico through Panama, and look for correlations between genetic relationships and biogeographic patterns related to the spread of the species.

Ctenosaura similis

C. similis individuals are excellent diggers and great climbers. They are also known as the fastest *Ctenosaura* species. Individuals are generally large and heavy animals. Adult females lack a clear crest while males have fully formed crests and small dewlaps that can be stretched under the throat. Coloration is highly variable for the individuals within the same population. In general, juveniles have color bands on green, gray or brown backgrounds. Adults are black and have black bands on a grey dorsal surface. They can have mottling on their backs. The head and throat of males turns orange and their jowls look yellowish with blue markings during breeding season (Kohler, 1996).

Mature individuals generally mate during spring. Some populations have different mating times (Halliday and Adler, 1992). The female individuals move to convenient places and lay approximately 30 eggs in a nest within ten weeks after mating. In 90 days, the hatchling digs its way out through the sand (Kohler, 1996). It takes 2 to 3 years for juveniles to be sexually active (Halliday and Adler, 1992).

Throughout life, all genera of iguanas are mostly herbivores, protein is necessary in the diet for growth. When *Ctenosaura* species become big enough, they can feed on other vertebrates. *C. similis* juveniles are generally insectivores and adults are herbivorous; however,

the diet of this species can also vary including arthropods and other smaller animals (Torres-Carvajal, 2007). More mature individuals tend to be more herbivorous (Van Devender, 1982).

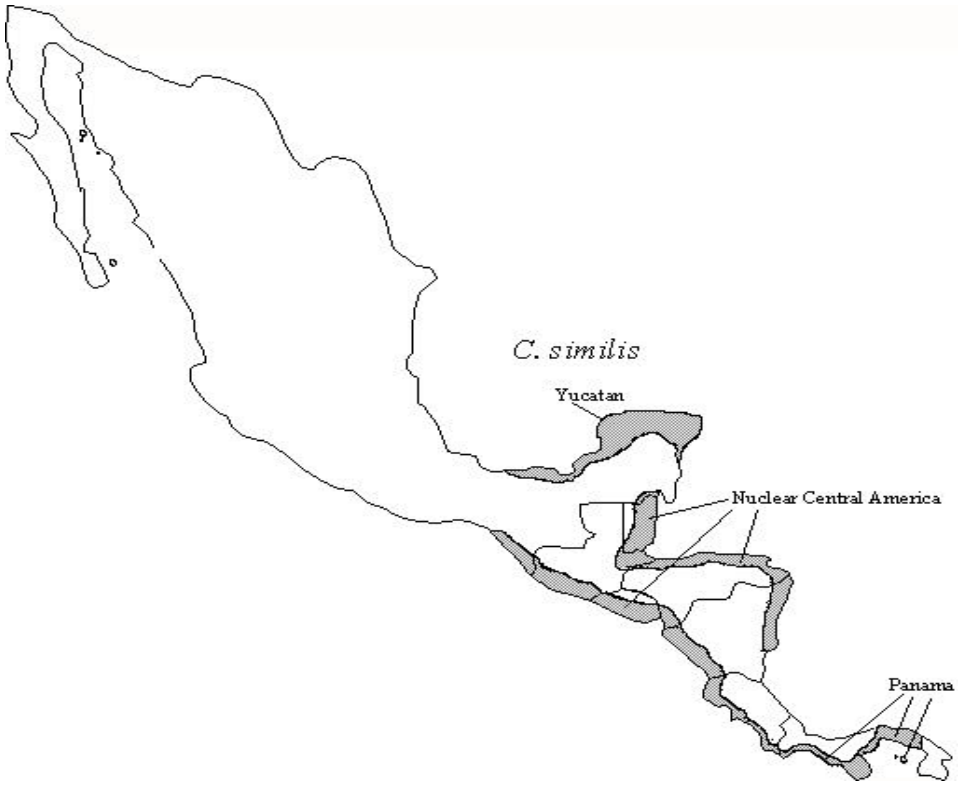

Figure.2. From "Outline of distribution of *C. similis* showing limits of Panamanian, Yucatan and Nuclear Central American populations" by Buckley L. J. Phylogeny and Evolution of the Genus Ctenosaura (Squamata: Iguanidae). Doctor of Philosophy Dissertation. Southern Illinois University at Carbondale. 1997. Reprinted with permission.

This species can be found in dry areas of the Pacific coast of northwestern Costa Rica, western Nicaragua, southern Mexico and southern Panama. The Atlantic coasts of the Yucatan Peninsula of Mexico, Honduras and some islands on the East of Nicaragua are also convenient areas for the individuals. The wet areas of Atlantic coast including eastern Nicaragua, northeastern Costa Rica and Panama are not favorable habitats for this species (Figure.2). High altitudes, cold climates, and rainy forests are not suitable for this species (Fitch and Henderson, 1978). It is hardly possible to find these black spiny-tailed iguanas 1,300 m above the sea levels

of Central America (Fitch and Henderson, 1978; Pasachnik and McCranie, 2010; Savage, 2002). Individuals are seen in varied climates and plant formations. Individuals can be found on rocky habitats, ruins, stone walls, nearby trees, and near forests and prefer open and dry areas such as arid savannas (Malfatti, 2007).

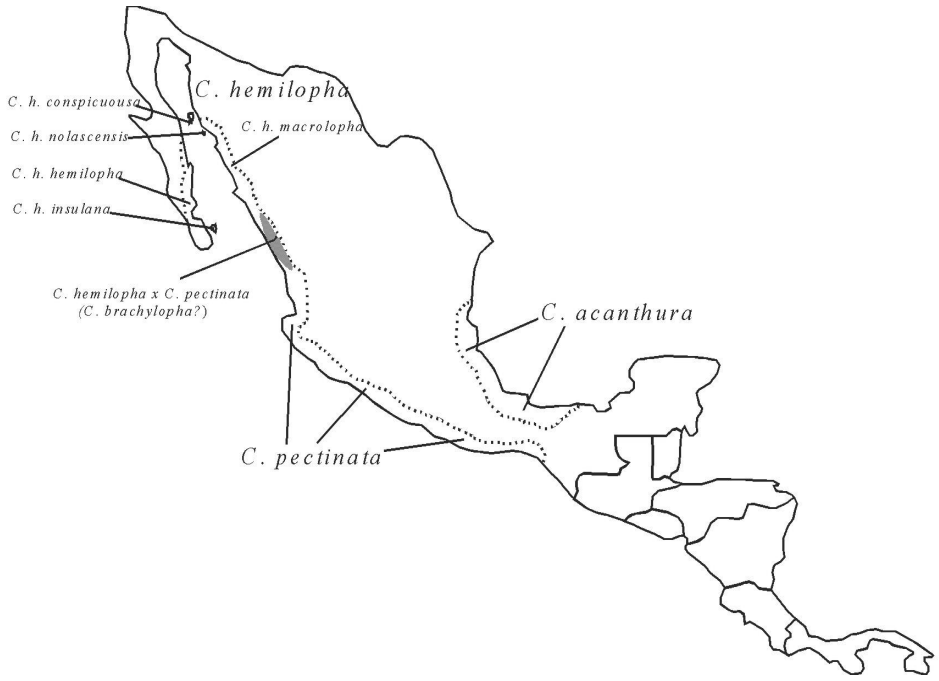

Figure.3. From "Outline of distribution of *C. pectinata* species group with area of potential hybrids between *C. hemilopha* and *C. pectinata* (*C. brachylopha*) in central Sinaloa indicated" by Buckley L. J. Phylogeny and Evolution of the Genus Ctenosaura (Squamata: Iguanidae). Doctor of Philosophy Dissertation. Southern Illinois University at Carbondale. 1997. Reprinted with permission.

C. similis individuals do not occupy habitats North of Tonala on the Pacific coast or west of Coatzocoalcos on the Atlantic coast of Mexico (Figure.3). On the other hand, the Mexican spiny-tailed iguana, *Ctenosaura pectinata* (Wiegmann, 1834), is commonly found on the Pacific coast, and the northeastern spiny-tailed iguana, *Ctenosaura acanthura* (Shaw, 1802), spreads on the Atlantic coast (Buckley, 1997). Both species are native to Mexico. These species show similar breeding, feeding, hiding habits and preying habitats ((Malfatti, 2007).*C. similis* has a

very broad distribution in Central America. On the other hand, having similar ecological niches with other two dominant species may prevent *C. similis* individuals spreading further.

Most of the *Ctenosaura* species are facing the possibility of becoming endangered. Some of the species of this genus are already on the IUCN Red list of Threatened species, a world-known and comprehensive list of endangered species. The black spiny-tailed iguana is not officially considered an endangered species even though it is commonly hunted in Central America (Pasachnik and McCranie, 2010). On the other hand, it is thought of as an invasive species since human carried it from Central America to other locations. Individuals eat the landscape plantings, other animals' food source and infest houses in southern Florida (Avery *et al*, 2014). Additionally, *C.similis* individuals are very popular as pets (Fitch and Henderson, 1978). Th**ey** are a particularly good meat source and locally eaten in Central America. People also believe this species has curative properties and gives spiritual strength to people (Savage, 2002). This species has listed as "Least Concern" yet individuals are still threatened and monitoring of the populations is needed because of human consumption and the pet trade in Central America (Pasachnik and McCranie, 2010).

Materials and Methods

Choice of DNA Sequence Data

Mitochondrial DNA: Cytochrome b

Mitochondria are the power source of human cells and are responsible for the synthesis of ATP. It is claimed that origin of mitochondria approximately dates back to 2 billion years ago as prokaryotic living things. In time, it became of an organelle of eukaryotic cells because of endosymbiotic relationship and transferred several genes to eukaryotic cell's nucleus (Margulis,

1981). Mitochondrial DNA is maternally inherited because of the scarcity and degradation of paternal mtDNA during fertilization. Mitochondria have their own DNA and genes. Molecular recombination does not occur in vertebrate mitochondrial genomes (Gillham, 1994). Any alteration in mtDNA may cause a negative effect on metabolism or fitness of organisms (Wei, 2009). Furthermore, there is no proofreading or mtDNA repair mechanism in the mitochondria. Therefore, the mutation rate is higher than the mutation rate of nuclear genome (Avise, 1994). MtDNA studies provide information about ancestral tracking and genetic relationships of individuals within a species. It also helps to identify evolutionary relationships between closely related species (Sarkissian, 2011).

There are many vital genes in mitochondria for the survival of organisms. Cytochrome b (*cytb*) is one of these important genes. It is an element of respiratory chain complex III in aerobic prokaryotes and eukaryotes. According to Esposti (1993), *cytb* is well understood in terms of its biochemistry and protein production. It is a very useful molecular marker for the study of phylogenetics of vertebrates because of its high sequence variability, and this gene provides broad information at the level of family and genus (Castresana, 2001). Additionally, new identified species can be assigned in the genus by using *cytb* gene (Giao *et al*., 1998).

Nuclear Gene: Rhodopsin

G protein-coupled receptors (GPCRs) comprise of the largest protein family of transmembrane receptors. These receptors are capable of sensing ligands outside the cell including ions, hormones, chemokines or photons. They stimulate signal transduction pathways inside the cell and finally activate cellular responses immediately (Hazell, 2012). Rhodopsin is a pigment that belongs to G-protein-coupled receptor (GPCR) family. This pigment is found in

photoreceptor cells of the retina and enables low light vision. Rhodopsin is bound to 11-cis retinal. When this molecule is exposed to light, it stimulates rhodopsin, which creates electrical signals. When these signals reach the brain, vision is created (Stuart &Brige, 1996).

According to Hunt *et al*. (1996), an organism may develop unique characteristics in its visual system due to environmental factors. Therefore, the effect of changes in these visual pigments may provide an opportunity to observe their function. The visual pigments are important in an organism since they trigger the visual cascade in the first place and are efficiently studied in the laboratory. Therefore, they are acceptable to be used in molecular evolutionary studies (Goldsmith, 1990).

Microsatellite DNA

Microsatellites or simple sequence repeats (SSRs) are randomly distributed short DNA sequences with different number of nucleotide repeats ranging from 1 to 6. The length of these repeats can change among individuals in a population. The fact that microsatellites are polymorphic and species-specific, make them useful as molecular markers (Miah *et al.*, 2013). Microsatellites have been used as molecular markers to study population genetics, conservation and linkage analysis (Chase *et al.*, 1996; Abdul-Muneer, 2014). In this study, the rhodopsin locus includes microsatellite region with 9-17 CT repeats.

DNA Amplification and Sequencing

Previously collected and extracted 182 samples were used in this study from localities presented in the figure.4 (Appendix.1). The complete mitochondrial *cytb* gene (1140 bp) was amplified by using L14919 and H16064 primers.

Figure.4.Map of the *Ctenosaurasimilis* localities used in this study.

PCR reactions were carried out in 100 µl reaction containing 50 µl GoTaq® Green Master Mix (2X), 1 µl each primer (1 µM), and 1 µl total DNA. Amplification conditions were as follows: denaturation for 2 min at 94 °C, followed by 37 cycles of denaturation at 94 °C for 45s, annealing at 56 °C for 45 s, extension at 72 °C for 1min, and a 5 min final extension at 72 °C. The third intron and flanking exon sequence of rhodopsin gene (847-878) was amplified by

using Rod3 and Rod4 primers. PCR reactions were conducted with 1 µl of extracted DNA in 25 µl reaction mixture containing 12.5 µl GoTaq® Green Master Mix (2X), 1 µl MgCl2 (1 mM), 1 µl each primer (1 µM). Amplification conditions were as follows: denaturation for 4 min at 94 °C, followed by 37 cycles of denaturation at 94 °C for 1min, annealing at 67 °C for 1min, extension at 72 °C for 1min, and a 5 min final extension at 72 °C. All PCR products were run in 1% agarose gel and visualized after staining with GelRed (Figure.5). The correct bands were purified by using EZ-10 Spin Column PCR Products Purification Kit, following the manufacturer's instructions (Bio Basic Inc.). The quality of the purified DNA was observed using a Nanodrop ND-1000 Spectrophotometer and the software ND-1000 v 3.2.1. (Figure.6).

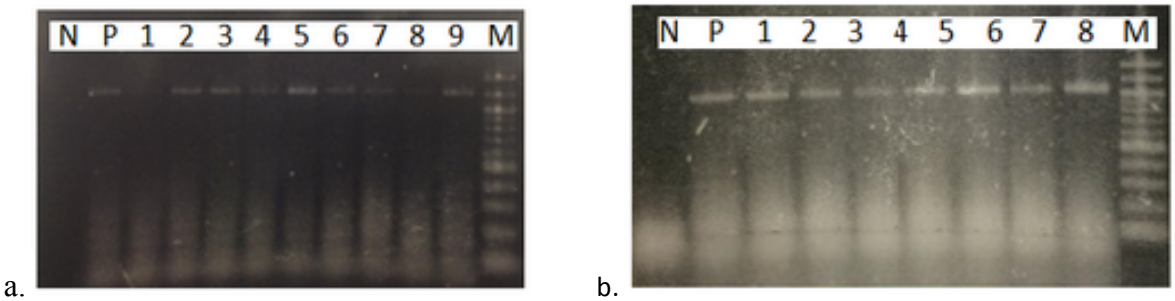

Figure.5. Agarose gel electrophoresis of amplification products. a) cytb gene 1140 bp b) rod gene ~850 bp M: 100 bp Marker, N:Negative control, P:Positive control. Other numbers: Amplified PCR products.

Sample ID	User ID	Date	Time	ng/ul	A260	A280	260/280
288 cytb	Default	8/15/2014	11:23 AM	30.77	0.615	0.325	1.89
288 cytb	Default	8/15/2014	11:23 AM	29.53	0.591	0.281	2.10
315 cytb	Default	8/15/2014	11:24 AM	29.49	0.410	0.222	1.85
315 cytb	Default	8/15/2014	11:24 AM	28.07	0.341	0.183	1.86
T1 cytb	Default	8/15/2014	11:25 AM	29.63	0.593	0.304	1.95
T1 cytb	Default	8/15/2014	11:26 AM	29.28	0.586	0.307	1.91
289 rod	Default	8/15/2014	11:27 AM	59.60	1.192	0.649	1.84
289 rod	Default	8/15/2014	11:28 AM	56.79	1.136	0.599	1.90
315 rod	Default	8/15/2014	11:28 AM	58.22	1.164	0.606	1.92
315 rod	Default	8/15/2014	11:29 AM	55.22	1.104	0.593	1.86
406 rod	Default	8/15/2014	11:29 AM	54.22	1.084	0.573	1.89
406 rod	Default	8/15/2014	11:30 AM	56.88	1.138	0.645	1.76

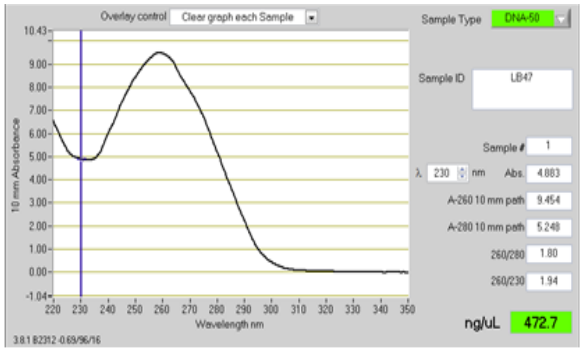

Figure.6. A typical Nanodrop ND-1000 v3.12 spectrophotometer reading.

The purified amplification products were sent to the GENEWIZ, Inc. for Sanger DNA sequencing (Sanger *et al.*, 1977). Eight primers were used for sequencing of cytochrome gene. Six primers were used for sequencing of rhodopsin gene. Five new primers were designed for rhodopsin gene locus by using online primer design tool Primer3Plus to sequence rhodopsin gene (Untergasser, 2012). All primers used in this study for *cytb* and rhodopsin genes are represented in the Table.1.

Table.1. Primers utilized for PCR amplifications and sequencing in this study. Amp.: Amplification. Seq.: Sequencing. H: High strands of mtDNA L: Light strands of mtDNA. Numbers are equivalent to position of each primer's 3' base in the mitochondrial genome of human (Anderson et al. 1981).

Locus	Primer Name	Primer Sequence (5′-3′)	Use	Reference
Cyt *b*	L14919	AACCACCGTTGTTATTCAACT		Burbrink *et al.,* 2000.
	H16064	CTTTGGTTTACAAGAACAATGCTTTA	Amp.	Burbrink *et al.,* 2000.
	L15136	ATAGCAACAGCATTTGTAG	Seq.	Krajewski *et al.,* 1992.
	L15416	GATAAAATCCCATTYCACCCHTACT		Krajewski *et al.,* 1994.
	L15613	GATCAATCCCAAACAAACTHGGMGG		Krajewski *et al.,* 1994.
	H15767	ATGAAGGGATGTTCTACTGGTT		Edwards *et al.,* 1991.
	H15500	CGGGGGTGAAGTTTTCTGGGTC		Krajewski *et al.,* 1992.
	H15149	AAACTGCAGCCCCTCAGAATGATATTTGTCCTCA		Kocher *et al.,* 1989.
Rod	Rod3	AGGTACATCCCAGAAGGCATGCAC		Glor *et al.,* 2004.
	Rod4	CAGGATTGTAGATGGCTGAGCT	Amp.	Glor *et al.,* 2004.
	RodF1	TGTACAGTTAAAGCGGTATGTAATCC	Seq.	Designed for this study.
	RodF2	AGGTGAGTGTGTGTGATGCAG		
	RodR2	ATGCGAGTGACTTCTTTCTCAG		
	RodR6	TGCAACAGTACAGCTTAGGAATGG		
	RodR7	CTCCTGCATCATAGAGACCATC		

DNA Alignment and Collapsing Identical Sequences

Individual DNA sequence alignments were completed by using Seqman Pro in the DNASTAR Lasergene software package version.12.2 (Burland, 2000). Necessary manual

corrections were carried out for the trace files. The final alignment comprised 1140 base pairs without any insertions or deletions for *cytb* locus for 159 individuals, and 847-878 base pairs with indels and different number of "CT" repeats for rhodopsin locus for 127 individuals.

All of the consensus sequences were checked for stop codons and unusual amino acid substitutions (transitions and transversions), and aligned by using the Clustal W method in DAMBE, a molecular biology and evolutionary data analysis program (Xia, 2013). Seventy-one unique sequences were found for the *cytochrome b* locus and 40 unique sequences were found for the rhodopsin locus. Collapsed sequences were relabeled for both data sets (Appendix.4a&4b). Identical sequences were collapsed together to create unique sequences (haplotypes) in order to prevent unresolved clusters and save time while branch swapping. There are approximately 4.9518×10^{38} ways to create possible trees for a size of 30 taxa (Figure.3.1 in Felsenstein, 2004). A branch swapping method while constructing trees may be time consuming, and since the genetic distances are so close to each other in an intraspecific population, so swapping may cause unresolved tree topology (Soltis and Soltis, 2003).

Molecular Data Analyses

Choice of Out-group: None of the *Ctenosaura* species are genetically close to the *C. similis.* All other species appear to be sister groups to this species (Buckley, 1997). Therefore, *Ctenosaura melanosterna* (Buckley & Axtell, 1997), the black-chested spiny-tailed iguana, was chosen as out-group for this study because it is found in Honduras where *C. similis* individuals can be found. *C.melanosterna* is categorized as an endangered species in part because of its habitat loss (Pasachnik *et al.,* 2012).

Phylogenetic Tree Analysis

Finding a unique method to infer phylogenies is a very complicated process. There are a number of assumptions to reconstruct phylogenies from a given dataset of DNA or protein sequences. The results may or may not display the true phylogenetic tree (Salemi and Vandamme, 2003). Each method applies different criteria to construct a tree. Therefore, the consensus trees can be compared to each other and a final decision can be made based on the results (Buckley, 1997).

In this study, collapsed sequences (i.e., haplotypes) for both data sets were used to perform phylogenetic tree analyses in PAUP* version 4.0 (Swofford, 2002), a computational phylogenetics program. Phylogenetic trees were constructed using maximum parsimony (MP), maximum likelihood (ML) and minimum evolution (ME) approaches.

MP chooses the tree with the shortest length to explain the observed data; namely, it searches tree space for topologies with the minimum amount of change to construct a phylogenetic tree. A phylogenetic tree chosen by parsimony supports the minimum total amount of evolutionary change (i.e., mutations) (Felsenstein, 2004). It evaluates a subset of all reasonable topologies (branch and bound method) and chooses the one that has the least number of changes as the best tree (Salemi and Vandamme, 2003).

Maximum likelihood uses an explicit DNA substitution model to construct phylogenies. It produces a number of different trees and evaluates each tree by using a nucleotide substitution model. Since different tree topologies are evaluated with different mathematical calculations, it is computationally demanding (Salemi and Vandamme, 2003). After searching for all reasonable trees, it chooses the tree with the highest likelihood as the best tree. The assumption

for ML is that hypothesizing an evolutionary history can be explained better by a higher probability than lower probability for a given dataset.

Desper and Gascuel (2005) define ME distance-based method as a very common approach to construct phylogenies by a given large number of datasets. Similar to ML, ME uses a nucleotide substitution model to estimate evolutionary distances; however, the mathematical calculations are less complicated since it creates a matrix of pairwise evolutionary distances among taxa to compute the best tree.

To understand the evolutionary process of a certain locus, it is important to predict the substitution changes by building nucleotide substitution models. The best-fit nucleotide substitution model is chosen based on a given data set and a topology. In this study, the best-fit model was ascertained using Modeltest version 3.7 (Posada and Crandall, 1998) and found to the generalized time-reversible (GTR +I+G, Tavaré, 1986) model of evolution that was then used to construct phylogenies for *cytochrome b* locus. Analyses were performed with gaps for rhodopsin locus. The HKY85 (Hasegawa, Kishino and Yano, 1985) model of evolution was used to construct phylogenies for rhodopsin locus.

All phylogenies were estimated under the heuristic search algorithms with the appropriate DNA substitution model. Tree-bisection-reconnection (TBR) was chosen as the branch swapping option for both data sets. Consensus trees were created for MP, ML, and ME approaches. A consensus tree is the sum of all possible outputs or remaining trees that occur more than 50% of the time ((Bryant, 2003). Therefore, the strict consensus and 50% Majority-rule trees were calculated to combine all possible solutions and obtain a single topology for each approach (Appendix.2a-v).

The bootstrap analysis is a statistical method used to estimate the support of nodes by evaluating the number of times a node is found in multiple searches of re-sampled data sets during bootstrap replicate data set searches. A bootstrap consensus tree displays how often a node occurs in a tree when data are randomly sampled more than once (Felsenstein, 1985). As the number of bootstrap samples (replicates) constructed increases, the computing resources necessary to complete the bootstrap search increases. In this study, bootstrap values were generated from 100 replicates of heuristic searches, and TBR branch swapping option was used for both data sets.

The threshold for a bootstrap value is accepted as 70%. Anything below 50% is not shown on the tree (Hillis and Bull, 1993). Nodes with bootstrap values between 75% and 95% are moderately supported, and above 90% are very well supported.

In this study, consensus trees for both loci were displayed using the ML best tree topology with bootstrap values from all approaches placed on corresponding branches as likelihood, parsimony, minimum evolution bootstrap values, respectively (Figure.7a & 7b).

Estimates of genetic distances were conducted in PAUP* by using the appropriate model for each locus (Appendix.3a & 3b.)

Phylogenetic Network Analysis:

According to Bryant and Moulton (2004), evolutionary networks can give more comprehensive information about closely related genotypes (compared to evolutionary trees) because of their ability to document recombination, hybridization, gene conversion or gene transfer more accurately. NETWORK is a software program used "to reconstruct phylogenetic networks and trees, infer ancestral types and potential types, evolutionary branchings and

variants, and to estimate datings" (NETWORK User Guide, 2012). Median joining (MJ) is one of most commonly used methods in this software package. It finds a minimum spanning tree first. Then, it adds new median vectors (i.e., hypothetical or missing ancestors) to a single network. This method handles large datasets and works fast. In this study, NETWORK.4.6.1.1 was used to compute an unrooted phylogenetic network for the generated data sets, and the MJ method was implemented for both data sets without using out groups (Bandelt and Forster, 1997). Phylogenetic networks for both datasets are represented in the figure 8a and 8b.

Molecular Data Analyses

Choice of Out-group: None of the *Ctenosaura* species are genetically close to the *C. similis.* All other species appear to be sister groups tothis species (Buckley, 1997). Therefore, *Ctenosauramelanosterna*(Buckley & Axtell, 1997), the black-chested spiny-tailed iguana was chosen as out-group for this study because it is found in Honduras where *C. similis* individuals can be found. *C.melanosterna* is categorized as an endangered species in part because of its habitat loss (Pasachnik*et al.,* 2012).

Phylogenetic Tree Analysis

Finding a unique method to infer phylogenies is a very complicated process. There are a number of assumptions to reconstruct phylogenies from a given dataset of DNA or protein sequences. The results may or may not display the true phylogenetic tree (Salemi and Vandamme, 2003). Each method applies different criteria to construct a tree. Therefore, the consensus trees can be compared to each other and a final decision can be made based on the results (Buckley, 1997).

In this study, collapsed sequences (i.e., haplotypes) for both data sets were used to perform phylogenetic tree analyses in PAUP* version 4.0 (Swofford, 2002), a computational phylogenetics program. Phylogenetic trees were constructed using maximum parsimony (MP), maximum likelihood (ML) and minimum evolution (ME) approaches.

MP chooses the tree with the shortest length to explain the observed data; namely, it searches tree space for topologies with the minimum amount of change to construct a phylogenetic tree. A phylogenetic tree chosen by parsimony supports the minimum total amount of evolutionary change (i.e., mutations) (Felsenstein, 2004). It evaluates a subset of all reasonable topologies (branch and bound method) and chooses the one that has the least number of changes as the best tree (Salemi and Vandamme, 2003).

Maximum likelihood uses an explicit DNA substitution model to construct phylogenies. It produces a number of different trees and evaluates each tree by using a nucleotide substitution model. Since different tree topologies are evaluated with different mathematical calculations, it is computationally demanding (Salemi and Vandamme, 2003). After searching for all reasonable trees, it chooses the tree with the highest likelihood as the best tree. The assumption for ML is that hypothesizing an evolutionary history can be explained better by a higher probability than lower probability for a given dataset.

Desper and Gascuel (2005) define ME distance-based method as a very common approach to construct phylogenies by a given large number of datasets. Similar to ML, ME uses a nucleotide substitution model to estimate evolutionary distances; however, the mathematical calculations are less complicated since it creates a matrix of pairwise evolutionary distances among taxa to compute the best tree.

To understand the evolutionary process of a certain locus, it is important to predict the substitution changes by building nucleotide substitution models. The best-fit nucleotide substitution model is chosen based on a given data set and a topology. In this study, the best-fit model was ascertained using Modeltest version 3.7 (Posada and Crandall, 1998) and found to the generalized time-reversible (GTR +I+G, Tavaré, 1986) model of evolution that was then used to construct phylogenies for *cytochrome b* locus. Analyses were performed with gaps for rhodopsin locus. The HKY85 (Hasegawa, Kishino and Yano, 1985) model of evolution was used to construct phylogenies for rhodopsin locus.

All phylogenies were estimated under the heuristic search algorithms with the appropriate DNA substitution model. Tree-bisection-reconnection (TBR) was chosen as the branch swapping option for both data sets. Consensus trees were created for MP, ML, and ME approaches. A consensus tree is the sum of all possible outputs or remaining trees that occur more than 50% of the time ((Bryant, 2003). Therefore, the strict consensus and 50% Majority-rule trees were calculated to combine all possible solutions and obtain a single topology for each approach (Appendix.2a-v).

The bootstrap analysis is a statistical method used to estimate the support of nodes by evaluating the number of times a node is found in multiple searches of re-sampled data sets during bootstrap replicate data set searches. A bootstrap consensus treedisplays how often a node occurs in a tree when data are randomly sampled more than once (Felsenstein, 1985). As the number of bootstrap samples (replicates) constructed increases, the computing resources necessary to complete the bootstrap search increases. In this study, bootstrap values were generated from 100 replicates of heuristic searches, and TBR branch swapping option was used for both data sets.

The threshold for a bootstrap value is accepted as 70%. Anything below 50% is not shown on the tree (Hillis and Bull, 1993). Nodes with bootstrap values between 75% and 95% are moderately supported, and above 90% are very well supported.

In this study, consensus trees for both loci were displayed using the ML best tree topology with bootstrap values from all approaches placed on corresponding branches as likelihood, parsimony, minimum evolution bootstrap values, respectively (Figure.7a & 7b).

Estimates of genetic distances were conducted in PAUP* by using the appropriate model for each locus (Appendix.3a & 3b.)

Phylogenetic Network Analysis:

According to Bryant and Moulton (2004), evolutionary networks can give more comprehensive information about closely related genotypes (compared to evolutionary trees) because of their ability to document recombination, hybridization, gene conversion or gene transfer more accurately. NETWORK is a software program used "to reconstruct phylogenetic networks and trees, infer ancestral types and potential types, evolutionary branchings and variants, and to estimate datings" (NETWORK User Guide, 2012). Median joining (MJ) is one of most commonly used methods in this software package. It finds a minimum spanning tree first. Then, it adds new median vectors (i.e., hypothetical or missing ancestors) to a single network. This method handles large datasets and works fast. In this study, NETWORK.4.6.1.1 was used to compute an unrooted phylogenetic network for the generated data sets, and the MJ method was implemented for both data sets without using out groups (Bandelt and Forster, 1997). Phylogenetic networks for both datasets are represented in the figure 8a and 8b.

Results

This study sequenced and aligned 1140 bp from *cytb* locus for 159 individuals and 847-878 bp rhodopsin locus for 127 *C. similis* individuals. One out-group, *C. melanosterna,* was added to both data sets while constructing gene trees. No out-group was used for the network analyses.

The genetic distances were conducted by using the appropriate model for each locus. The highest genetic distance is 1.85% for rhodopsin locus and the highest genetic distance for *cytb* locus is 3.7 % (Appendix.3a & 3b).

Phylogenetic Tree Analyses:

Results of DAMBE program analysis indicate 71 cytb mtDNA haplotypes from 159 individuals and 40 rhodopsin haplotypes from 127 individuals represented in Appendix 4a&4b. Not all individuals were successfully genotyped (sequenced) from both loci.

Gene tree of cytochrome *b:*

The phylogenetic relationships inferred from *cytb* sequences, using MP, ML and ME approaches, are quite similar to each other. The Southern Mexico haplogroup (C2) is supported as the sister to the Yucatan haplogroup (C1) weakly by ML analysis (63%). It is placed as the sister to all other C. similis haplogroups by MP and ME analyses (lower dashed line) but this placement has no bootstrap support (<50%). One of the Western Costa Rica haplogroups (CBP32_05/06, CBP46) and the Panama haplogroup (CBB00_21_01/02) are placed as sister to the remaining C. similis haplogroups but with no bootstrap support (<50%) so their relationships remain of uncertain affinity. Moreover, some haplotype topologies and branching within the clades are different for each approach, especially for the ME best tree. However,

most clades are consistent among the ML, MP and ME best trees. The maximum likelihood best tree with ML, MP and ME bootstrap values shows 3 major clades and the group, C6. The first clade C7 is defined by 26 haplotypes. C1, the subclade of C7, is defined by 21 haplotypes representing Northern Mexico, the Yucatan Peninsula of Mexico, and the Utila island of Honduras populations. C2 is defined by 5 haplotypes representing Southern Mexico, the Yucatan Peninsula of Mexico populations. The clade C3 is defined by 8 haplotypes representing El Salvador, Southern Mexico, and Southern and Central Guatemala populations. The clade C8 comprises 2 subclades, C4 and C5. The subclade C4 is defined by 17 haplotypes representing Southern Florida, Northern Honduras including the Utila Island, Nicaragua including the Corn islands, and Western and Central Costa Rica populations. The subclade C5 is defined by 15 haplotypes representing Southern Florida, Northern Honduras including the Utila and Guanaja islands populations. C6 comprises 5 haplotypes representing Utila island of Honduras, Western Costa Rica, and Southern Panama populations. Figure.9b shows the biogeographic distributions of these clades and subclades.

The bootstrap values from all methods are shown on a single consensus tree (Figure.7a). In general, anything below 50% for bootstrap values are not displayed on the phylogenetic trees since those nodes are not supported. The overall bootstrap values of MP, ML and ME trees are very close to each other in most cases. Some clades show high confidence with high bootstrap values. For example, C3 is supported with bootstrap values, 88%, 100%, and 82% for likelihood, parsimony and minimum evolution respectively. Some subclades of C3 are also supported by well supported bootstrap values. C1 within itself represents polytomy, where more than two taxa are rooted together (Lin *et al.,* 2011), and some subclades show well supported

bootstrap values such as Northern Mexico, the Yucatan Peninsula and the Utila island haplotypes.

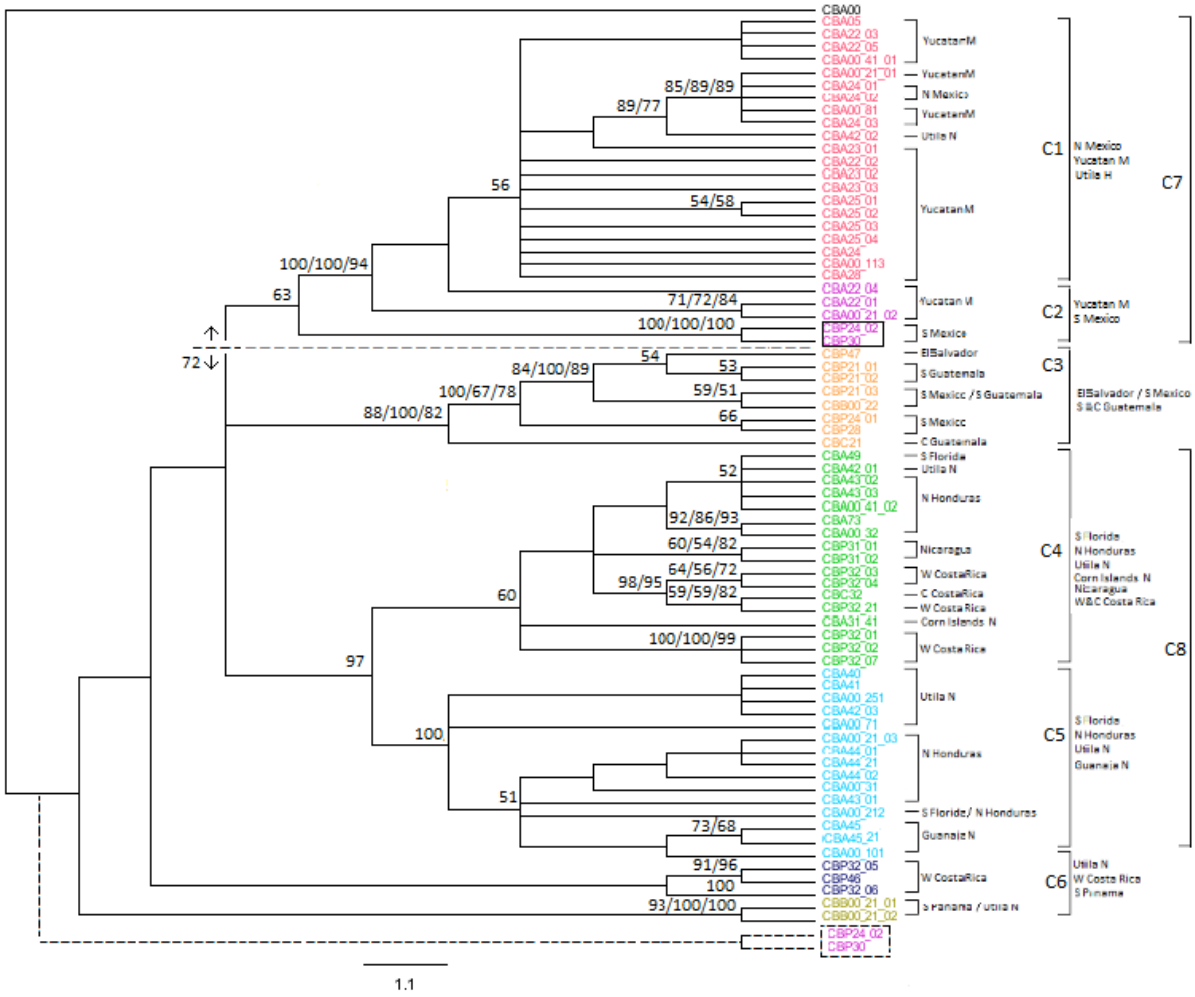

Figure.7a. Maximum likelihood best tree with bootstrap values of all methods used in this study for *cytb* locus

The node for the haplotypes CBP24_02 and CBP30 in C2 results in bootstrap values 100%, 100%, 100% for likelihood, parsimony, and minimum evolution respectively. Some subclades of C4 resulted in strongly supported bootstrap values such as some Honduras and Western Costa Rica haplotypes 100%, 100%, and 99%. The node for the major clade C8 is only supported with likelihood bootstrap values of 97%. The node for the subclade C5 is only

supported with a parsimony bootstrap value of 100%. C6 is not supported with well supported bootstrap values; however, each small clade within the group shows high bootstrap values such as Western Costa Rica, Panama and the Utila island haplotypes. Some single resolved nodes are also seen in the tree.

Gene tree of rhodopsin:

The phylogenetic relationships inferred from rhodopsin sequences using the MP, ML and ME approaches are almost identical. The only discrepancy among gene trees is the haplotype RDC46, representing Central Guatemala that is grouped by the upper clade for the ME tree (shown by dashed line) and the lower clade for MP and ML trees (Figure.7b). Additionally, some haplotype topologies and branching within the clades are different for each tree, especially for the ME best tree. However, clades are consistent among the ML, MP and ME best trees. The maximum likelihood haplotype tree with ML, MP and ME bootstrap values show 2 major clades: the first major clade includes subclades R1, R2, and R3. The second major clade comprises subclade R4, R5 and R6. In the first major clade, subclade R1 is defined by 11 haplotypes representing Southern Florida, Northern Mexico, Northern Honduras, El Salvador, Nicaragua and Western Costa Rica populations. The subclade R2 is defined by 5 haplotypes representing Northern Honduras including mostly the Guanaja island populations. The subclade R3 is defined by 3 haplotypes representing Southern Mexico and Western Guatemala populations. In the second major clade, subclade R4 is defined by 12 haplotypes representing the Yucatan peninsula of Mexico, the Corn islands of Nicaragua, Western Costa Rica and Southern Panama populations. The group R5 is defined by 6 haplotypes representing Northern Honduras, Nicaragua, and Western Costa Rica populations have relationships that possess either weak or no bootstrap support such that their phylogenetic affinities remain unresolved. The

group R6 is defined by 3 haplotypes representing Central Guatemala and Western Mexico populations. Figure.9a shows the biogeographic distributions of these clades and subclades.

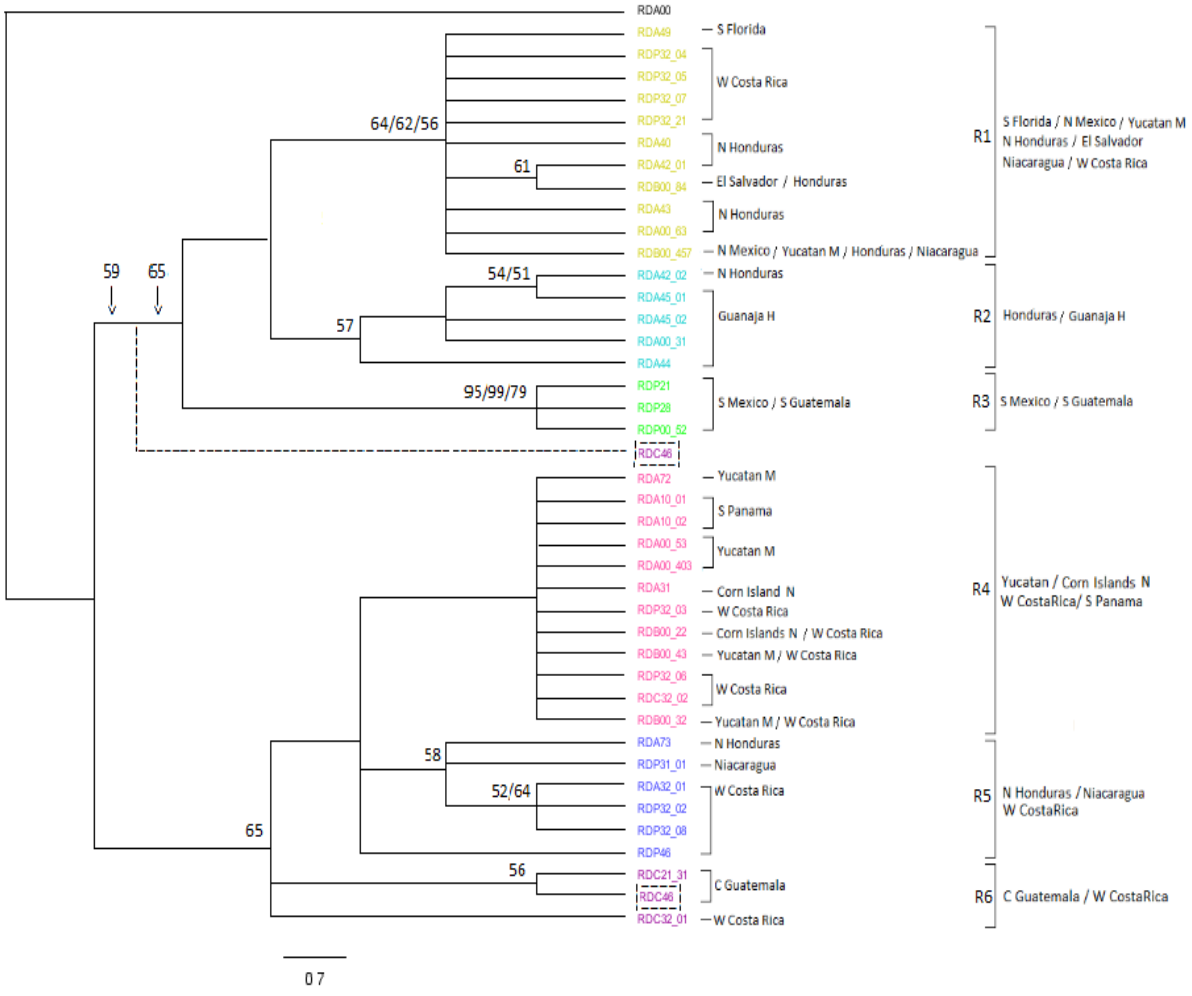

Figure.7b. Maximum likelihood best tree with bootstrap values of all methods used in this study for rhodopsin locus.

All bootstrap values are shown on a single summary tree and are similar to each other for MP, ML and ME trees (Figure.7b). In general, most nodes are supported by bootstrap values are between 52-65%, which is weak support. The only exception is that the clade R3 which results in bootstrap values 95%, 99%, 79% for ML, MP, and ME trees respectively. The clade R1 is supported with weak bootstrap values, 64%, 62%, and 56% respectively. Additionally, it

represents a polytomy. The clade R4 is not supported with strongly supported bootstrap values for all trees. At the same time, it also shows a polytomy. Even if R3 has high bootstrap values, it depicts a polytomy as well. In some cases, single resolved nodes are also seen on the tree.

Haplotype Network Analyses:

Among 171 sequences for the *cytb* locus, 68 mtDNA haplotypes were found, and a total of 40 haplotypes were detected from 153 rhodopsin sequences according to NETWORK.

Haplotype network of cytochrome *b:*

In this network, most clusters are widely separated. They are also mostly in agreement with the maximum likelihood best tree. The clades were colored by sample locations and grouped by clades and groups found in the maximum likelihood best tree. As it shows in the ML tree, the clades C3, C4, C5, and C6 are well separated while C1 and C2 are considerably clustered in the network. The cluster C12 comprises C1 and three haplotypes of clade C2 in the ML tree. C1 has 20 haplotypes instead of 21 in the ML tree. The haplotype CB24_03, Yucatan Peninsula, Mexico population is grouped with the haplotype CBA0081 that also represents the Yucatan Peninsula (#1 shown in the Figure.8b). There are 23 haplotypes in the clade C12 from 2 main localities, the Yucatan Peninsula of Northern Mexico, and Honduras. The subclade C22 has only 2 haplotypes, representing Southern Mexico. The clade C3 has 10 haplotypes from three localities, Southern Mexico, Southern Guatemala, and El Salvador, as it appears the same in the ML tree. The clades C4, C5, and C6 are clustered as it appears in the ML tree. On the other hand, C4 has 16 haplotypes instead of 17 in the ML tree. The haplotype CB43_02, Northern Honduras population is grouped with the haplotype CBA00212 that also represents Northern Honduras (#2 shown in the Figure.8b). Additionally, C5 has 14 haplotypes

instead of 15 in the ML tree. The haplotype CB41, the Utila island of Honduras population is grouped with the haplotype CBA00251 that also represents Utila Island (#3 shown in Figure.8a).

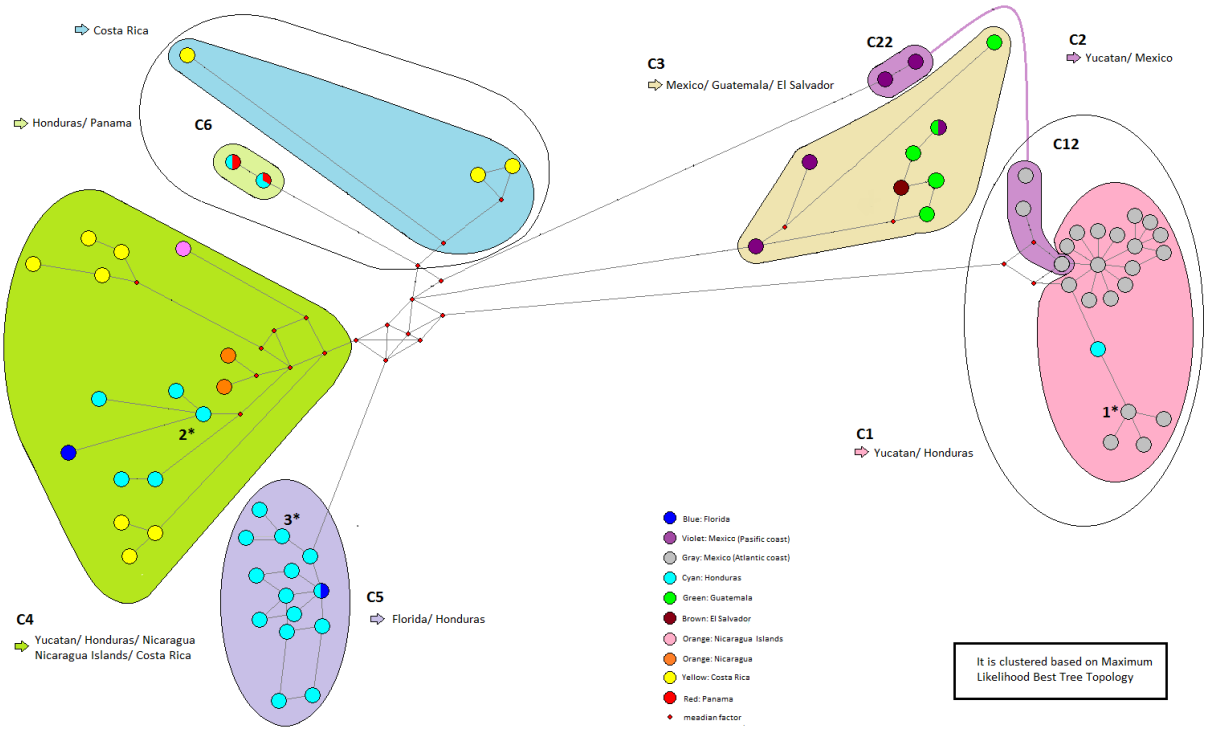

Figure.8a. The median-joining network of *C. similis* based on cytochrome *b* sequences. The branch length is proportional to the number of mutations. In general, the circle size is proportional to the haplotype frequency and it is not showed on the figure since the sampling data has sampling bias.

Haplotype network of rhodopsin:

In this network, clades are not as well separated as it appears in the *cytb* network. However, it is mostly in agreement with the maximum likelihood best tree (Figure.8b). When the clades are colored by sample locations and grouped by clades and unresolved groups found in the maximum likelihood best tree, the separation of the clades is more understandable. While R1, R4, R5, and R6 are partially grouped, R2 and R3 are well separated, as small clades. R2 has

5 haplotypes, representing all Honduras populations. R3 has only 3 haplotypes, representing Southern Mexico and Southern Guatemala, as it appears the same in the ML tree.

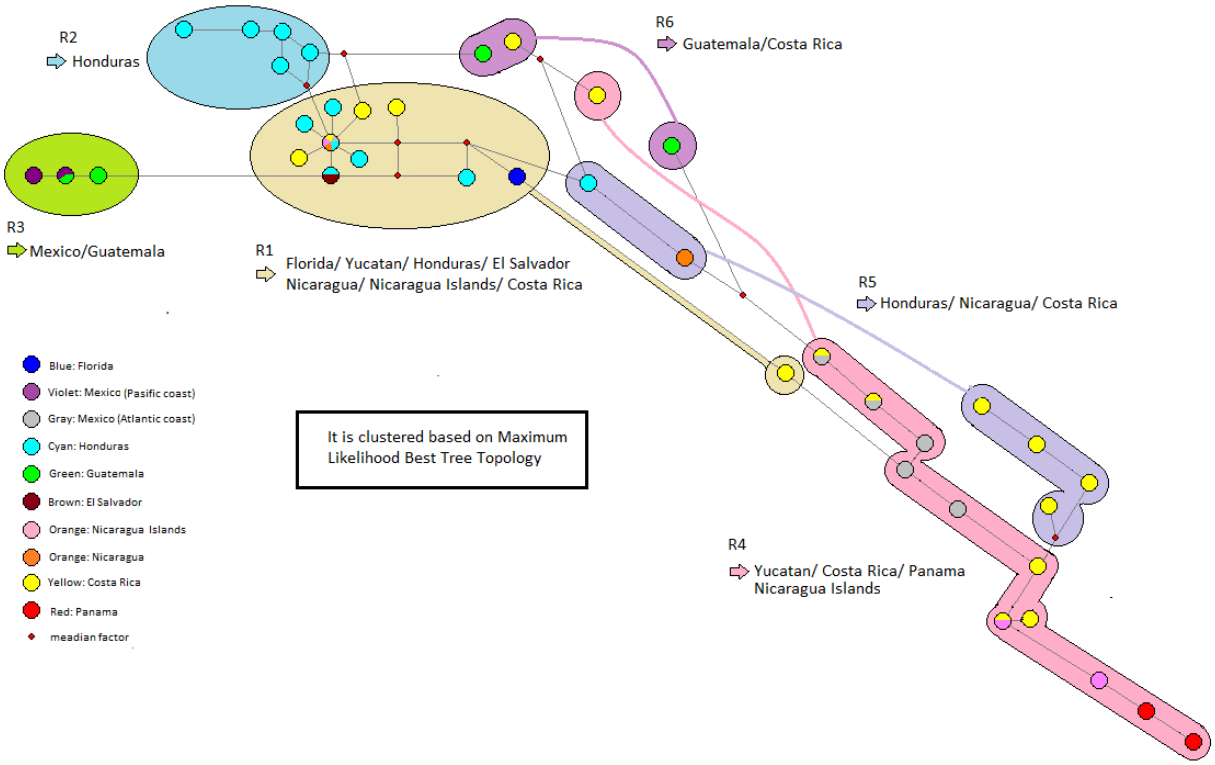

Figure.8b. The median-joining network of *C. similis* based on rhodopsin sequences. The branch length is proportional to the number of mutations. In general, the circle size is proportional to the haplotype frequency and it is not showed on the figure since the sampling data has sampling bias.

Haplotype Diversity:

The biogeographic distributions of the clades and subclades for both loci are showed on figure.9.a and figure.9.b, rhodopsin and *cytb* respectively. Each line represents a clade or unresolved group found in the trees. Additionally, the numbers of haplotypes based on the localities are displayed on the maps.

Cytochrome *b:*

According to figure.9a, there are only two different haplotypes from Southern Florida. Both haplotypes of Southern Florida are closely related with the Honduras haplotypes. There is one unique haplotype for Southern Florida. The other haplotype of Southern Florida is exactly as same as one of Honduras haplotypes. There is one unique haplotype for Nicaragua Islands, one unique haplotype for El Salvador. Four unique haplotypes were found on Southern Mexico and another four unique haplotypes on Guatemala. There is one unique haplotypes that is shared by Guatemala and Southern Mexico populations. There are two unique haplotypes from Western Nicaragua. Costa Rica, Honduras (including islands) and the Yucatan Peninsula have the highest haplotype numbers; 10, 19, and 22 respectively. There are no unique haplotypes for Panama. There are 22 unique haplotypes on the Pacific coast and 46 unique haplotypes on the Atlantic coast.

Rhodopsin:

Figure 9.b shows only one unique haplotype from Southern Florida, one unique haplotype from Nicaragua Islands. Two unique haplotypes are shared by Honduras and Costa Rica, and one unique haplotype is shared by Nicaragua Islands and Panama. There is also one unique haplotype in Southern Mexico, and three unique haplotypes from Guatemala. Southern Mexico and Guatemala populations share one unique haplotype.

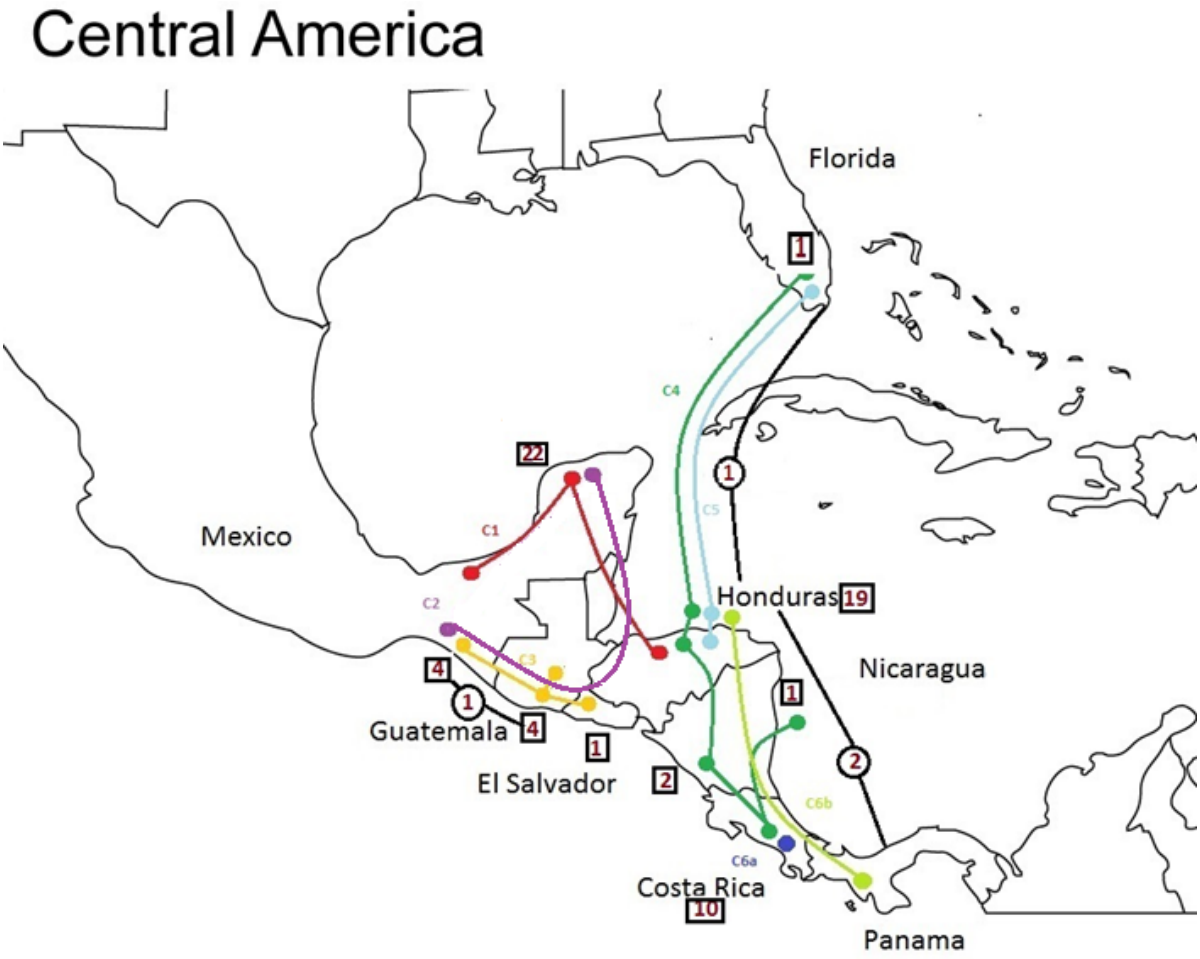

Figure.9a. The biogeographic distributions of these clades and subclades for *cytb* locus

There is only one unique haplotype in Western Nicaragua. El Salvador and Honduras populations share another unique haplotype. There are three haplotypes in the Yucatan Peninsula, and two unique haplotypes for Panama. Costa Rica and Honduras (including islands) have the highest haplotype numbers; 12 and 10 respectively. There are 20 unique haplotypes on the Pacific coast and 18 unique haplotypes on the Atlantic coast. Another unique haplotype is shared by five different localities.

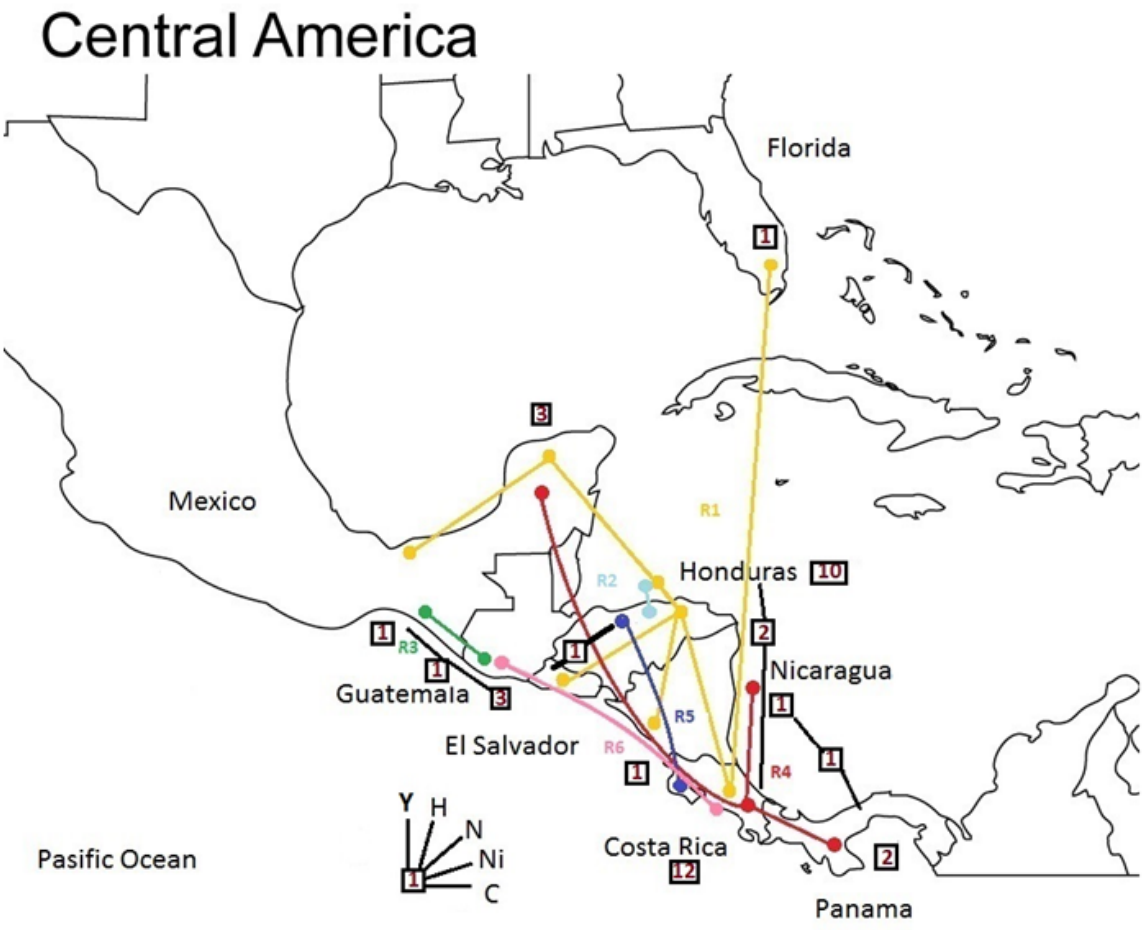

Figure.9b.The biogeographic distributions of these clades and subclades for rhodopsin locus

Discussion

This study confirms that there are 71 haplotypes of *cytb*locus and 40 haplotypes of rhodopsin in Central America. The highest genetic distance for 40 rhodopsin haplotypes is 1.85% and the highest genetic distance for the 71 cytbhaplotypes is 3.7 %. There is a consistency between the genetic distance and number of haplotypes based on the genetics distances. The mitochondrial DNA is evolving more rapidly than nuclear DNA so that the genetic diversity of *cytb* locus is about 2 times higher than rhodopsin, and the number of haplotypes for cytb is also about 2 times higher than the number of haplotypes of rhodopsin.

For the cytochrome *b* gene tree, it appears that there are 3 main clades (C7, C3, and C8) with several haplogroups of uncertain phylogenetic affinity (S. Mexico, Panama, some W. Costa Rica) that are not strongly supported as members of any other larger haplogroup. Most of the subclades haplotypes are well separated in the gene tree based on their locations. There are only two different haplotypes from Southern Florida and both of them are grouped by main clade C8. One of them shares a more recent common ancestor with some Northern Honduras haplotypes in the subclade C4. The other haplotype of Southern Florida is exactly as same as one of Honduras haplotypes, and shares a common ancestor with other Northern Honduras haplotypes including the islands. Both haplotypes of Southern Florida are closely related with the Honduras haplotypes. Because of pet trade between Central America and the United States, it is expected to see this close relationship between Southern Florida and Honduras haplotypes in the*cytb* gene tree if there were released or escaped animals since the climate in southern Florida is subtropical.

The Yucatan Peninsula haplotypes appear to occur only in the clade C1, and share a common ancestor with Northern and Southern Mexico, and some Utila island haplotypes. There is only one Honduras haplotype that shares a common ancestor with Yucatan Peninsula haplotypes in the clade C7. These broad northern haplotypes are well separated on the Atlantic coast. C3 seems to have all Guatemala haplotypes, some Southern Mexico and El Salvador haplotypes. Additionally, this clade is supported by high bootstrap values, and well separated on the Pacific coast. Most of the Western Costa Rica haplotypes are found in the clade C8. It appears there is no Costa Rican haplotype in the two main clades (C7 and C3). The Western Costa Rica haplotypes in the clade C4 share a common ancestor with Nicaragua, Honduras haplotypes. Some Western Costa Rica and Panama/Utila haplotypes seem to have the deepest

split in the rhodopsin tree. This small Western Costa Rica clade seems to be well separated on the Pacific coast, and may share a more recent common ancestor with all haplotypes except Panama/Utila haplogroup, but this relationship has low bootstrap support.

The rhodopsin tree splits into two distinct lineages (Figure.7b). Both lineages have haplotypes from the Yucatan Peninsula, Northern Honduras, Nicaragua, and especially Western Costa Rica. The Panama haplotypes only appear in the lower major clade as a recent split compared to other subclades in the main clade, and seem to have a common ancestor with some Yucatan Peninsula, Nicaragua Island and Western Costa Rica haplotypes. Additionally, the Island haplotypes of Nicaragua only appear in the lower major clade (specifically inR4). The Southern Florida haplotype only appears in the upper major clade (in the subclade R1), and it has a more recent common ancestor with some Northern Honduras, Northern Mexico including the Yucatan Peninsula, El Salvador, Nicaragua, and some Western Costa Rica haplotypes. It also has a recent split or recent dispersal compared to some Guanaja Island, Southern Mexico and Southern Guatemala haplotypes. R3 (only Southern Mexico haplotypes and some Central Guatemala haplotypes) and R6 (some Western Costa Rica and Central Guatemala haplotypes) seem to have the deepest split in the rhodopsin tree within their main clades. In general, Western Costa Rica haplotypes are dispersed through all main clades in this gene tree.

It appears that haplotypes from almost all locations share a common ancestor with haplotypes from Costa Rican populations (Figure.9a). Additionally, most of the subclades are not well supported (low bootstrap values) in the gene tree based on their locations except some small clades such as R2 (Northern Honduras haplotypes) and R3 (Southern Mexico and Guatemala haplotypes, on the Pacific Coast) and R6 (Central Guatemala and Western Costa Rica haplotypes, on the Pacific Coast). According to the gene tree of rhodopsin, Costa Rican

haplotypes are present in almost all areas in Central America and therefore Costa Rica may represent an original source area for *C. similis* before individuals dispersed through Central America. It appears that individuals were not able to go west of the Isthmus of Tehuantepec and *C. similis* is replaced by ecologically similar species *C. pectinata* and *C. acanthura* to the west and north. Panama has both coasts to the Pacific and the Atlantic Oceans. It has also been a physical bridge between Central and South America, allowing animals to migrate between continents. Due to natural events and genetic drift, some old alleles are lost in populations while some new alleles are added over time leaving only a portion of the original alleles in wild populations. This rate of this natural process of allele emergence and extinction differs in mitochondrial vs. nuclear genomes (Avise, 1994). Since they have higher substitution rates, mtDNA genomes tend to accumulate new alleles faster and show shorter coalescence times and more cohesive clades (stronger bootstrap support). Nuclear genomes replace alleles more slowly and alleles can survive in populations through multiple range expansions leaving nuclear alleles spread over wide geographic areas. This pattern is seen the *C. similis* data presented here.

In networks, branch lengths are adjusted based on the number of mutations between taxa. A network displays the distance between taxa and shows all possible pathways among haplotypes. For example, most of the subclades of the clades in the cytb tree display polytomy, especially C1. Moreover, the clades of rhodopsin gene tree show polytomy in most cases with low bootstrap values on most clades. These unresolved nodes are represented in a different way in networks. In another way, networks can show an intraspecific DNA sequence variation more clearly (Mardulyn, 2012).

According to the *cytb* gene tree, the Costa Rican haplotypes seem to be the oldest haplotypes in Central America. Moreover, the rhodopsin gene tree supports this idea due to

some the topology of some haplotypes, the broad distribution of Costa Rica haplotypes all around Central America. On the other hand, the individuals from Panama and Utila share the same haplotype for the *cytb* gene tree. The Panama haplotypes for rhodopsin have a more recent split and, a common ancestor with some Yucatan Peninsula, Nicaragua Island and Western Costa Rica haplotypes (clade C4). However, clade C4 shows polytomy and it is not clear that which haplotypes are closely related to Panama haplotypes in the rhodopsin gene tree. In this case, the network of rhodopsin shows that Panama haplotypes are closely related Nicaragua Islands, and Western Costa Rica haplotypes (Figure.8a). In the *cytb* network, even Panama haplotypes are not exactly in the clade C4, it is also close the Nicaragua and Western Costa Rica haplotypes (Figure.8b).

Every population has its own dynamics. In a population, new alleles appear because of mutation, and allele frequency changes over time as a result of natural selection, genetic drift, mutation, and migration. As a population goes through a speciation event, alleles may be completely transferred to all lineages and may stay in the population, this is complete lineage sorting. On the other hand, some alleles may be lost over time and cannot be presented in the subpopulations; this is incomplete lineage sorting (Degnan and Rosenberg, 2006). It is possible that gene trees can be different from each other due to lineage sorting. Since lineage sorting appears before speciation, and genes have different characteristics, gene trees for the same species can be different in terms of tree topology and branch length (Oren and Papke, 2010).

In this study, the rod and *cytb* gene trees do not exactly match each other. There are both similarities and dissimilarities. Molecular recombination does not occur in mitochondrial genomes and only one parent is able to transfer its genetic data. Therefore, the molecular clock for mitochondrial genes is faster than nuclear genes. With an 8 million year history for

Ctenosaura genus and approximately 2.5 million year history for *C. similis*, mitochondrial haplotypes can easily be replaced with newer, closely related haplotypes compared to slower haplotype replacement for nuclear genes. Therefore, it is highly possible to see gene trees with similarities and dissimilarities.

Central America is a broad area to study with its species diversity and geographic characteristics. *C. similis* individuals are distributed through Southern Mexico to Panama. Individuals prefer to live on the coasts in most places. The coasts of Central America can be open to any natural events since it is in the middle of the Pacific and the Atlantic Oceans. Also, the widths of the areas of the coast where *C. similis* live are not geographically broad. The general genetic diversity is very low based on genetic distance between individuals (shown in Appendix). Considering the areas where *C.similis* lives, the availability of natural disasters in these areas, heavy climate changes, the width of the coast, physical barriers, and ecological niche problems, it is possible that *C.similis* individuals may have gone through important evolutionary processes such as bottleneck or genetic drift which may cause a decrease of genetic diversity in its 2.5 million year history in Central America. On the other hand, the high haplotype diversity for single species may have originated from its broad distribution and physical barriers in Central America over time.

According to figure.9a, Costa Rica, Honduras (including islands) and the Yucatan Peninsula have the highest mitochondrial haplotype numbers; 10, 19, and 22 respectively, based on localities. The Yucatan Peninsula is a very old, broad and favorable area for this species to diverse. Additionally, there are less physical barriers in the area to disperse between countries. It has high haplotype diversity and haplotype endemism. Honduras, relatively another broad habitat for this species compared to other places, has also a high number of unique haplotypes.

T his higher haplotype diversity and haplotype endemism may indicate an older distribution of *C.similis* in these areas. At the same time, gene trees support that there is still ongoing migration between Honduras and the Yucatan Peninsula. The distribution of *C.similis* in Costa Rica is not as broad as Honduras or the Yucatan Peninsula. The haplotype diversity less than these areas; however, it is higher than all other localities in Central America. Figure.9b shows the number of unique haplotypes for rhodopsin. Costa Rica and Honduras have the highest number of unique haplotype, 12 and 10 respectively. All other habitats do not have more than 3 unique haplotypes. The high number for unique haplotypes in Honduras may be again because of older dispersion of populations to these habitats. Both loci display relatively higher number of unique haplotypes for Costa Rica. Overall, the Costa Rica may indicate the origin of this species in Central America while considering the haplotype endemism and haplotype diversity based on localities.

As explained before, mutation rate is faster and more unique haplotypes can be produced for mitochondrial DNA. The reason why there are higher unique haplotypes in certain areas can be because of an earlier dispersion of this species and ongoing migration.

By observing haplotype numbers based on localities, the Atlantic coast has higher haplotype diversity and lower haplotype endemism than the Pacific coast for both loci. This can also be because the width of the areas, and earlier dispersion but isolation of the populations on the Pacific coast, broad areas, less physical barriers between countries, and ongoing migration on the Atlantic coast, and not having the same sample number from each localities (Sampling Bias).

Some general discussion

Bootstrap values are assigned to nodes in trees. A bootstrap value higher than 70% increases the confidence of the topology at a particular internal node. In this study, the bootstrap values are lower than 70% in most cases. Despite low bootstrap values for most branches and lower bootstrap values within the trees, the relationships between the taxa are similar for likelihood, parsimony and minimum evolution trees. As seen in the rhodopsin tree, there are less bootstrap values compared to *cytb* gene tree.

For an intraspecific population, it is most likely to see lower bootstrap values or not to have low values for the nodes of a tree (Soltis and Soltis, 2003). Moreover, close genetic distances can result in poorly solved branches. In this case, networks can help to explain the unresolved branches in more detail (Mardulyn, 2012). In this study, the results for gene trees and networks are close to each other. There is a clear consistency between the results of two different analyses for the same data sets. However, clades and taxa in the networks show clearer representation of haplotypes for both data sets compared to gene trees due to unresolved nodes and polytomy, and the low bootstrap values in the trees.

Median vectors are represented by red diamond shaped symbols in the networks. The rhodopsin network has relatively less median vectors while the *cytb* network has more median vectors. Since median vectors represent missing or possible ancestral haplotypes, and mitochondrial genes are only inherited maternally and have a higher mutation ratio, it is expected that more ancestral information will be lost over time. Therefore, more median vectors are likely to be seen in the cytochrome *b* network.

In the networks, the area of circles are proportional to the haplotype frequency but it is not shown in this study and on the figures since the sample numbers are not the same from every locality. This study has samples from every locality; however, the numbers of samples are not the same for each population. Therefore, all individuals are not equally distributed. This sampling bias could be influencing the results of this study to a small degree.

Future Work

A gene tree is defined as a tree constructed from a single DNA locus. It provides information about the evolutionary history of the locus used in the study. A species tree can be inferred from multiple gene trees, collections of genes, or a combination of morphological and genetic data, it highlights overall pattern. Species trees can enhance the taxa genealogy. Species trees may or may not match the gene trees and these differences may be due to horizontal gene transfer, gene duplication or extinction (Cranston *et al*., 2009) and especially incomplete lineage sorting. Different genes have different characteristics, and this causes different gene histories. Combining different sources (i.e. data sets) may lead to a better estimation of strong evolutionary history, or tell a different story of interesting species (Baum, 1992; Oren and Papke, 2010).

This study used *cytochrome b* and rhodopsin loci to construct gene trees. For a future study, a species tree will be constructed by combining *cytb* and rod sequences for 117 individuals from all Central America, ranging from southern Mexico to Panama.

Genes do not evolve at a constant rate. Because of this, divergence time estimation can be difficult to construct. However, timing of important events in evolutionary history is as important as understanding the relationships of species and populations as well (Arbogast *et al*., 2002)

Estimating divergence times of lineages helps to have a better understanding of the timing of evolutionary processes. As a future study, divergence times will be estimated by using multiple loci, mitochondrial and nuclear.

Conclusion

In this study, the phylogeographic patterns and genetic population structure of *C. similis* were investigated in Central America by analyzing the sequences of one mitochondrial (cytochrome b, Cytb) and one nuclear DNA (rhodopsin, rod) locus. *Ctenosaura* genus has about 6-12 million year history (approximately 8 million years) based on a recent study about Galapagos Marine Iguana (MacLeod *et al*., 2015). *C.similis* has successfully occupied and dispersed in Central America and Southern Mexico with at least 2-3 million-year history. The origin of this species could be the Costa Rica and Panama region due to high haplotype diversity for both data sets, and deeper splits between existing haplotypes are visible on both gene trees and networks. There appears to be somewhat less haplotype diversity on the Pacific Coast, except Costa Rica, but more deep divergence among haplotypes. In most cases, there appears to be ongoing gene flow, migration on both coasts from South (Costa Rica-Panama) to North (The Isthmus of Mexico) and possible areas between countries especially on the Atlantic coast as shown by several haplotypes shared at both ends of the distribution of *C. similis* (Mexico and Panama). In the 2.5 million years history of this species, it appears that there may have been multiple or ongoing migration events and alleles have been mixed by the force of migration in several areas of Central America and Mexico. There is no major, clear separation based on geographical distribution except recent dispersal for small clades in certain areas.

Monitoring *Ctenosaura similis* is necessary for two reasons. First, conservation is needed in existing habitats since genetic diversity may be too low to sustain health populations (W.

Mexico, Panama). Second, this species can be very invasive in some areas such as Florida and Northern South America. Even though there are many studies that have been conducted on *Ctenosaura genus* and other species of the genus, a few of the studies focus on *C. similis.* This study provides an opportunity to infer some general conclusions on *C. similis* in Central America. With regards to this study, it is expected to increase the interest and research of *C. similis* to better understand its evolutionary history.

Literature Cited

Abdul-Muneer, P. M. (2014). Application of microsatellite markers in conservation genetics and fisheries management: recent advances in population structure analysis and conservation strategies. *Genetics Research International*, 2014, 691759.

Anderson, S., A. T. Bankier, B.G., M. H. L. DeBruijn, A. R. Coulson, J. Drouin, I. C. Eperon, D. P. Nierlich, B. A. Roe, F. Sanger, P. H. Schreier, A. J. H. Smith, R. Staden, and I. G. Young. (1981). Sequence and organization of the human mitochondrial genome. *Nature* 290, 457-465. doi.org/10.1038/290457a0

Arbogast, B. S., Edwards, S. V., Wakeley, J., Beerli, P., & Slowinski, J. B. (2002). Estimating divergence times from molecular data on phylogenetic and population genetic times cales. *Annual Review of Ecology and Systematics*.

Avise, J. C. (1994) Molecular Markers, Natural History and Evolution. Chapman and Hall, Inc. 511 pp. New York.

Avery, M.L., Tillman E.A., Spurfeld C., Engeman R.M., Maciejewski K.P., Brown J.D., Fetzer E.A. (2014) Invasive black spiny-tailed iguanas, *Ctenosaura similis*, on Gasparilla Island, Florida, USA. *Integrative Zoology*; 9: 590–597. doi: 10.1111/1749-4877.12085.

Bailey, J. W. (1928) A revision of the lizards of the genus Ctenosaura. *Proc. US Natl. Mus.* 73: 1-55.

Bandelt, H-J., Forster, P. (1997) The myth of bumpy hunter-gatherer mismatch distributions. *American Journal of Human Genetics*. 61:980-983.

Bryant, D. (2003). A Classification of Consensus Methods for Phylogenetics. *DIMACS Series in Discrete Mathematics and Theoretical Computer Science*, *61*, 163–184.

Berglee, R. (2012). Middle America. *Regional geography of the world: Globalization, people, and places: Chapter 5: Middle America* [Creative Commons] (Vol.1.0). Retrieved from: http://2012books.lardbucket.org/books/regional-geography-of-the-world-globalization-people-and-places/s08-middle-america.html

Bernard, R. B. (1992) Combining Trees as a Way of Combining Data Sets for Phylogenetic Inference, and the Desirability of Combining Gene Trees. Vol. 41. No.1.pp.3-10.

Bryant, D., Moulton, V. (2004).Neighbor-Net: An Agglomerative Method for the Construction of Phylogenetic Networks. *Molecular Biology and Evolution*, 21(2), 255–265.

Buckley L. J. (1997) Phylogeny and Evolution of the Genus Ctenosaura (Squamata: Iguanidae). Doctor of Philosophy Dissertation. Southern Illinois University at Carbondale.

Burbrink, F. T., Lawson, R., &Slowinski, J. B. (2000). Mitochondrial DNA phylogeography of the polytypic North American rat snake (Elapheobsoleta): a critique of the subspecies concept. *Evolution; International Journal of Organic Evolutio*n, 54(6), 2107–2118.

Burland, T. G. (2000). DNASTAR's Lasergene sequence analysis software. Methods in Molecular Biology (Clifton, N.J.), 132, 71–91.

Castresana, J. (2001). Cytochrome b phylogeny and the taxonomy of great apes and mammals. *Molecular Biology and Evolution*, 18(4), 465–471.

Chase, M., Kesseli, R., &Bawa, K. (1996). Microsatellite markers for population and conservation genetics of tropical trees. *American Journal of Botany*, 83(1), 51–57.

Cranston, K. A., Hurwitz, B., Ware, D., Stein, L., & Wing, R. A. (2009). Species trees from highly incongruent gene trees in rice. *Systematic Biology*, 58(5), 489–500.

Degnan, J.H., Rosenberg, N.A. (2006) Discordance of Species Trees with Their Most Likely Gene Trees. *PLoS Genetics*. 2(5)-68.

Desper, R., &Gascuel, O. (2005).The minimum evolution distance-based approach to phylogenetic inference. In O. Gascuel (Ed.), Mathematics of Evolution and Phylogeny (pp. 1–32).Oxford University Press. Retrieved from http://www.lirmm.fr/~w3ifa/MAAS/Articles-en-ligne/DesperGascuel_MEP05.pdf

Edwards, S. V, Arctander, P., & Wilson, A. C. (1991).Mitochondrial resolution of a deep branch in the genealogical tree for perching birds. *Proceedings. Biological Sciences / The Royal Society*, 243(1307), 99–107.

Esposti, M. D., De Vries, S., Crimi, M., Ghelli, A., Patarnello, T., & Meyer, A. (1993). Mitochondrial cytochrome b: evolution and structure of the protein. *Biochimica et Biophysica Acta*, 1143(3), 243–271.

Felsenstein, J. (2004) Inferring Phylogenies. Sunderland, Massachusetts - Sinauer Associates, Inc. - ISBN: 0-87893-177-5

Fitch H.S., Henderson R.W. (1978) Ecology and Exploitation of *Ctenosaura similis*. Univ. Kansas Sci. Bull. 5 1 (5): 483-500.

Fortunato, Helena M. (2008). *The Central American land bridge: evolution at work*. Schriften des Naturwissenschaftlichen Vereins fÃ¼r Schleswig-Holstein, 70: 56-72.

Giao, P. M., Tuoc, D., Dung, V. V, Wikramanayake, D. E., Amato, G., & MacKinnon, J. R. (1998). Description of Muntiacustrungsonensis, a new species of muntjac (Artiodactila: Muntiacidae) from Central Vietnam, and implications for conservation. *Animal Conservation*, 1(1), 61–68.

Gillham, N.W. (1994) Organelle Genes and Genomes, Oxford University Press.

Glor, R. E., Gifford, M. E., Larson, A., Losos, J. B., Schettino, L. R., Chamizo Lara, A. R., & Jackman, T. R. (2004). Partial island submergence and speciation in an adaptive radiation: a multilocus analysis of the Cuban green anoles. *Proceedings. Biological Sciences / The Royal Society*, 271(1554), 2257–2265.

Goldsmith, T. H. (1990). Optimization, constraint, and history in the evolution of eyes. *The Quarterly Review of Biology*, 65(3), 281–322.

Halliday T., Adler D. (1992) The Encyclopedia of Reptiles and Amphibians. New York: Facts on File Inc.

Harvey, C. A., Komar, O., Chazdon, R., Ferguson, B.G., Finegan, B., Griffith, D.M., Martinez-Ramos, M., Morales, H., Nigh, R., Soto-Pinto, L., Breugel, M.V., Wishnie, M. (2008) Integrating Agricultural Landscapes with Biodiversity Conservation in the Mesoamerican Hotspot. *Conservation Biology* 22, 8-15.

Hazell, G. G. J., Hindmarch, C. C., Pope, G. R., Roper, J. a, Lightman, S. L., Murphy, D., …Lolait, S. J. (2012). G protein-coupled receptors in the hypothalamic paraventricular and supraoptic nuclei--serpentine gateways to neuroendocrine homeostasis. *Frontiers in Neuroendocrinology*, 33(1), 45–66. http://doi.org/10.1016/j.yfrne.2011.07.002

Hunt, D. M., Fitzgibbon, J., Slobodyanyuk, S. J., &Bowmaker, J. K. (1996). Spectral tuning and molecular evolution of rod visual pigments in the species flock of cottoid fish in Lake Baikal. Vision Research, 36(9), 1217–1224.

Huson, D. H., & Bryant, D. (2006). Application of phylogenetic networks in evolutionary studies. *Molecular Biology and Evolution*. 23(2): 254-267.

Kocher, T. D., Thomas, W. K., Meyer, A., Edwards, S. V, Pääbo, S., Villablanca, F. X., & Wilson, A. C. (1989). Dynamics of mitochondrial DNA evolution in animals: amplification and sequencing with conserved primers. *Proceedings of the National Academy of Sciences of the United States of America*, 86(16), 6196–6200.

Kohler G. (1996) Notes on the systematic status of the taxa acanthura, pectinata, and similis of the genus Ctenosaura". *Senckenbergiana Biologica*. 30 (1): 33-43.

Krajewski, C., Driskell, A. C., Baverstock, P. R., & Braun, M. J. (1992). Phylogenetic relationships of the thylacine (Mammalia: Thylacinidae) among dasyuroid marsupials: evidence from cytochrome b DNA sequences. *Proceedings. Biological Sciences / The Royal Society*, 250(1327), 19–27.

Krajewski, C., & Fetzner, J. W. Jr. (1994). Phylogeny of cranes (Gruiformes: Gruidae) based on cytochrome-b DNA sequences. The Auk, 111(2), 351–365. Retrieved from http://www.jstor.org/stable/10.2307/4088599

Krysko K. L., King F. W., Enge K. M., Reppas A. T. (2003) Distribution of the introduced black spiny-tailed iguana (*Ctenosaura similis*) on the southwestern coast of Florida.- Florida Scientist, Lawrence, Kansas; 66 (2): 74-79.

Laurin, M., & Reisz, R. R. (1995). A reevaluation of early amniote phylogeny. *Zoological Journal of the Linnean Society*, *113*(2), 165–223. Retrieved from http://doi.wiley.com/10.1111/j.1096-3642.1995.tb00932.x

Lin, G., Zhang, C., & Xu, D. (2011). Polytomy identification in microbial phylogenetic reconstruction. *BMC Systems Biology,* **5**(Suppl 3):S2

MacLeod, A., Rodríguez, A., Vences, M., Orozco-terWengel, P., García, C., Trillmich, F., Gentile, G., Caccone, A., Quezada, G., Steinfartz, S. (2015) Hybridization masks speciation in the evolutionary history of the Galápagos marine iguana. *Proc. R. Soc. B,* 282: 20150425 doi:10.1098/rspb.2015.0425

Malfatti M. (2007) A look at the Genus Ctenosaura: Meet the World's fastest lizard and its kin. Reptiles Magazine. 15(11):64-73.

Miah, G., Rafii, M. Y., Ismail, M. R., Puteh, A. B., Rahim, H. A., Asfaliza, R., & Latif, M. A. (2013). Blast resistance in rice: A review of conventional breeding to molecular approaches. *Molecular Biology Reports*, 40(3), 2369–2388.

Mardulyn, P. (2012) Trees and/or Networks to display intraspecific DNA sequence variation. *Molecular Ecology.* Vol(21):14, 3385-3390.

Margulis L. (1981) Symbiosis in cell evolution. W. H. Freeman and Company.

Oren, A. R., Papke, T. (2010) Molecular Phylogeny of Microorganisms Horizon Scientific Press, Science - 220 pages.

Pasachnik, S. &McCranie, J.R. 2010. *Ctenosaura similis*. The IUCN Red List of Threatened Species.Version 2014.3. <www.iucnredlist.org>

Pasachnik, S., Montgomery, C.E. &Henningheim, E. 2012.*Ctenosaura melanosterna*.The IUCN Red List of Threatened Species. Version 2014.3.<www.iucnredlist.org>

Salemi, M., &Vandamme, A. M. (2003). The phylogenetic handbook: a practical approach to DNA and protein phylogeny. (M. Salemi& A.-M. Vandamme, Eds.) *American Journal of Human Biology* (Vol. Primera). Cambridge University Press. Retrieved from http://books.google.com/books?hl=en&lr=&id=Kq6xk_M5dVEC&oi=fnd&pg=PR17&dq=The+phylogenetic+handbook+:+A+practical+approach+to+DNA+and+protein+phylogeny&ots=dEw-uvVrE8&sig=_Gd9sPFRb7cfgZEa8Zi1BI1QbqE

Sarkissian C.D. (2011) Mitochondrial DNA in Ancient Human Populations of Europe. Doctor of Philosophy Dissertation. University of Adelaide. South Australia.

Savage J. M. (2002) The Amphibians and Reptiles of Costa Rica: A Herpetofauna between Two Continents, between Two Seas. University of Chicago Press. Chicago, Illinois.

Soltis, D. E., & Soltis, P. S. (2003). Applying the Bootstrap in Phylogeny Reconstruction. *Statistical Science*.18 (2): 256-267.

Stuart J.A., Brige R.R. (1996) "Characterization of the primary photochemical events in bacteriorhodopsin and rhodopsin". In Lee AG. Rhodopsin and G-Protein Linked Receptors, Part A (Vol 2) (2 Vol Set). Greenwich, Conn: JAI Press. 33–140

Templeton, A. R., Crandall, K. A., & Sing, C. F. (1992). A cladistic analysis of phenotypic associations with haplotypes inferred from restriction endonuclease mapping and DNA sequence data. III. Cladogram estimation. *Genetics*, 132(2), 619–633.

Torres-Carvajal O. (2007) Heterogeneous Growth of Marginal Teeth in the Black Iguana *Ctenosaura similis* (Squamata: Iguanidae). *Journal of Herpetology*, 41(3):528-531.

Townsend, J. H., Krysko, K. L., &Enge, K. M. (2003). The identity of spiny-tailed iguanas, Ctenosaura, introduced to Florida, USA (Squamata: Sauria: Iguanidae). *Herpetozoa*, 16(1-2), 67–72. Retrieved from <Go to ISI>://ZOOREC:ZOOR13900061387

Townsend, T. M., Mulcahy, D. G., Noonan, B. P., Sites, J. W., Kuczynski, C. A., Wiens, J. J., & Reeder, T. W. (2011). Phylogeny of iguanian lizards inferred from 29 nuclear loci, and a comparison of concatenated and species-tree approaches for an ancient, rapid radiation. *Molecular Phylogenetics and Evolution*, 61(2), 363–380.

Untergasser, A., Cutcutache, I., Koressaar, T., Ye, J., Faircloth, B. C., Remm, M., &Rozen, S. G. (2012).Primer3-new capabilities and interfaces. *Nucleic Acids Research*, 40(15).

Vitt, L. J., &Pianka, E. R. (2005). Deep history impacts present-day ecology and biodiversity. Proceedings of the National Academy of Sciences of the United States of America, 102(22), 7877–7881.

Xia, X. (2013). DAMBE5: A comprehensive software package for data analysis in molecular biology and evolution. *Molecular Biology and Evolution*, 30(7), 1720–1728.

Wei, Y.-H., Wu, S.-B., Ma, Y.-S., & Lee, H.-C. (2009). Respiratory function decline and DNA mutation in mitochondria, oxidative stress and altered gene expression during aging. *Chang Gung Medical Journal*, *32*(2), 113–32. Retrieved from http://www.ncbi.nlm.nih.gov/pubmed/19403001

Appendix.1. *Ctenosaura similis* tagging data from samples within Central America ordered by sample number/name. BF: Bruce Elfstrom; JWS: Jack W. Sites, Brigham Young University; KU: University of Kansas; LJB: Larry J.Buckley, Rochester Institute of Technology; SP: Stesha Pasachnik, Institute for Conservation Research, San Diego Zoo Global; USFWS: U.S. Fish & Wild Service. Check Mark (✓) indicates Presence of DNA Sequence for nuclear locus and/or mitochondrial locus.

Sample#	Rod	Cyt b	Location		Source	Latitude & Longitude
			Region	Country		
1	✓	✓	Cochino Grande Island	Honduras	KU	
5		✓	Yucatan Peninsula	Mexico	LJB	
8	✓	✓	Utila Island	Honduras	LJB	
47	✓	✓		El Salvador	BF	
49	✓	✓		Florida	BF	
72	✓	✓	Quintana Roo, 1.1 km. N. CobaRd.on Hwy 307	Mexico	JWS	
73	✓	✓	Louis Porras (Zoo Herp)	Honduras	JWS	
107		✓		Panama	LJB	
108	✓	✓		Panama	LJB	
109	✓	✓		Panama	LJB	
123	✓	✓	Coatzacoalcos, Veracruz (beach on west end of city)	Mexico	LJB	
127	✓	✓	Calla de Campos, Michoacan (Hwy 200), Veracruz	Mexico	LJB	
131	✓	✓	Coatzacoalcos, Veracruz	Mexico	LJB	
158	✓	✓	Conkal, Yucatán	Mexico	LJB	
210	✓	✓	Gualan	Guatemala	SP	
211	✓		Guastatoya	Guatemala	SP	
212	✓		Rio Grande	Guatemala	SP	
214	✓	✓	Aldea	Guatemala	SP	
215		✓	Candelaria	Guatemala	SP	
216	✓	✓	El Pumpo	Guatemala	SP	
217	✓	✓	El Pumpo	Guatemala	SP	

219	✓	✓	Ticul, Yucatan	Mexico	SP	
220		✓	Maxcanu, Yucatan	Mexico	SP	
221	✓	✓	Yucatan	Mexico	SP	
222	✓	✓	Dzibalchen, Yucatan	Mexico	SP	
223	✓	✓	Yucatan	Mexico	SP	
224	✓	✓	Chencho,Yucatan	Mexico	SP	
225		✓	Yucatan	Mexico	SP	
226	✓	✓	Maxcanu, Yucatan	Mexico	SP	
227	✓	✓	PocBoc,Yucatan	Mexico	SP	
228	✓	✓	Hecelchakan, Yucatan	Mexico	SP	
229	✓	✓	Xkumcheil, Yucatan	Mexico	SP	
230	✓	✓	Sevaba playa, Yucatan	Mexico	SP	
231	✓		Pixtun, Yucatan	Mexico	SP	
232	✓	✓	Candelaria, Campeche	Mexico	SP	
233	✓	✓	Yucatan	Mexico	SP	
234	✓	✓	San Hipolito, Yucatan	Mexico	SP	
235	✓	✓	Jonuta, Tabasco	Mexico	SP	
236	✓	✓	Yucatan	Mexico	SP	
237	✓	✓	Belen,Campeche	Mexico	SP	
239	✓	✓	Yucatan	Mexico	SP	
240	✓	✓	Arriaga	Mexico	SP	
241	✓	✓	Arriaga	Mexico	SP	
242	✓	✓	Tabasco	Mexico	SP	
243	✓		Puerto Ceiba, Tabasco	Mexico	SP	
244	✓	✓	Aquila Serra Racho	Mexico	SP	
245	✓	✓	Allende	Mexico	SP	
246	✓ ✓	✓	Neuvo	Mexico	SP	

247	✓	✓	Atasha,Tabasco	Mexico	SP	
248	✓	✓	Carmen, Quintana Roo	Mexico	SP	
249	✓ ✓	✓	Ticopo, Yucatan	Mexico	SP	
250	✓	✓	Hoctun, Yucatan	Mexico	SP	
251	✓ ✓		Statuto, Yucatan	Mexico	SP	
252	✓	✓	Kaua, Yucatan	Mexico	SP	
253	✓		Temozon, Yucatan	Mexico	SP	
254	✓ ✓		Temozon, Yucatan	Mexico	SP	
255		✓	Espita, Yucatan	Mexico	SP	
256	✓	✓	Cenotillo, Yucatan	Mexico	SP	
257	✓	✓	Cenotillo, Yucatan	Mexico	SP	
258	✓	✓	Tizimin, Yucatan	Mexico	SP	
259	✓ ✓	✓	Puerto Morelos, Quintana Roo	Mexico	SP	
261	✓ ✓	✓	Tulum, Quintana Roo	Mexico	SP	
262	✓	✓	Coba, Quintana Roo	Mexico	SP	
263	✓		Coba, Quintana Roo	Mexico	SP	
264	✓		Chunhua, Quintana Roo	Mexico	SP	
265	✓	✓	Chetumal, Quintana Roo	Mexico	SP	
287	✓	✓	Tonala	Mexico	LJB	
288		✓	Merida, Yucatan	Mexico	LJB	
290	✓		Champoton, Campeche	Mexico	LJB	
292	✓	✓	Conkal, Yucatan	Mexico	LJB	
293	✓	✓	Conkal, Yucatan	Mexico	LJB	
305	✓	✓	Chiapas, Tapachula, CantónVillaflor	Mexico	LJB	N15 11 19 7 W92 36 28 7
313	✓	✓	Yucatan, Hwy 180 D	Mexico	LJB	N20 88 23 6 W89 25 80 0
314	✓	✓	Morgan's Rock	Nicaragua	SP	
315	✓	✓	San Jorge	Nicaragua	SP	

316	✓	✓	Little Corn Island	Nicaragua	SP	
317	✓ ✓	✓	Little Corn Island	Nicaragua	SP	
318	✓	✓	Big Corn Island	Nicaragua	SP	
319	✓ ✓	✓	Big Corn Island	Nicaragua	SP	
320	✓	✓	Esparza	Costa Rica	SP	
321	✓ ✓	✓	Pt. Morena	Costa Rica	SP	
322	✓ ✓	✓	Samara	Costa Rica	SP	
323	✓ ✓	✓	Casitas	Costa Rica	SP	
324	✓ ✓	✓	,Lepanto	Costa Rica	SP	
325	✓	✓	Dominical	Costa Rica	SP	
326	✓ ✓	✓	Rica Jaco	Costa Rica	SP	
327	✓ ✓	✓	Rica Tarcoles	Costa Rica	SP	
328	✓ ✓	✓	Rica Lurdes	Costa Rica	SP	
329	✓ ✓	✓	Rica Playa Brasilito	Costa Rica	SP	
373		✓	Key Biscayne	Florida	USFWS	
374		✓	Key Biscayne	Florida	USFWS	
375		✓	Key Biscayne	Florida	USFWS	
376		✓	Key Biscayne	Florida	USFWS	
377		✓	Key Biscayne	Florida	USFWS	
378		✓	Key Biscayne	Florida	USFWS	
379		✓	Key Biscayne	Florida	USFWS	
380		✓	Key Biscayne	Florida	USFWS	
381		✓	Key Biscayne	Florida	USFWS	
382		✓	Key Biscayne	Florida	USFWS	
383		✓	Key Biscayne	Florida	USFWS	
384		✓	Key Biscayne	Florida	USFWS	
385		✓	Key Biscayne	Florida	USFWS	

386	✓	✓	West side, Utila Island	Honduras	SP	
387	✓	✓	Iguana Road, Utila Island	Honduras	SP	
388		✓	Iguana Road, Utila Island	Honduras	SP	
389	✓	✓	Iguana Road, Utila Island	Honduras	SP	
390		✓	DBE, Utila Island	Honduras	SP	
391	✓	✓	NDEVEL, Utila Island	Honduras	SP	
392		✓	FND, Utila Island	Honduras	SP	
393	✓	✓	FND, Utila Island	Honduras	SP	
394		✓	FND, Utila Island	Honduras	SP	
395		✓	Pumpkin HillHouse, Utila Island	Honduras	SP	
396	✓	✓	Pumpkin HillHouse, Utila Island	Honduras	SP	
397	✓	✓	Annie Mar, Utila Island	Honduras	SP	
398		✓	West side, Utila Island	Honduras	SP	
399		✓	West side, Utila Island	Honduras	SP	
400	✓	✓	TH, Utila Island	Honduras	SP	
401	✓	✓	FND, Utila Island	Honduras	SP	
402	✓	✓ ✓	FND, Utila Island	Honduras	SP	
403	✓	✓	Pumpkin HillHouse, Utila Island	Honduras	SP	
404	✓	✓	FND, Utila Island	Honduras	SP	
405	✓	✓	FND, Utila Island	Honduras	SP	
406	✓	✓	Old Airport, Utila Island	Honduras	SP	
407		✓	Annie Mar, Utila Island	Honduras	SP	
408	✓	✓	FND, Utila Island	Honduras	SP	
409		✓	Tradewinds, Utila Island	Honduras	SP	
410	✓	✓	NDEVEL, Utila Island	Honduras	SP	
411		✓	NDEVEL, Utila Island	Honduras	SP	
412		✓	NDEVEL, Utila Island	Honduras	SP	

413		✓	Annie Mar, Utila Island	Honduras	SP	
414		✓	IB, Utila Island	Honduras	SP	
415	✓	✓	RH, Utila Island	Honduras	SP	
416		✓	Old Airport, Utila Island	Honduras	SP	
417	✓	✓	Annie Mar, Utila Island	Honduras	SP	
418b	✓	✓	Annie Mar, Utila Island	Honduras	SP	
419a	✓	✓	Annie Mar, Utila Island	Honduras	SP	
419b		✓	Annie Mar, Utila Island	Honduras	SP	
420a		✓	Pumpkin HillHouse, Utila Island	Honduras	SP	
420b	✓	✓	Pumpkin HillHouse, Utila Island	Honduras	SP	
421a		✓	Annie Mar, Utila Island	Honduras	SP	
421b		✓	Annie Mar, Utila Island	Honduras	SP	
422		✓	Annie Mar, Utila Island	Honduras	SP	
423		✓	FND, Utila Island	Honduras	SP	
424		✓	NDEVEL, Utila Island	Honduras	SP	
425		✓	Sambo Creek, Honduras North	Honduras	SP	
426	✓	✓	AguaCal, Honduras North	Honduras	SP	N15 25 45 8 W86 53 41 6
427	✓ ✓	✓	AguaCal, Honduras North	Honduras	SP	N15 25 45 8 W86 53 41 6
428	✓	✓	AguaCal, Honduras North	Honduras	SP	
429	✓ ✓	✓	Tornabe, Honduras North	Honduras	SP	
430		✓	Miami, Honduras North	Honduras	SP	
431		✓	Tornabe, Honduras North	Honduras	SP	
432		✓	Sambo Creek, Honduras North	Honduras	SP	
433	✓	✓	Sambo Creek, Honduras North	Honduras	SP	
434		✓	Sambo Creek, Honduras North	Honduras	SP	
435		✓	AguaCal, Honduras North	Honduras	SP	N15 25 45 8 W86 53 41 6
436		✓	Puerto Castillo, Honduras North	Honduras	SP	N16 00 26 4 W85 58 23 1

437	✓	✓	Puerto Castillo, Honduras North	Honduras	SP	N16 00 26 4 W85 58 23 1
438	✓ ✓	✓	Puerto Castillo, Honduras North	Honduras	SP	N16 00 26 4 W85 58 23 1
439	✓	✓ ✓	Puerto Castillo, Honduras North	Honduras	SP	N16 00 26 4 W85 58 23 1
440	✓	✓	Puerto Castillo, Honduras North	Honduras	SP	N16 00 26 4 W85 58 23 1
441	✓	✓	Punta Sal, Honduras North	Honduras	SP	N15 54 48 9 W87 37 36 9
442		✓	Punta Sal, Honduras North	Honduras	SP	N15 54 48 9 W87 37 36 9
443		✓	Punta Sal, Honduras North	Honduras	SP	N15 54 48 9 W87 37 36 9
444		✓	Punta Sal, Honduras North	Honduras	SP	N15 54 48 9 W87 37 36 9
445		✓	Coral Bay, Guanaja Island	Honduras	SP	N16 26 97 6 W85 53 36 7
446	✓	✓	Coral Bay, Guanaja Island	Honduras	SP	N16 26 97 6 W85 53 36 7
447	✓ ✓	✓	Manati Resort, Guanaja Island	Honduras	SP	N16 27 40 5 W85 52 07 9
448	✓ ✓	✓	Manati Resort, Guanaja Island	Honduras	SP	N16 27 40 5 W85 52 07 9
449		✓	Rd. to Marty's, Guanaja Island	Honduras	SP	N16 27 06 5 W85 54 71 1
450	✓	✓	Rd. to Marty's, Guanaja Island	Honduras	SP	N16 27 06 5 W85 54 71 1
451	✓	✓	Marty's, Guanaja Island	Honduras	SP	N16 27 60 5 W85 54 61 3
452	✓	✓	Marty's, Guanaja Island	Honduras	SP	N16 27 60 5 W85 54 61 3
453	✓	✓	SW Cay, Guanaja Island	Honduras	SP	N16 24 31 7 W85 53 09 5
454	✓	✓	SW Cay, Guanaja Island	Honduras	SP	N16 24 31 7 W85 53 09 5
455	✓ ✓	✓	Red Cliff, Guanaja Island	Honduras	SP	N16 25 75 7 W85 54 89 3
456		✓	Red Cliff, Guanaja Island	Honduras	SP	N16 25 75 7 W85 54 89 3
457	✓		West End, Guanaja Island	Honduras	SP	
458	✓ ✓	✓	Joshua's Cay, Guanaja Island	Honduras	SP	N16 27 57 5 W85 49 87 8
459	✓		Bobo's, Guanaja Island	Honduras	SP	N16 29 09 2 W85 53 83 8
460	✓	✓	NE Bight, Guanaja Island	Honduras	SP	N16 30 25 2 W85 50 29 1
461		✓	NE Bight, Guanaja Island	Honduras	SP	N16 30 25 2 W85 50 29 1
462	✓ ✓		Morazan	Guatemala	SP	
463	✓	✓	Golfito	Costa Rica	SP	

Appendix.2a. Phylogram of Maximum parsimony phylogenetic tree for *Ctenosaura similis* generated from rhodopsin sequences.

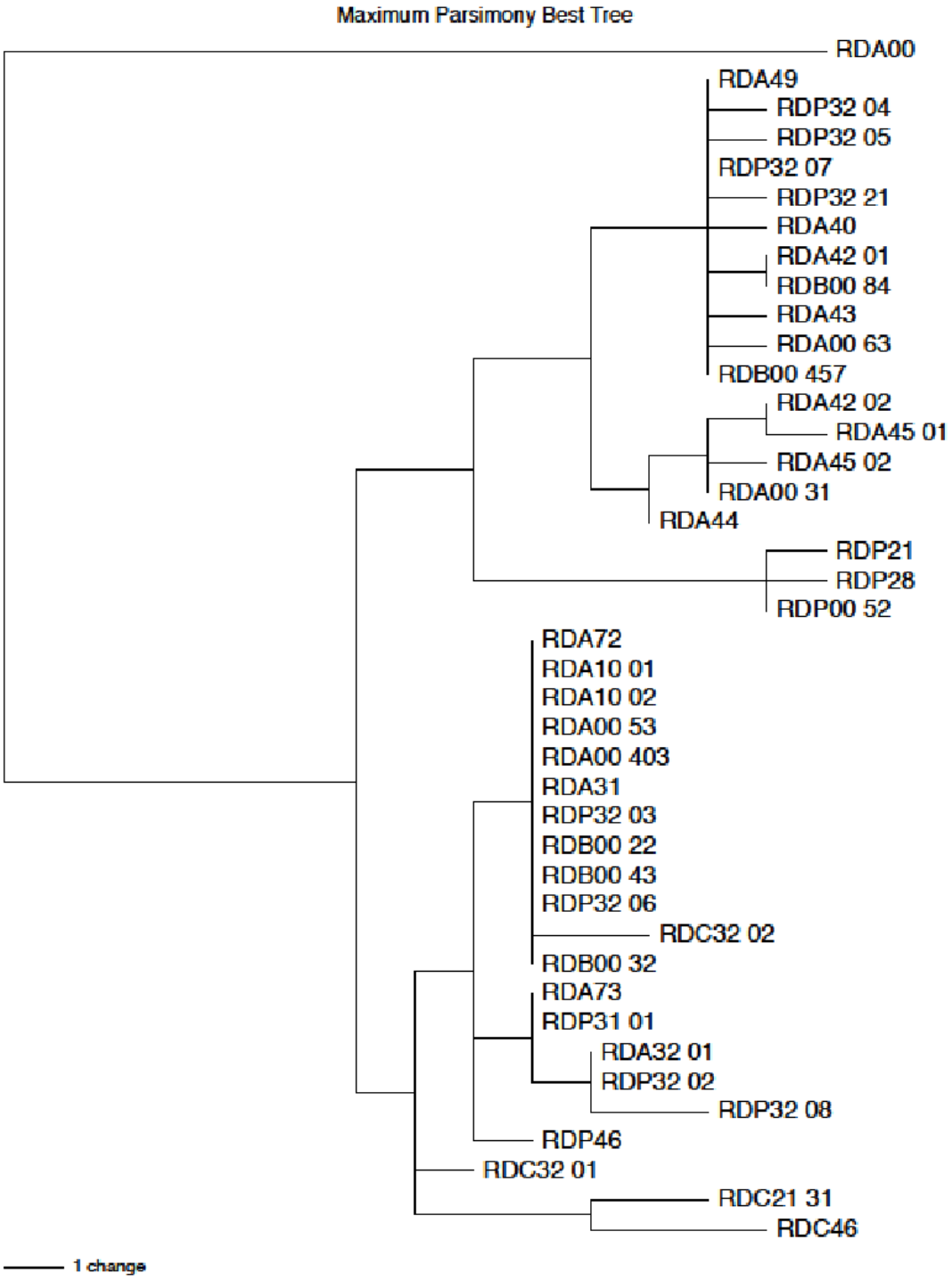

Appendix.2b. Cladogram of Maximum parsimony phylogenetic tree for *Ctenosaura similis* generated from rhodopsin sequences.

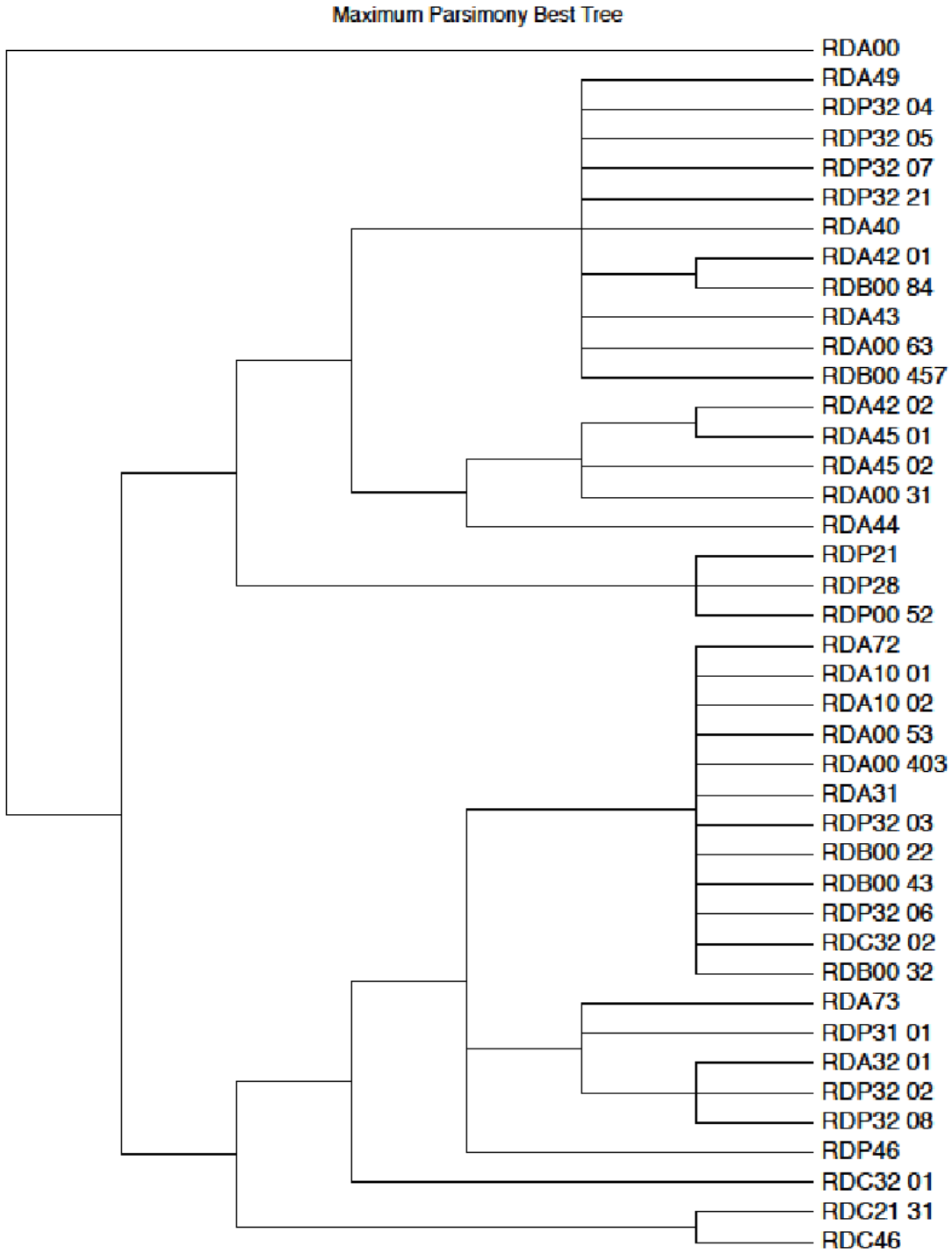

Appendix.2c. Cladogram of Maximum parsimony phylogenetic tree for *Ctenosaura similis* generated from rhodopsin sequences with strict consensus rule.

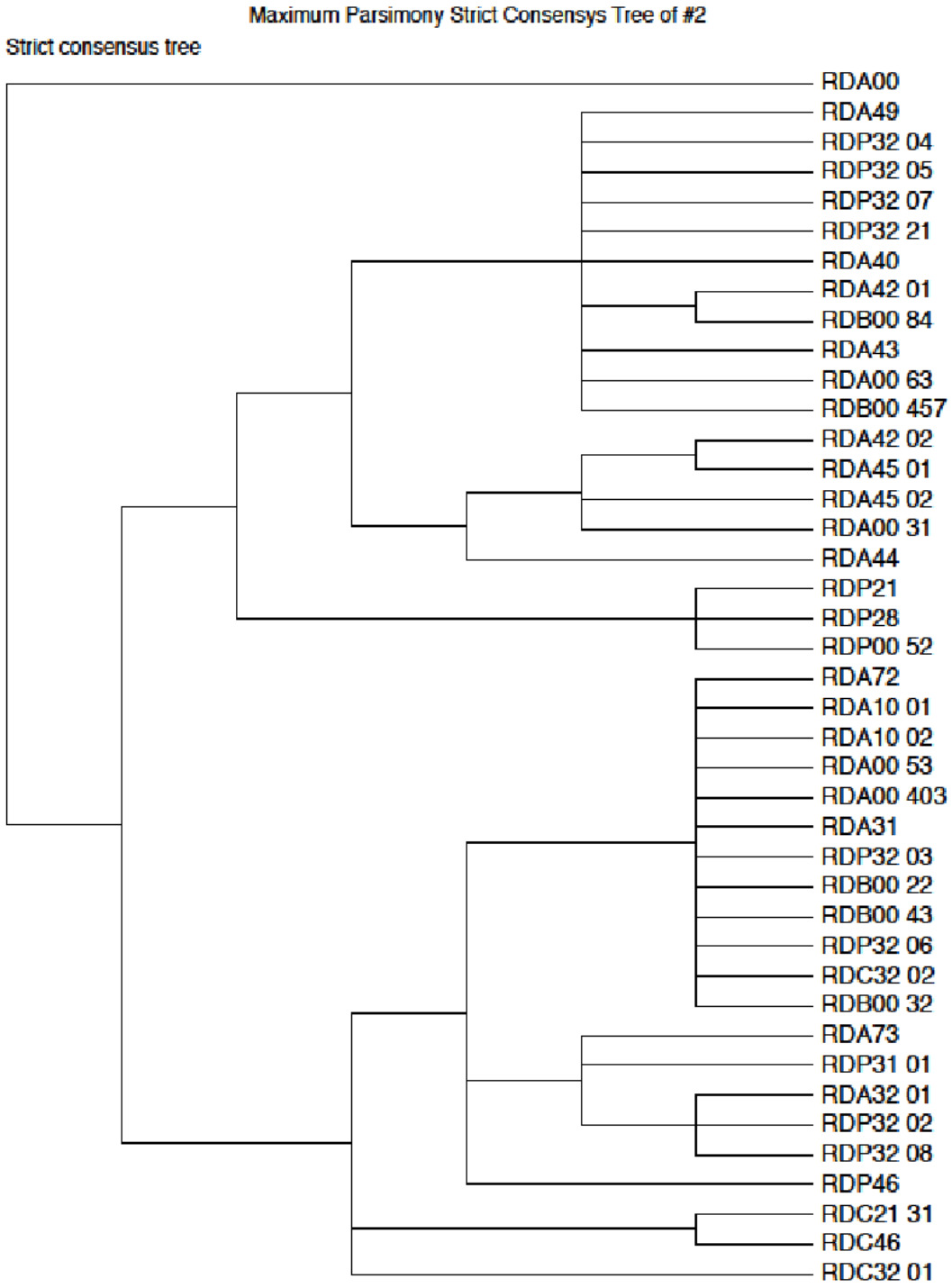

Appendix.2d. Cladogram of Maximum parsimony bootstrap tree for *Ctenosaura similis* generated from rhodopsin sequences.

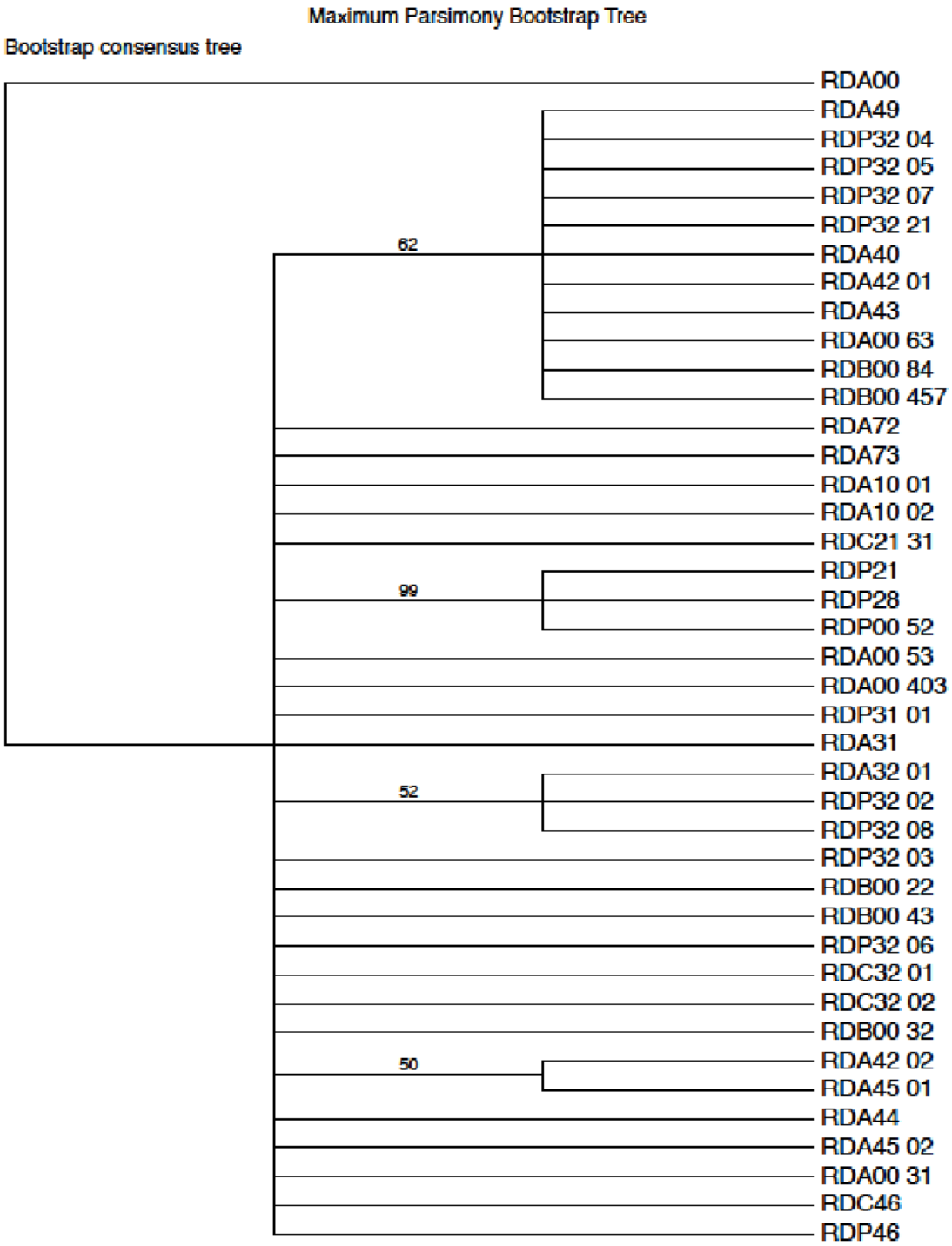

Appendix.2e. Phylogram of Maximum likelihood phylogenetic tree for *Ctenosaura similis* generated from rhodopsin sequences.

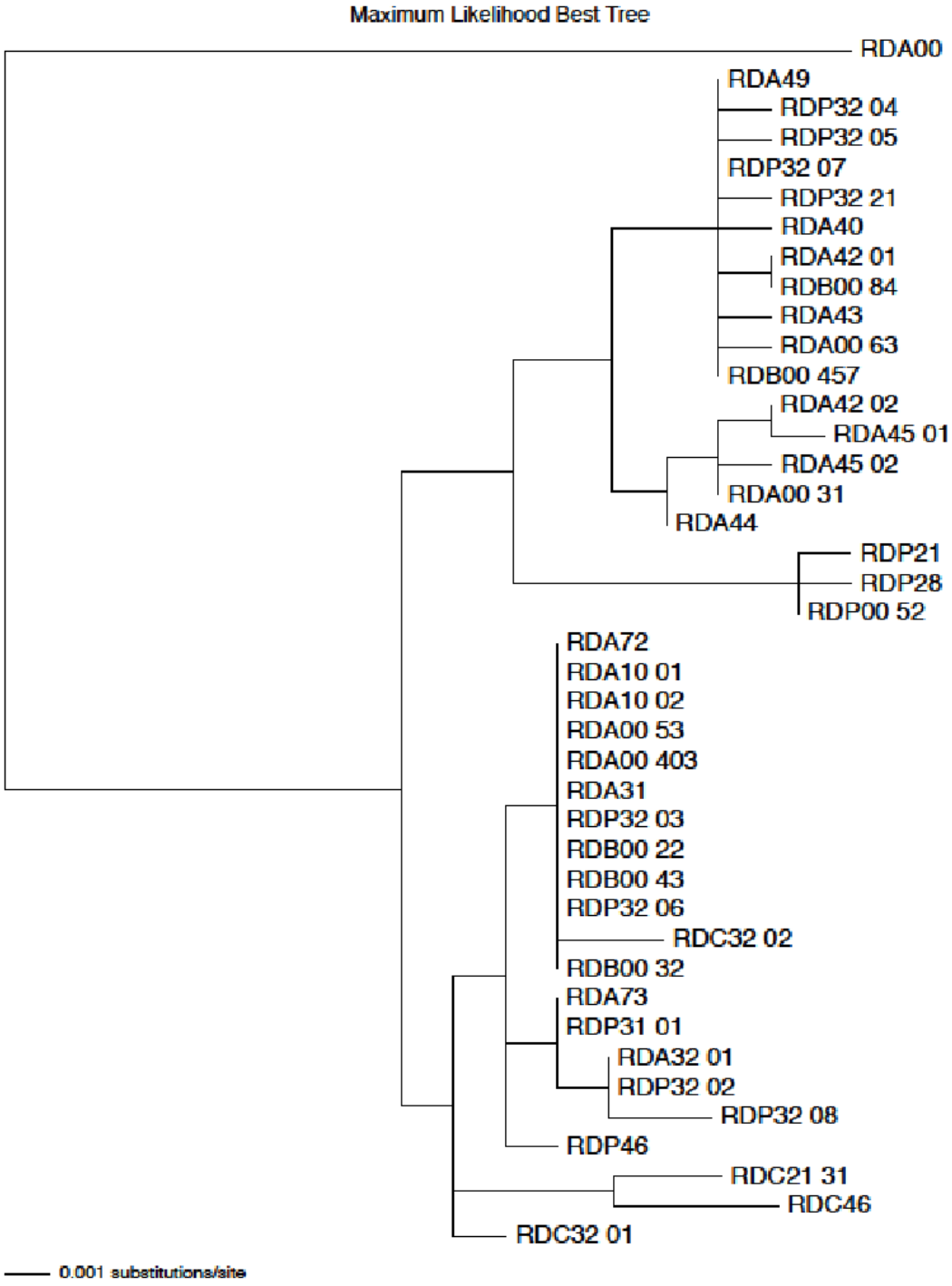

Appendix.2f. Cladogram of Maximum likelihood phylogenetic tree for *Ctenosaura similis* generated from rhodopsin sequences.

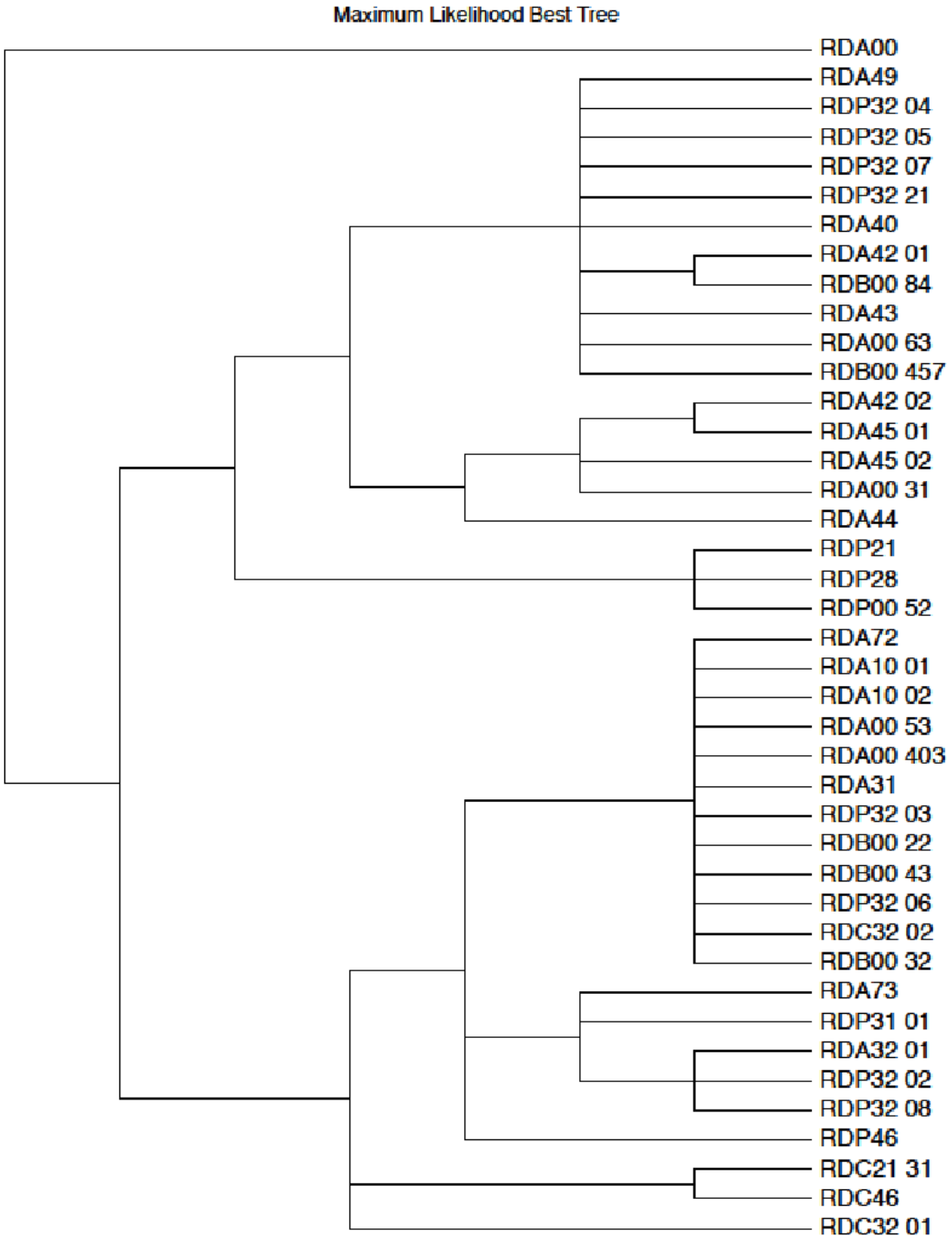

Appendix.2g. Cladogram of Maximum likelihood bootstrap tree for *Ctenosaura similis* generated from rhodopsin sequences.

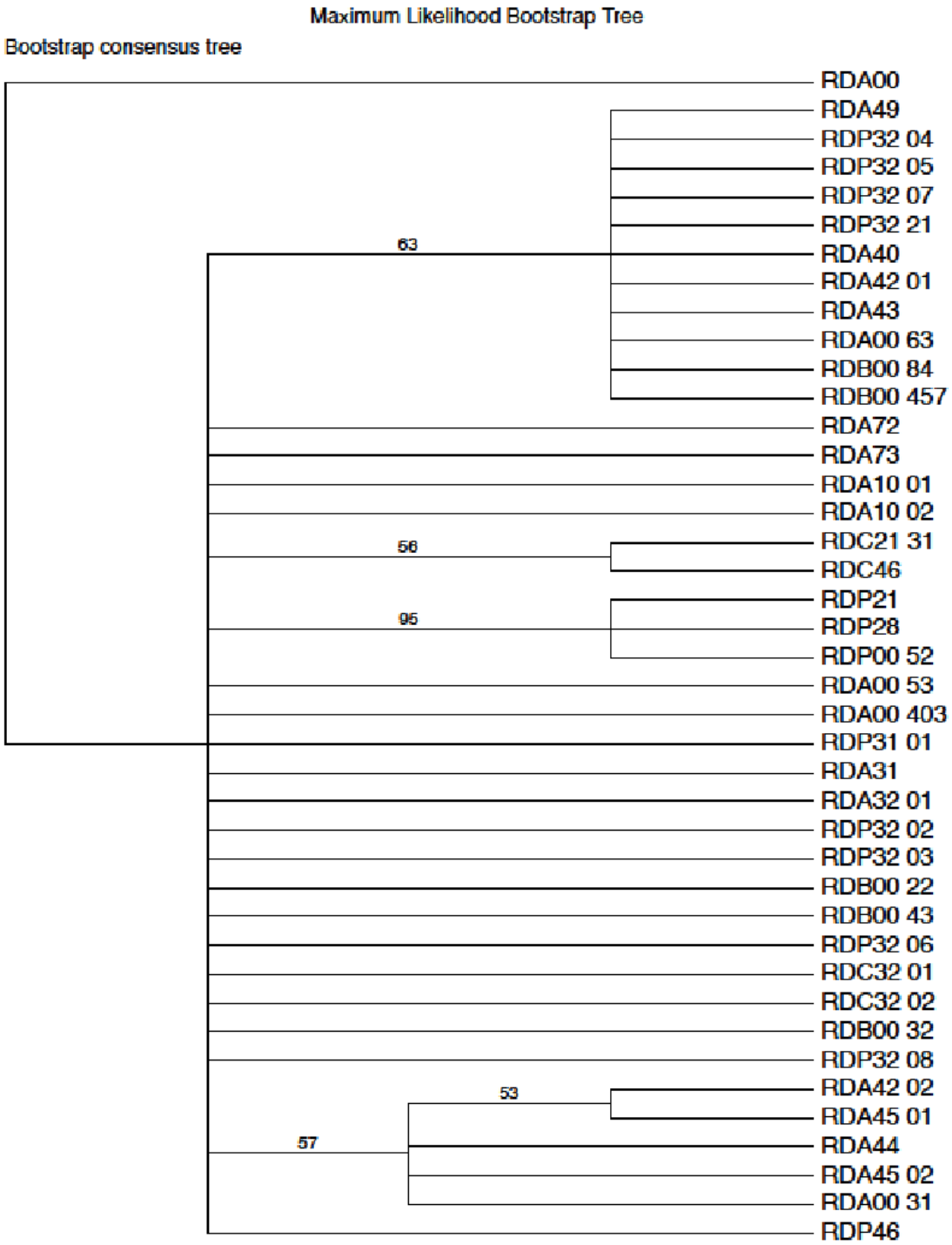

Appendix.2h. Phylogram of Minimum Evolution phylogenetic tree for *Ctenosaura similis* generated from rhodopsin sequences.

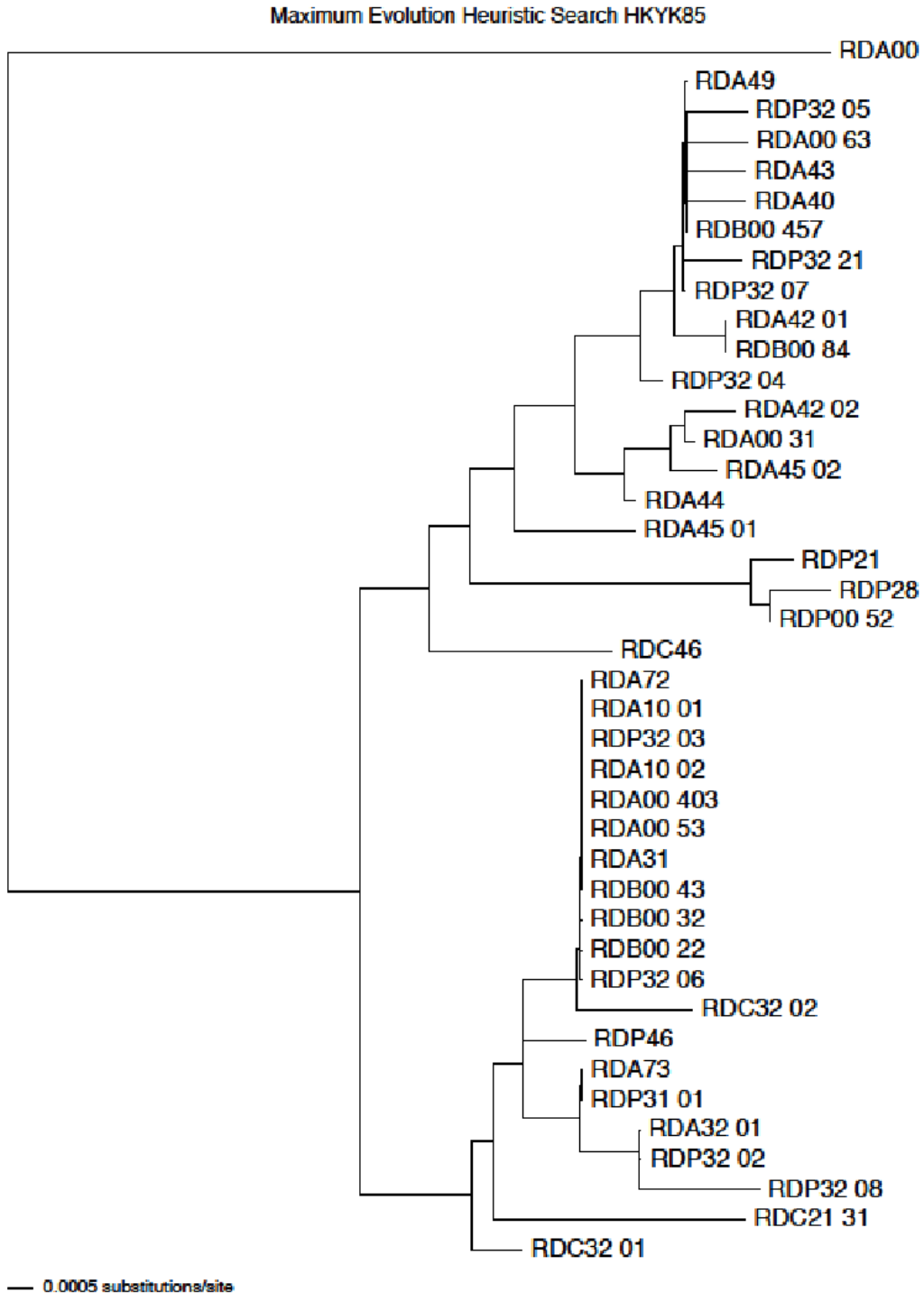

Appendix.2i. Cladogram of Minimum Evolution phylogenetic tree for *Ctenosaura similis* generated from rhodopsin sequences.

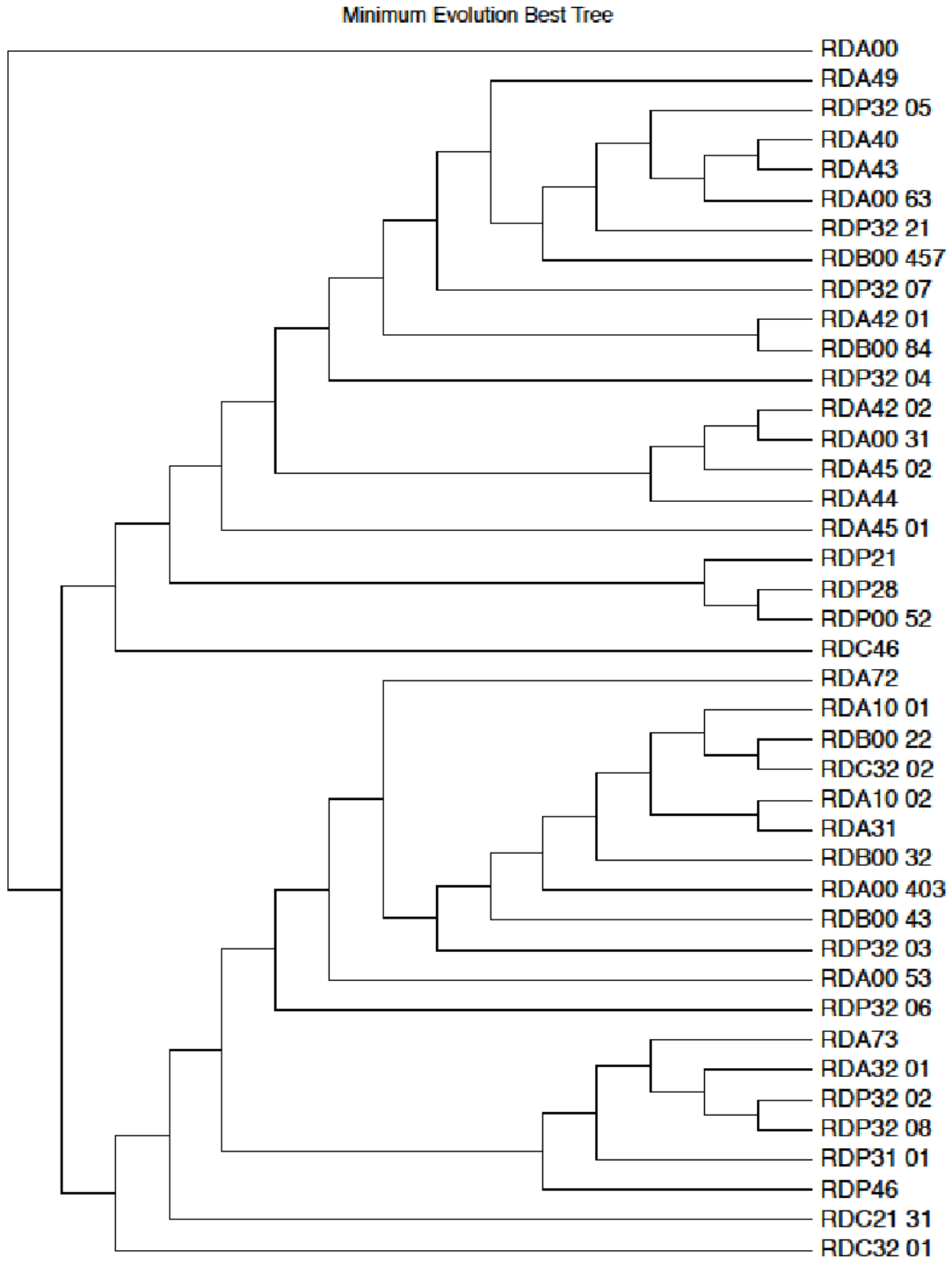

Appendix.2j. Cladogram of Minimum Evolution phylogenetic tree for *Ctenosaura similis* generated from rhodopsin sequences with strict consensus rule.

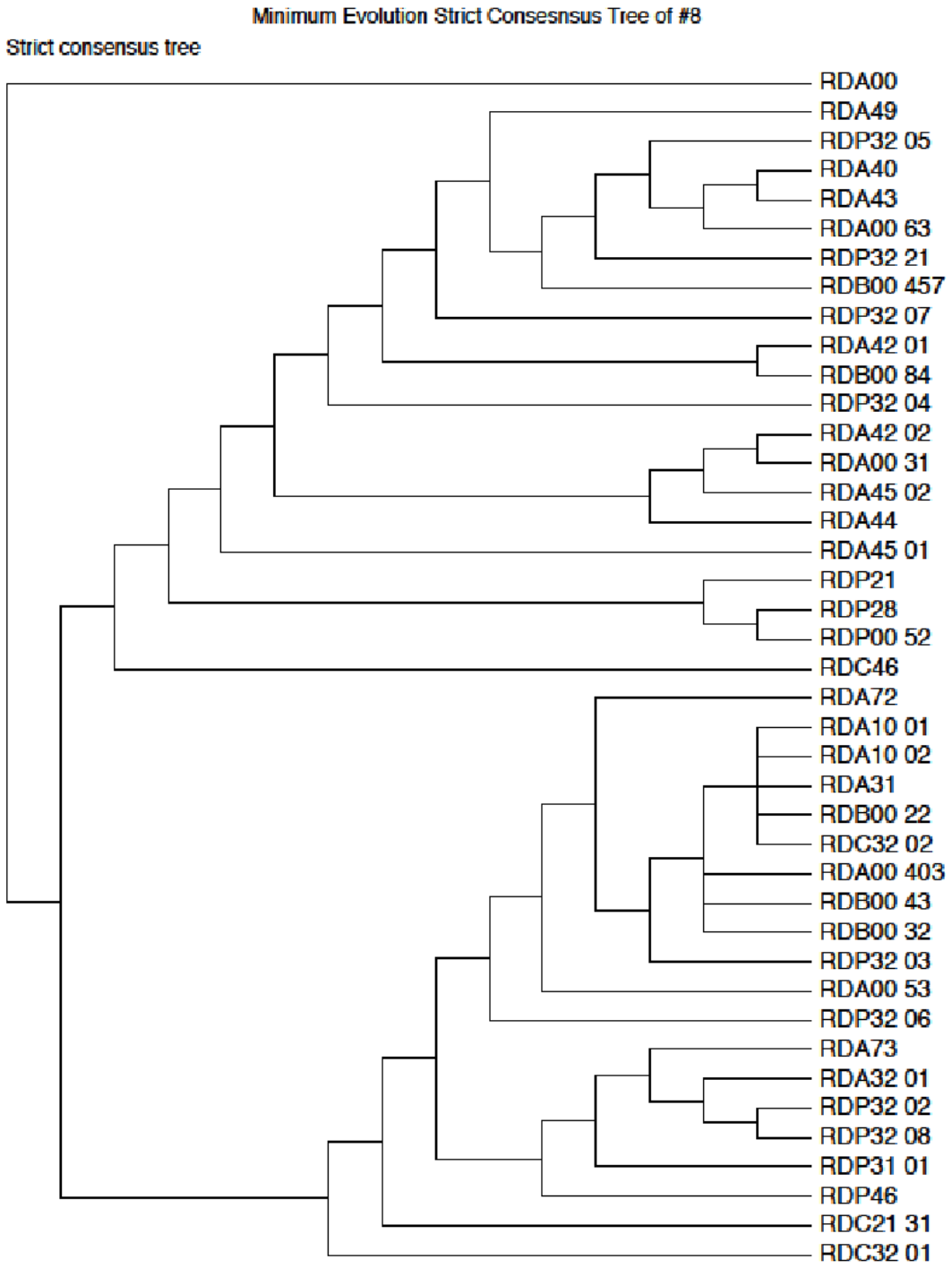

Appendix.2k. Cladogram of Minimum Evolution bootstrap tree for *Ctenosaura similis* generated from rhodopsin sequences.

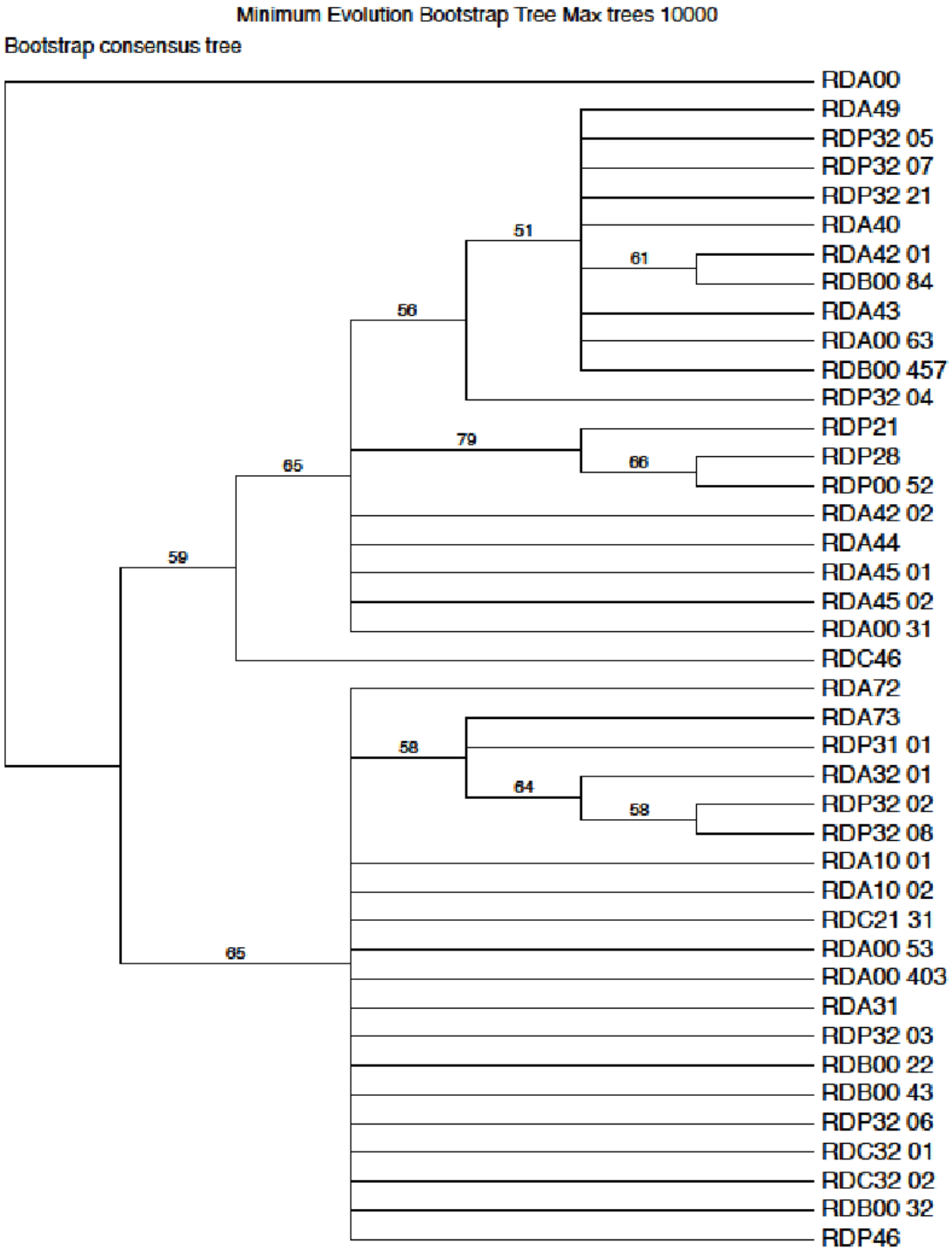

Appendix.2l. Cladogram of Maximum parsimony phylogenetic tree for *Ctenosaura similis* generated from cytochrome *b* sequences.

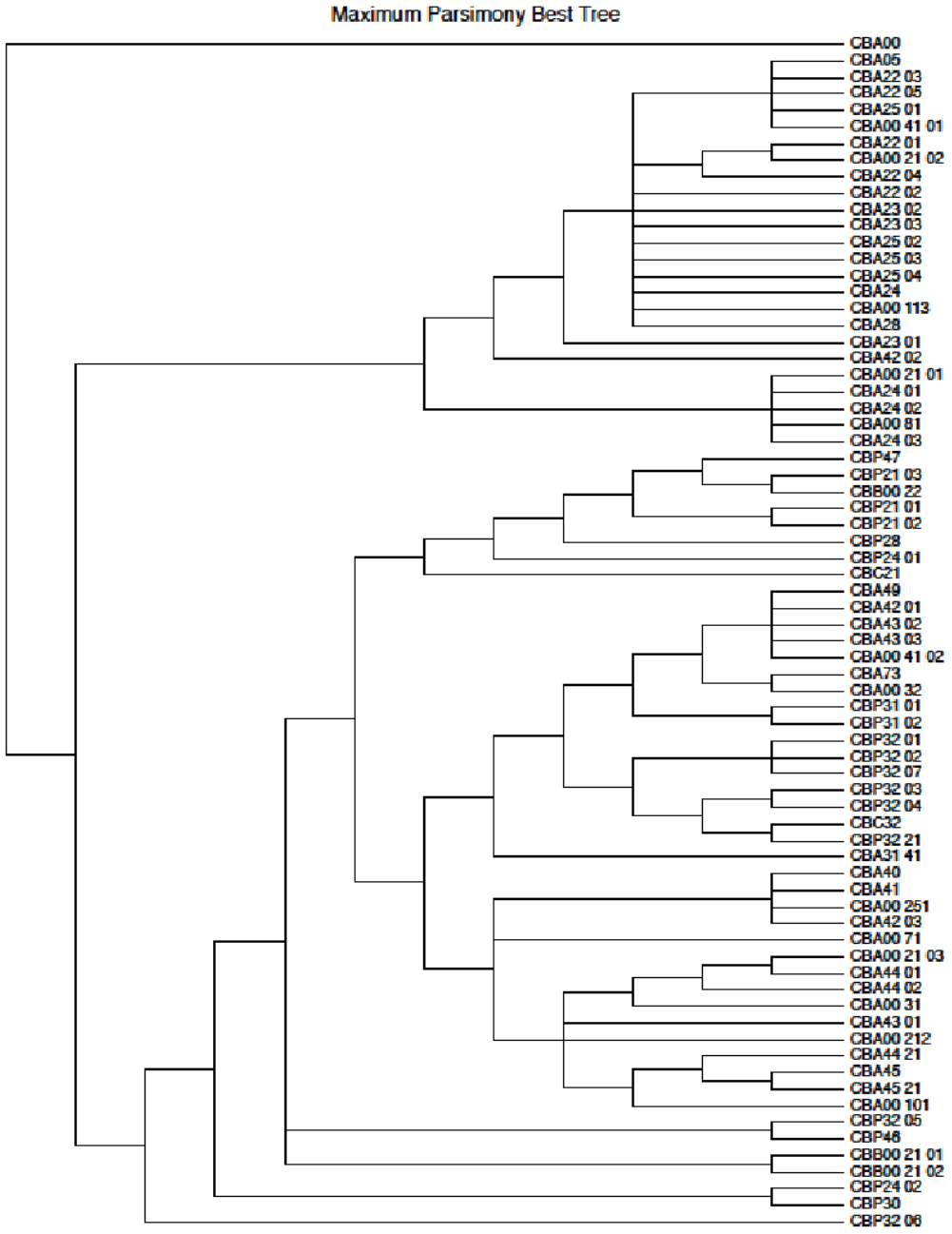

Appendix.2m. Cladogram of Maximum parsimony phylogenetic tree for *Ctenosaura similis* generated from cytochrome *b* sequences with strict consensus rule.

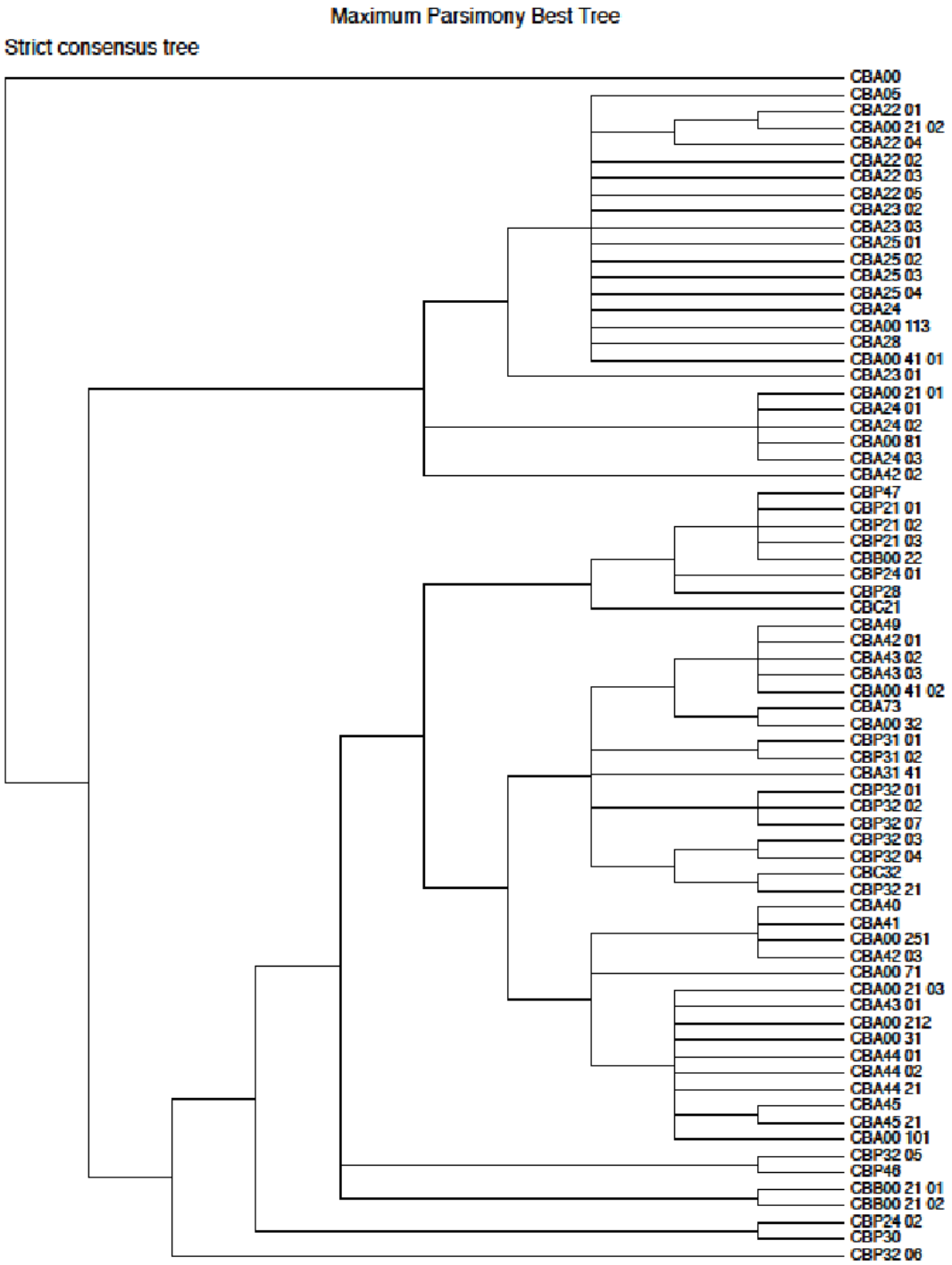

Appendix.2n. Cladogram of Maximum parsimony phylogenetic tree for *Ctenosaura similis* generated from cytochrome *b* sequences with 50% majority rule.

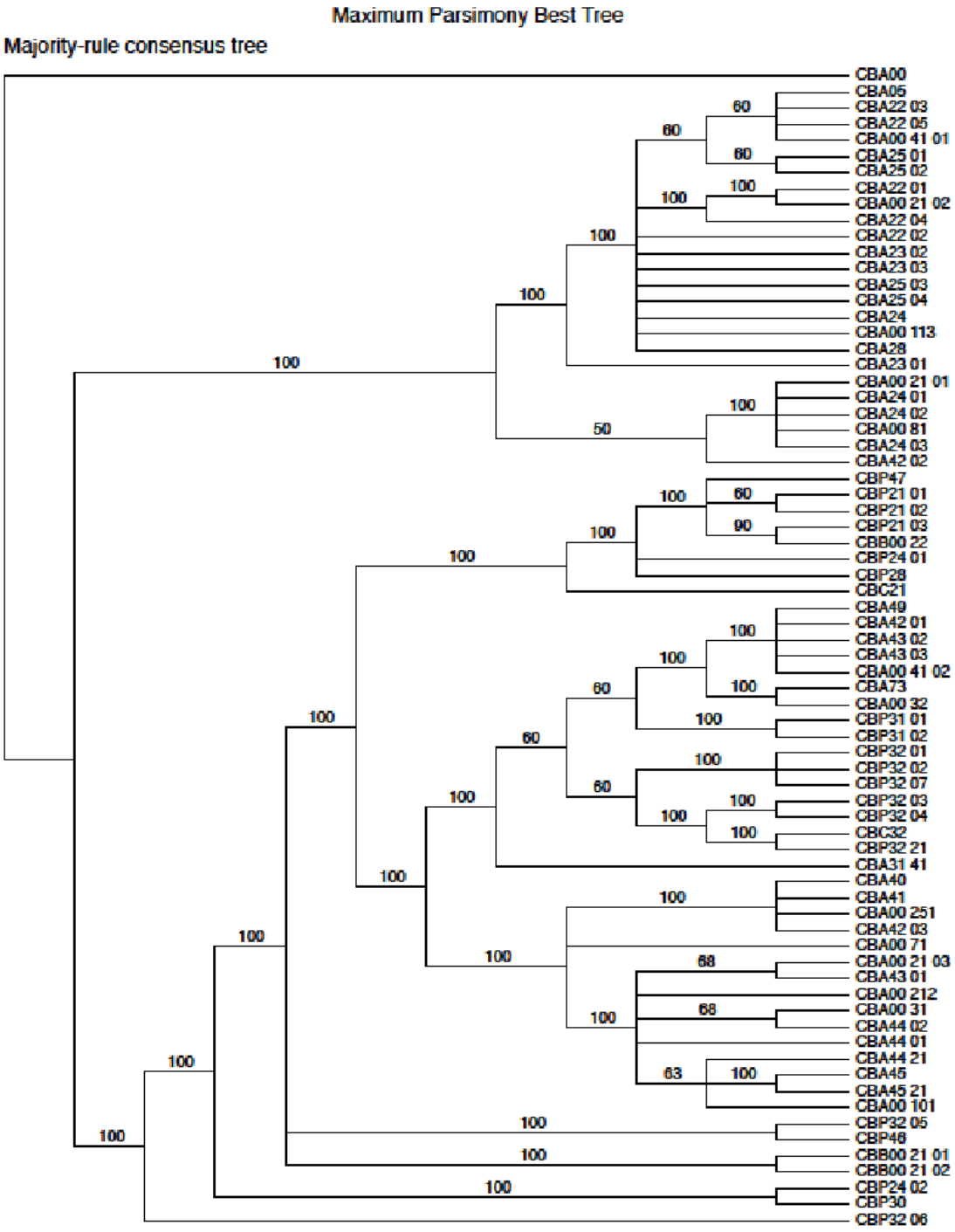

Appendix.2o. Cladogram of Maximum parsimony bootstrap tree for *Ctenosaura similis* generated

from cytochrome *b* sequences.

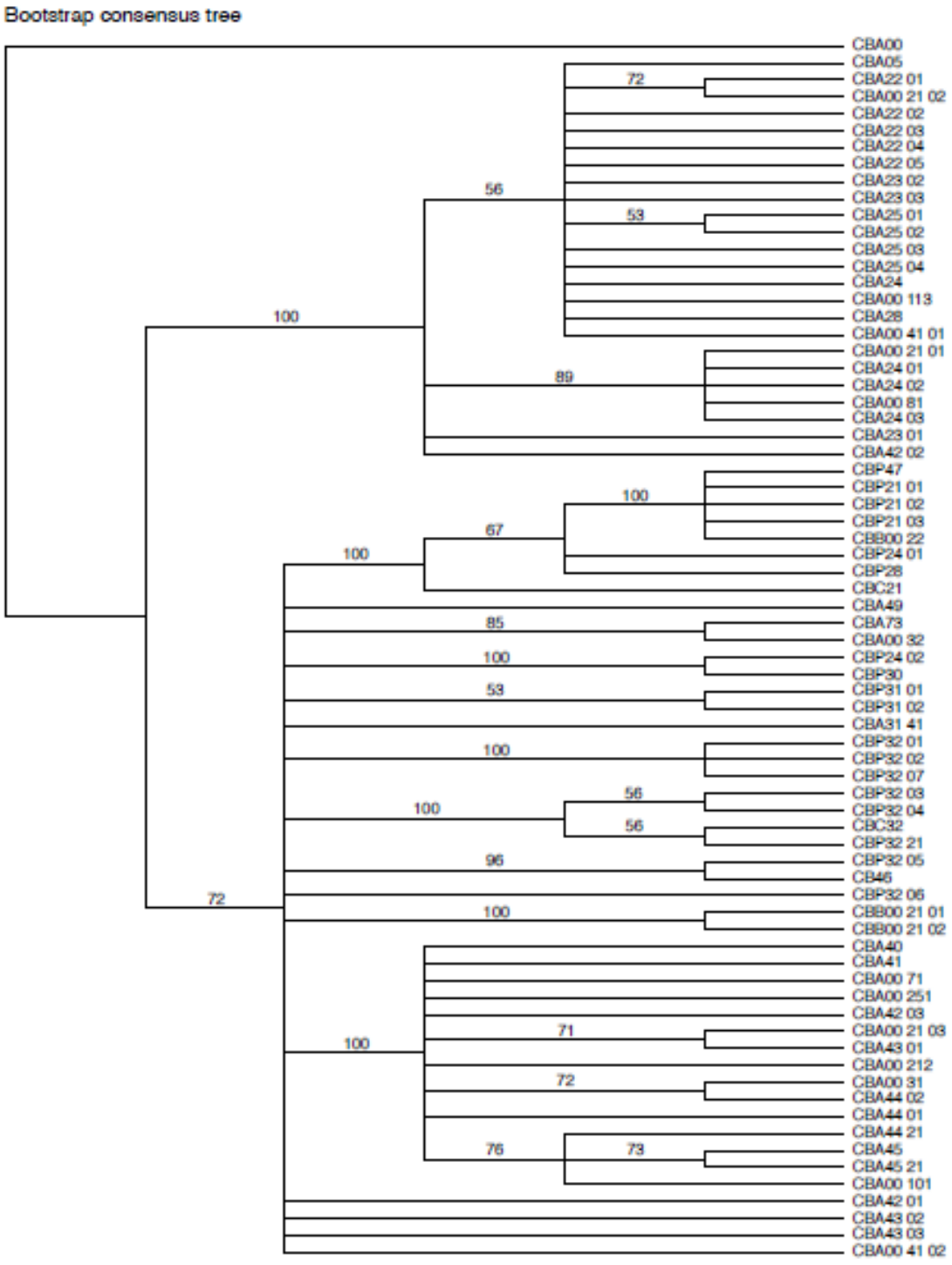

Appendix.2p. Phylogram of Maximum likelihood phylogenetic tree for *Ctenosaura similis* generated from cytochrome *b* sequences.

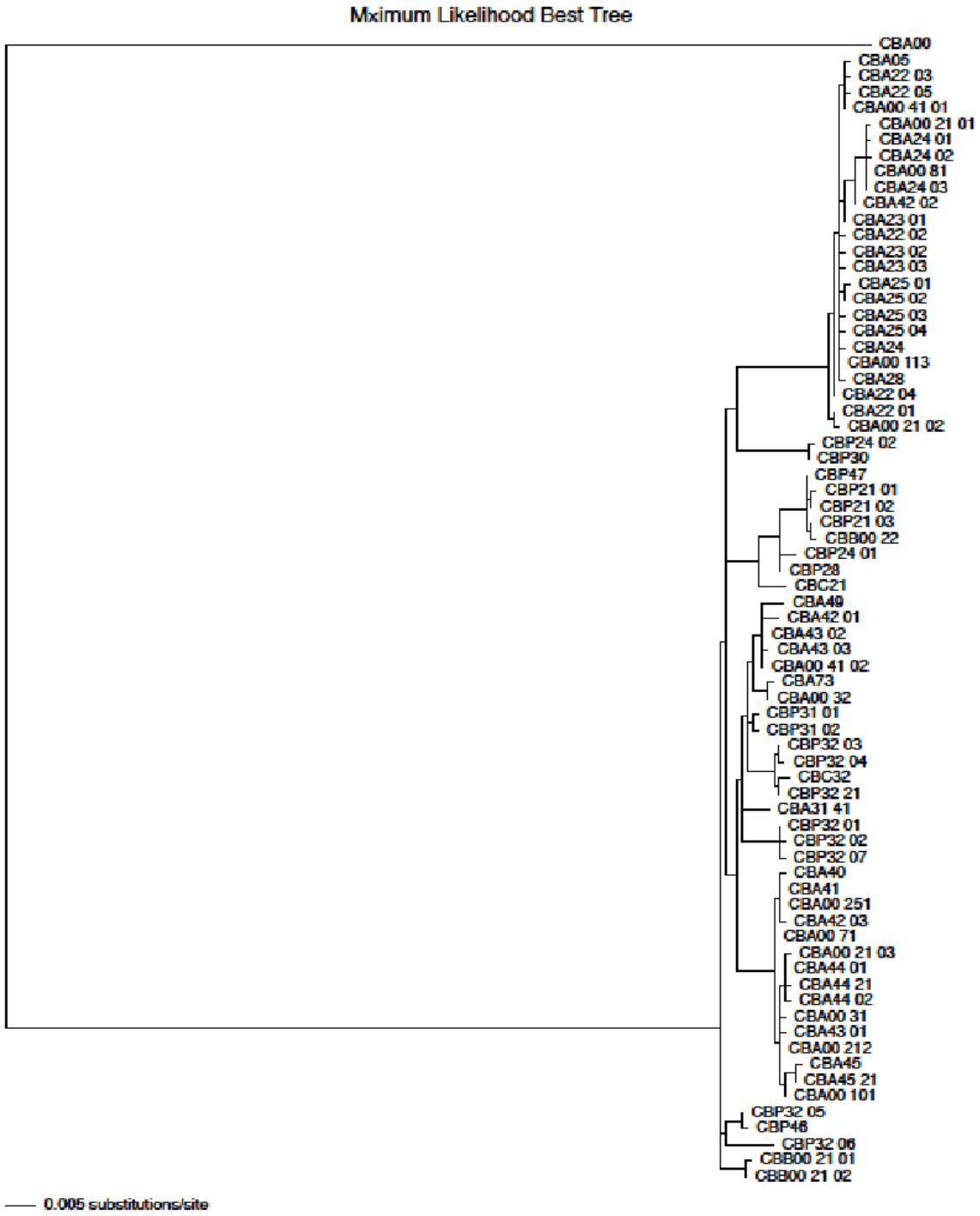

Appendix.2q. Cladogram of Maximum likelihood phylogenetic tree for *Ctenosaura similis* generated from cytochrome *b* sequences.

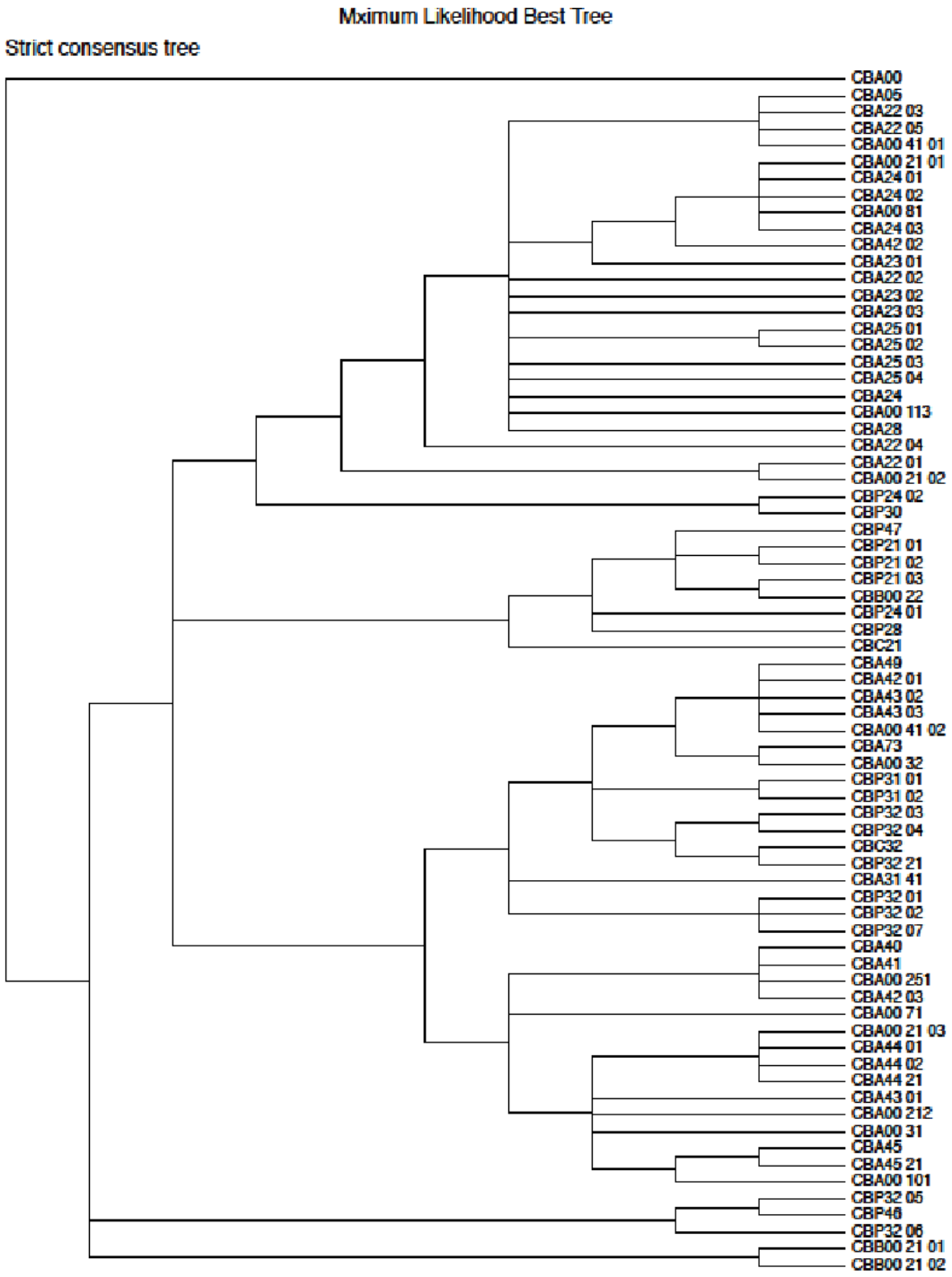

Appendix.2r. Cladogram of Maximum likelihood phylogenetic tree for *Ctenosaura similis* generated from cytochrome *b* sequences with strict consensus rule.

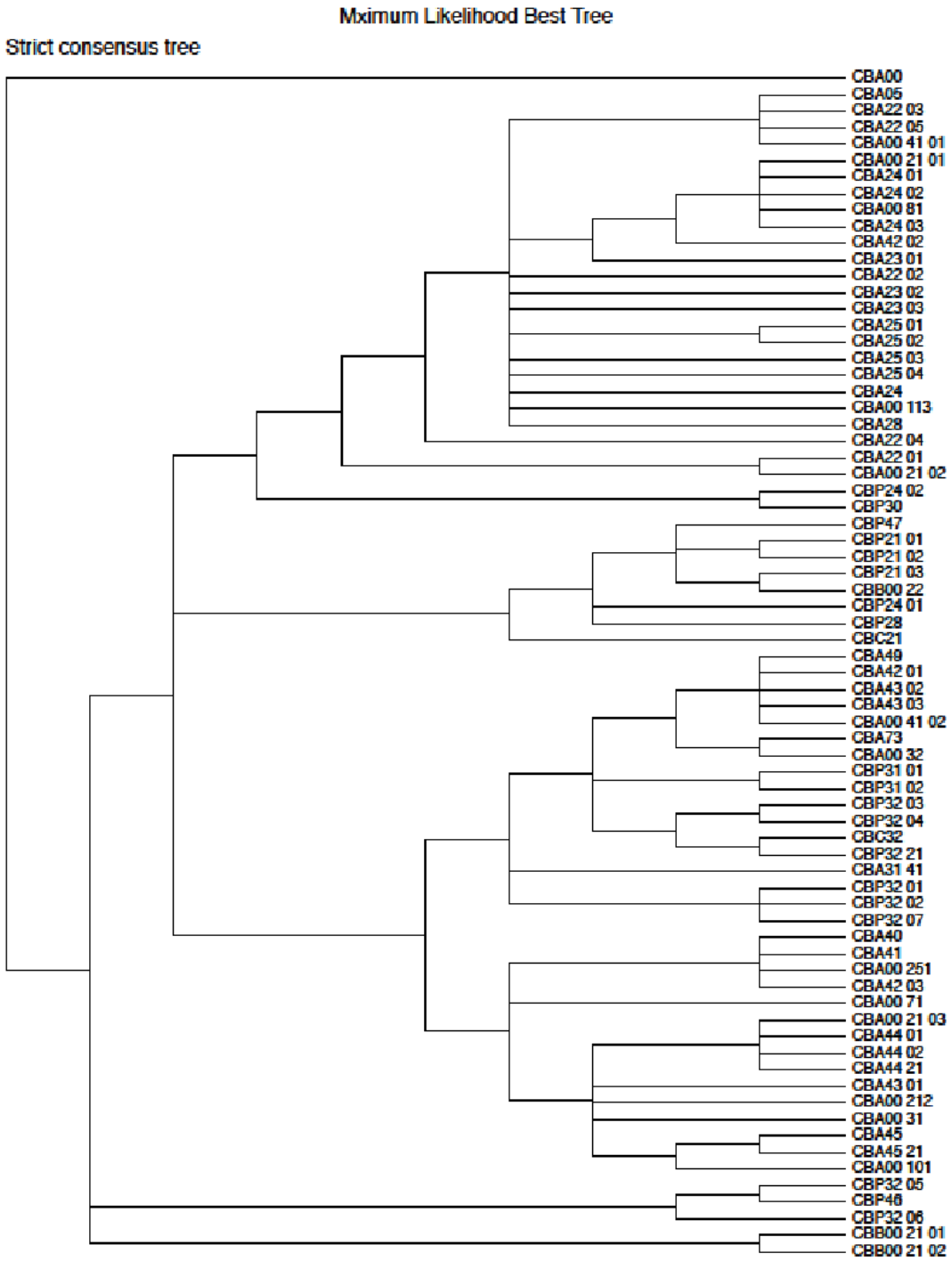

Appendix.2s. Cladogram of Maximum likelihood bootstrap tree for *Ctenosaura similis* generated from cytochrome *b* sequences.

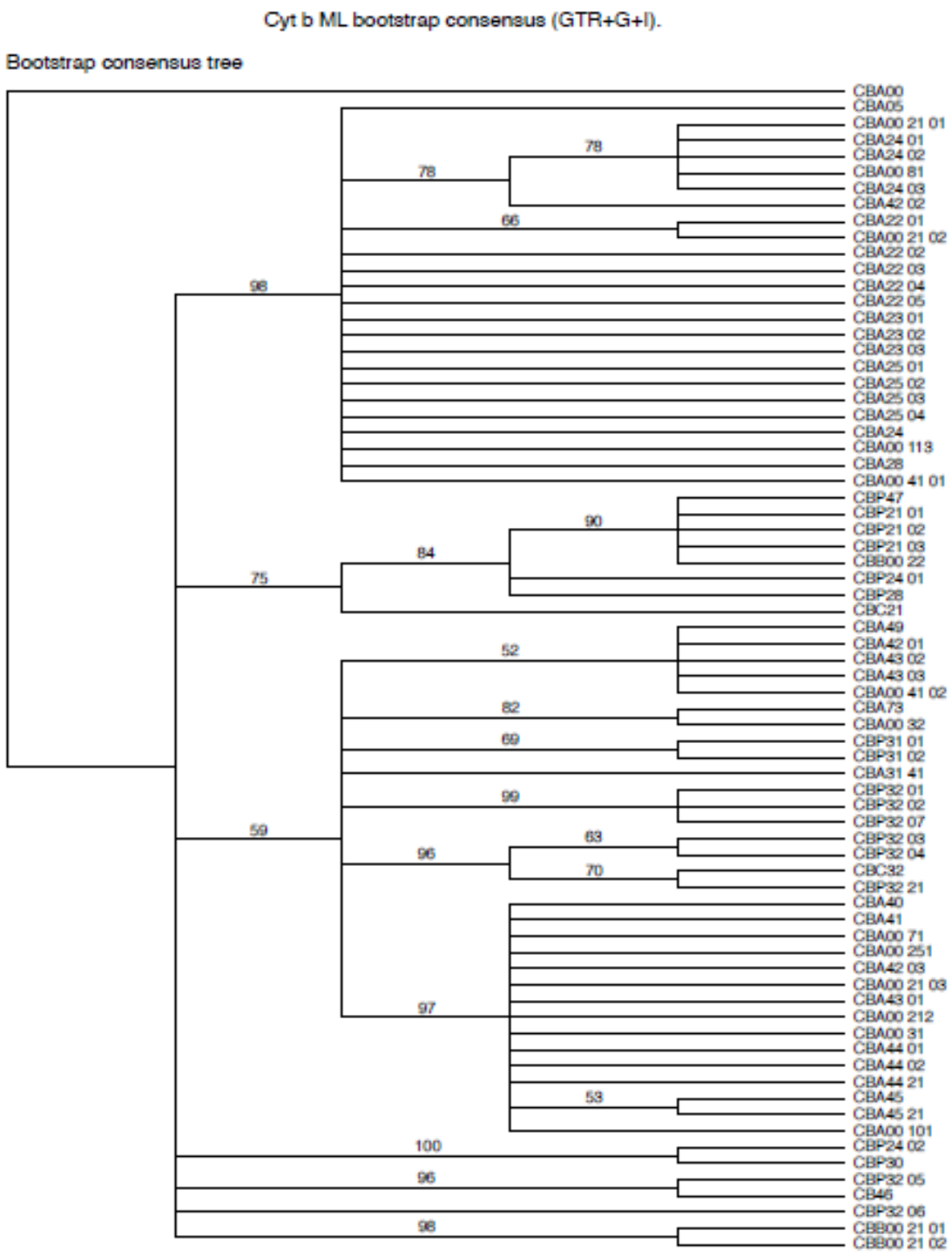

Appendix.2t. Cladogram of Minimum evolution phylogenetic tree for *Ctenosaura similis* generated from cytochrome *b* sequences with strict consensus rule.

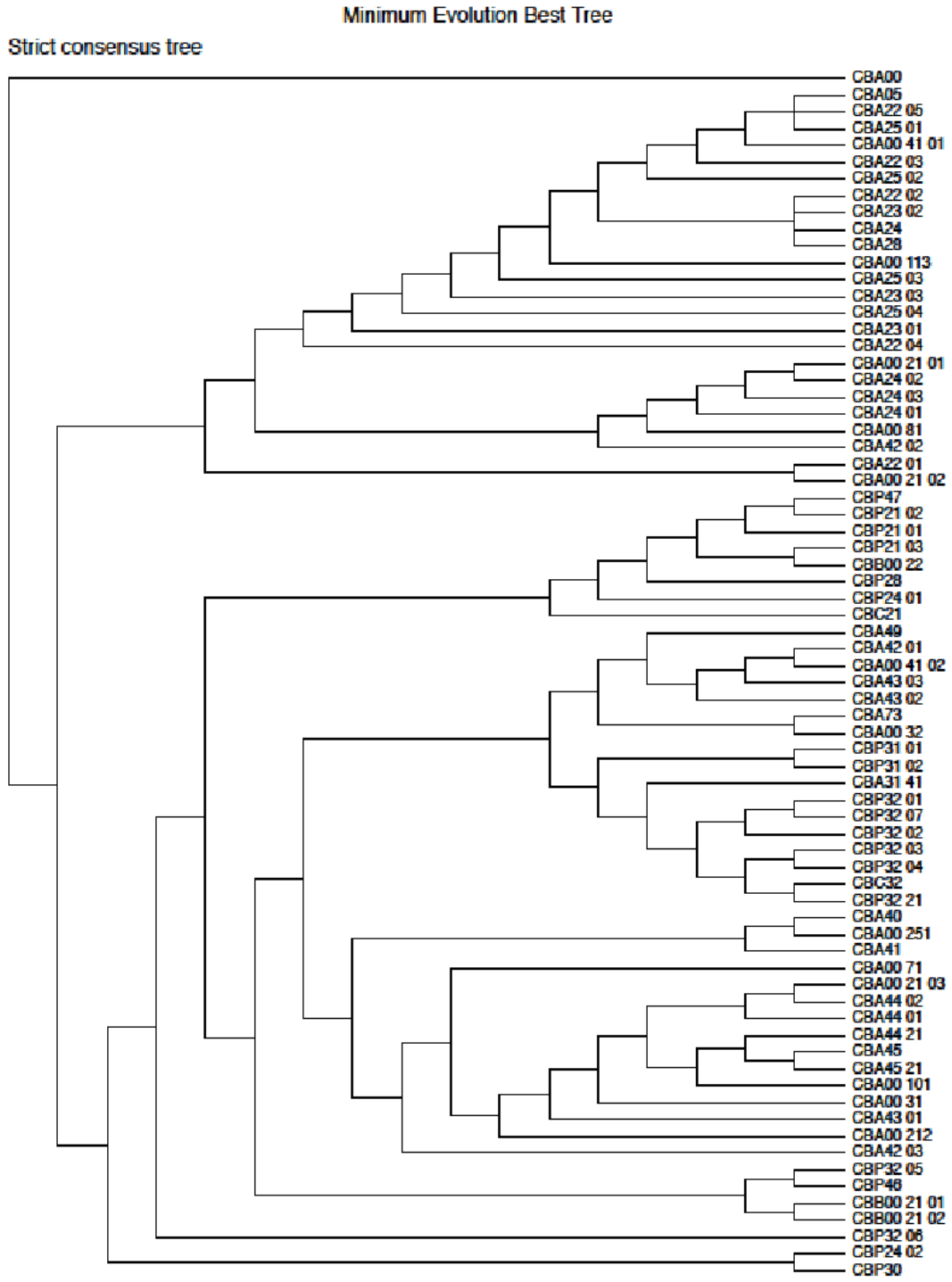

Appendix.2u. Cladogram of Minimum evolution bootstrap tree for *Ctenosaura similis* generated from cytochrome *b* sequences.

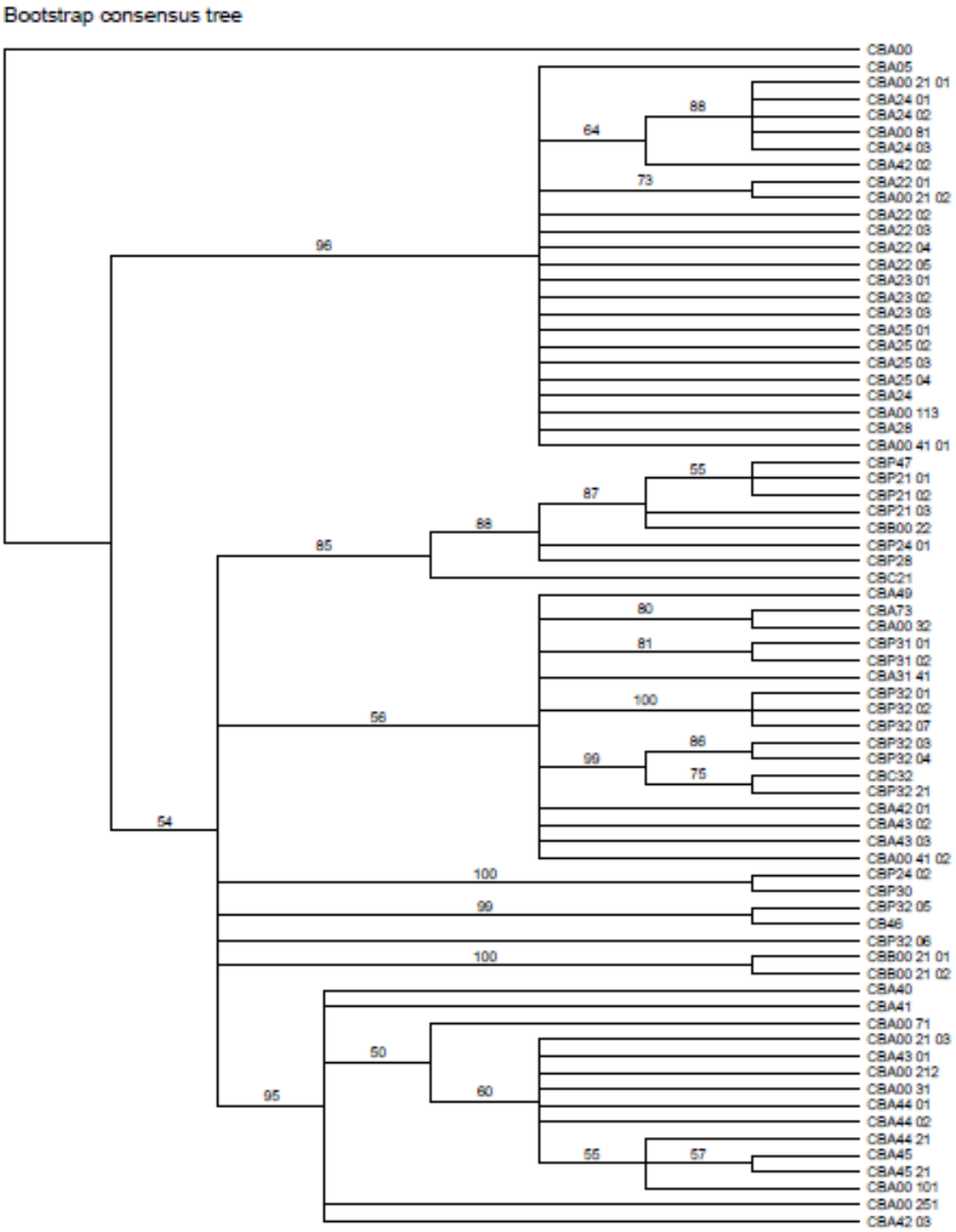

Appendix.3a. Pairwise nucleotide divergence matrix estimated according to HKY85 model (Hasegawa, Kishino and Yano 1985) based on 878 base pairs of the rhodopsin locus for 1 sequence of *Ctenosaura melanosterna* and 40 haplotype sequence of *Ctenosaura similis*

	RDA00	RDA49	RDA72	RDA73	RDA10 01	RDA10 02	RDC21 31	RDP21	RDA00 53	RDP28	RDP00 52	RDA00 403	RDP31 01	RDA31	RDA32 01	RDP32 02	RDP32 03	RDP32 04	RDB00 22	RDP32 05	RDB00 43
RDA00																					
RDA49	0.0353																				
RDA72	0.0329	0.0113																			
RDA73	0.0328	0.0113	0.0024																		
RDA10 01	0.0328	0.0113	0	0.0024																	
RDA10 02	0.0328	0.0113	0	0.0024	0																
RDC21 31	0.0378	0.0154	0.0060	0.0086	0.0060	0.0060															
RDP21	0.0431	0.0101	0.0142	0.0142	0.0142	0.0142	0.0185														
RDA00 53	0.0329	0.0113	0	0.0024	0	0	0.0060	0.0142													
RDP28	0.0431	0.0131	0.0142	0.0142	0.0142	0.0142	0.0185	0.0024	0.01424												
RDP00 52	0.0407	0.0116	0.0127	0.0127	0.0127	0.0127	0.0169	0.0012	0.01275	0.0012											
RDA00 403	0.0329	0.0113	0	0.0024	0	0	0.0060	0.0142	0	0.0142	0.0127										
RDP31 01	0.0328	0.0113	0.0024	0.0000	0.0024	0.0024	0.0085	0.0142	0.00236	0.0142	0.0127	0.0024									
RDA31	0.0328	0.0113	0	0.0024	0	0	0.0060	0.0142	0	0.0142	0.0127	0	0.0024								
RDA32 01	0.0312	0.0126	0.0035	0.0012	0.0035	0.0035	0.0098	0.0156	0.00353	0.0156	0.0141	0.0035	0.0012	0.0035							
RDP32 02	0.0312	0.0126	0.0035	0.0012	0.0035	0.0035	0.0098	0.0156	0.00353	0.0156	0.0141	0.0035	0.0012	0.0035	0						
RDP32 03	0.0329	0.0113	0	0.0024	0	0	0.0060	0.0142	0	0.0142	0.0127	0	0.0024	0	0.0035	0.0035					
RDP32 04	0.0372	0.0012	0.0101	0.0101	0.0101	0.0101	0.0141	0.0115	0.01007	0.0145	0.0130	0.0101	0.0101	0.0101	0.0114	0.0114	0.0101				
RDB00 22	0.0328	0.0113	0	0.0024	0	0	0.0060	0.0142	0	0.0142	0.0127	0	0.0024	0	0.0035	0.0035	0	0.0101			
RDP32 05	0.0371	0.0012	0.0127	0.0127	0.0127	0.0127	0.0168	0.0115	0.01271	0.0145	0.0130	0.0127	0.0127	0.0127	0.0141	0.0141	0.0127	0.0024	0.0127		
RDB00 43	0.0329	0.0113	0	0.0024	0	0	0.0060	0.0142	0	0.0142	0.0127	0	0.0024	0	0.0036	0.0036	0	0.0101	0	0.0127	
RDP32 06	0.0328	0.0113	0	0.0024	0	0	0.0060	0.0142	0	0.0142	0.0127	0	0.0024	0	0.0035	0.0035	0	0.0101	0	0.0127	0
RDP32 07	0.0353	0	0.0112	0.0113	0.0112	0.0112	0.0153	0.0101	0.01117	0.0131	0.0116	0.0112	0.0113	0.0112	0.0125	0.0125	0.0112	0.0012	0.0112	0.0012	0.0112
RDP32 21	0.0337	0.0012	0.0128	0.0127	0.0127	0.0127	0.0169	0.0115	0.01275	0.0145	0.0130	0.0128	0.0127	0.0127	0.0141	0.0141	0.0128	0.0024	0.0127	0.0024	0.0128
RDC32 01	0.0315	0.0101	0.0036	0.0024	0.0036	0.0036	0.0073	0.0129	0.00358	0.0129	0.0115	0.0036	0.0024	0.0036	0.0036	0.0036	0.0036	0.0088	0.0036	0.0114	0.0036
RDC32 02	0.0369	0.0142	0.0024	0.0036	0.0024	0.0024	0.0087	0.0173	0.00239	0.0173	0.0157	0.0024	0.0036	0.0024	0.0048	0.0048	0.0024	0.0129	0.0024	0.0157	0.0024
RDB00 32	0.0329	0.0113	0	0.0024	0	0	0.0060	0.0142	0	0.0142	0.0127	0	0.0024	0	0.0036	0.0036	0	0.0101	0	0.0127	0
RDP32 08	0.0345	0.0154	0.0059	0.0036	0.0059	0.0059	0.0124	0.0185	0.00596	0.0185	0.0169	0.0060	0.0036	0.0059	0.0023	0.0023	0.0059	0.0141	0.0059	0.0168	0.0060
RDA40	0.0377	0.0012	0.0129	0.0128	0.0128	0.0128	0.0170	0.0116	0.01286	0.0146	0.0131	0.0129	0.0128	0.0128	0.0142	0.0142	0.0129	0.0024	0.0128	0.0024	0.0129
RDA42 01	0.0371	0.0012	0.0127	0.0127	0.0127	0.0127	0.0168	0.0088	0.01269	0.0117	0.0102	0.0127	0.0127	0.0127	0.0140	0.0140	0.0127	0.0024	0.0127	0.0024	0.0127
RDA42 02	0.0367	0.0062	0.0126	0.0126	0.0126	0.0126	0.0167	0.0116	0.01264	0.0116	0.0101	0.0126	0.0126	0.0126	0.0140	0.0140	0.0126	0.0075	0.0126	0.0075	0.0126
RDA43	0.0372	0.0012	0.0128	0.0127	0.0127	0.0127	0.0169	0.0115	0.01275	0.0145	0.0130	0.0128	0.0127	0.0127	0.0141	0.0141	0.0128	0.0024	0.0127	0.0024	0.0128
RDA44	0.0333	0.0037	0.0100	0.0100	0.0100	0.0100	0.0140	0.0116	0.00999	0.0116	0.0101	0.0100	0.0100	0.0100	0.0113	0.0113	0.0100	0.0049	0.0100	0.0049	0.0100
RDA00 63	0.0372	0.0012	0.0127	0.0127	0.0127	0.0127	0.0169	0.0115	0.01275	0.0145	0.0130	0.0127	0.0127	0.0127	0.0141	0.0141	0.0127	0.0024	0.0127	0.0024	0.0127
RDA45 01	0.0334	0.0075	0.0100	0.0100	0.0100	0.0100	0.0140	0.0116	0.01000	0.0116	0.0101	0.0100	0.0100	0.0100	0.0113	0.0113	0.0100	0.0088	0.0100	0.0088	0.0100
RDA45 02	0.0372	0.0037	0.0127	0.0127	0.0127	0.0127	0.0169	0.0115	0.01275	0.0145	0.0130	0.0127	0.0127	0.0127	0.0141	0.0141	0.0127	0.0049	0.0127	0.0049	0.0127

RDB00 84	0.0372	0.0012	0.0128	0.0127	0.0127	0.0127	0.0169	0.0088	0.01275	0.0117	0.0102	0.0128	0.0127	0.0127	0.0141	0.0141	0.0128	0.0024	0.0127	0.0024	0.0128
RDA00 31	0.0350	0.0049	0.0113	0.0113	0.0113	0.0113	0.0153	0.0130	0.01131	0.0130	0.0115	0.0113	0.0113	0.0113	0.0126	0.0126	0.0113	0.0062	0.0113	0.0062	0.0113
RDB00 457	0.0355	0	0.0114	0.0114	0.0114	0.0114	0.0155	0.0101	0.01140	0.0131	0.0116	0.0114	0.0114	0.0114	0.0127	0.0127	0.0114	0.0012	0.0114	0.0012	0.0114
RDC46	0.0363	0.0088	0.0099	0.0099	0.0099	0.0099	0.0061	0.0142	0.00991	0.0142	0.0127	0.0099	0.0099	0.0099	0.0112	0.0112	0.0099	0.0075	0.0099	0.0101	0.0099
RDP46	0.0332	0.0114	0.0024	0.0024	0.0023	0.0023	0.0086	0.0143	0.00236	0.0144	0.0128	0.0024	0.0024	0.0023	0.0035	0.0035	0.0023	0.0101	0.0023	0.0128	0.0024

	RDP32 06	RDP32 07	RDP32 21	RDC32 01	RDC32 02	RDB00 32	RDP32 08	RDA40	RDA42 01	RDA42 02	RDA43	RDA44	RDA00 63	RDA45 01	RDA45 02	RDB00 84	RDA00 31	RDB00 457	RDC46	RDP46	
RDP28																					
RDP00 52																					
RDA00 403																					
RDP31 01																					
RDA31																					
RDA32 01																					
RDP32 02																					
RDP32 03																					
RDP32 04																					
RDB00 22																					
RDP32 05																					
RDB00 43																					
RDP32 06																					
RDP32 07	0.0112																				
RDP32 21	0.0127	0.0012																			
RDC32 01	0.0036	0.0100	0.0115																		
RDC32 02	0.0024	0.0141	0.0157	0.0036																	
RDB00 32	0.0000	0.0113	0.0128	0.0036	0.0024																
RDP32 08	0.0059	0.0152	0.0169	0.0060	0.0074	0.0060															
RDA40	0.0128	0.0012	0.0024	0.0116	0.0159	0.0129	0.0170														
RDA42 01	0.0127	0.0012	0.0024	0.0114	0.0157	0.0127	0.0168	0.0024													
RDA42 02	0.0126	0.0062	0.0075	0.0114	0.0156	0.0126	0.0167	0.0076	0.0049												
RDA43	0.0127	0.0012	0.0024	0.0115	0.0157	0.0128	0.0169	0.0024	0.0024	0.0075											
RDA44	0.0100	0.0037	0.0049	0.0087	0.0128	0.0100	0.0140	0.0050	0.0049	0.0024	0.0049										
RDA00 63	0.0127	0.0012	0.0024	0.0115	0.0157	0.0127	0.0169	0.0024	0.0024	0.0075	0.0024	0.0049									
RDA45 01	0.0100	0.0075	0.0088	0.0088	0.0129	0.0100	0.0140	0.0089	0.0062	0.0012	0.0088	0.0036	0.0088								
RDA45 02	0.0127	0.0037	0.0049	0.0115	0.0157	0.0127	0.0169	0.0049	0.0049	0.0024	0.0049	0.0024	0.0049	0.0036							
RDB00 84	0.0127	0.0012	0.0024	0.0115	0.0157	0.0128	0.0169	0.0024	0.0000	0.0049	0.0024	0.0049	0.0024	0.0062	0.0049						
RDA00 31	0.0113	0.0049	0.0062	0.0101	0.0142	0.0113	0.0153	0.0063	0.0062	0.0012	0.0062	0.0012	0.0062	0.0024	0.0012	0.0062					
RDB00 457	0.0114	0.0000	0.0012	0.0101	0.0143	0.0114	0.0155	0.0012	0.0012	0.0062	0.0012	0.0037	0.0012	0.0075	0.0037	0.0012	0.0049				
RDC46	0.0099	0.0088	0.0101	0.0087	0.0127	0.0099	0.0139	0.0102	0.0101	0.0100	0.0101	0.0074	0.0101	0.0100	0.0101	0.0101	0.0087	0.0088			
RDP46	0.0023	0.0112	0.0128	0.0036	0.0049	0.0024	0.0060	0.0130	0.0128	0.0127	0.0128	0.0101	0.0128	0.0101	0.0128	0.0128	0.0114	0.0115	0.0100		

Appendix.3b. Pairwise nucleotide divergence matrix estimated according to Generalized time-reversible (GTR) model (Tavaré, 1986) based on 1140 base pairs of the cytochrome b locus for 1 sequence of *Ctenosaura melanosterna* and 71 haplotype sequence of *Ctenosaura similis*

	CBA00	CBA05	CBP47	CBA49	CBA73	CBA00 2101	CBC21	CBP21 01	CBP21 02	CBP21 03	CBA22 01	CBA22 02	CBA22 03	CBA22 04	CBA22 05	CBA23 01	CBB00 22	CBA23 02	CBA23 03	CBP24 01	CBP24 02	CBA24 01	CBA24 02	CBA00 81
CBA00																								
CBA05	0.3129																							
CBP47	0.3014	0.0360																						
CBA49	0.2890	0.0278	0.0214																					
CBA73	0.2989	0.0257	0.0213	0.0072																				
CBA00 21 01	0.3077	0.0072	0.0359	0.0278	0.0278																			
CBC21	0.3069	0.0314	0.0129	0.0192	0.0172	0.0335																		
CBP21 01	0.3048	0.0360	0.0017	0.0214	0.0214	0.0359	0.0130																	
CBP21 02	0.3040	0.0371	0.0009	0.0224	0.0224	0.0370	0.0139	0.0009																
CBP21 03	0.2958	0.0347	0.0009	0.0203	0.0202	0.0346	0.0119	0.0026	0.0017															
CBA22 01	0.3057	0.0045	0.0324	0.0245	0.0224	0.0081	0.0279	0.0324	0.0335	0.0311														
CBA22 02	0.3111	0.0027	0.0347	0.0266	0.0245	0.0063	0.0301	0.0347	0.0358	0.0334	0.0035													
CBA22 03	0.3094	0.0018	0.0335	0.0277	0.0255	0.0072	0.0312	0.0336	0.0347	0.0323	0.0044	0.0026												
CBA22 04	0.3057	0.0027	0.0324	0.0245	0.0224	0.0063	0.0279	0.0324	0.0335	0.0311	0.0018	0.0018	0.0026											
CBA22 05	0.3094	0.0018	0.0358	0.0277	0.0255	0.0072	0.0312	0.0358	0.0369	0.0345	0.0044	0.0026	0.0018	0.0026										
CBA23 01	0.3055	0.0027	0.0324	0.0245	0.0244	0.0045	0.0301	0.0324	0.0335	0.0311	0.0035	0.0018	0.0026	0.0018	0.0026									
CBB00 22	0.2980	0.0358	0.0017	0.0213	0.0212	0.0357	0.0129	0.0035	0.0026	0.0009	0.0322	0.0345	0.0334	0.0322	0.0356	0.0322								
CBA23 02	0.3111	0.0027	0.0347	0.0266	0.0245	0.0063	0.0301	0.0347	0.0358	0.0334	0.0035	0.0018	0.0026	0.0018	0.0026	0.0018	0.0345							
CBA23 03	0.3049	0.0027	0.0347	0.0267	0.0245	0.0063	0.0301	0.0347	0.0358	0.0334	0.0035	0.0018	0.0026	0.0018	0.0026	0.0018	0.0345	0.0018						
CBP24 01	0.3033	0.0315	0.0071	0.0215	0.0194	0.0337	0.0092	0.0071	0.0080	0.0081	0.0281	0.0303	0.0292	0.0281	0.0314	0.0302	0.0090	0.0303	0.0280					
CBP24 02	0.3048	0.0319	0.0244	0.0211	0.0191	0.0319	0.0244	0.0245	0.0255	0.0233	0.0285	0.0307	0.0318	0.0285	0.0318	0.0285	0.0243	0.0307	0.0307	0.0267				
CBA24 01	0.3022	0.0072	0.0360	0.0278	0.0278	0.0018	0.0336	0.0360	0.0371	0.0347	0.0082	0.0063	0.0072	0.0063	0.0072	0.0045	0.0358	0.0063	0.0063	0.0338	0.0319			
CBA24 02	0.3023	0.0072	0.0360	0.0279	0.0278	0.0018	0.0336	0.0360	0.0371	0.0347	0.0082	0.0063	0.0072	0.0063	0.0072	0.0045	0.0358	0.0063	0.0063	0.0338	0.0319	0.0018		
CBA00 81	0.3054	0.0063	0.0348	0.0267	0.0267	0.0009	0.0324	0.0348	0.0359	0.0335	0.0072	0.0054	0.0063	0.0054	0.0063	0.0036	0.0346	0.0054	0.0054	0.0326	0.0308	0.0009	0.0009	
CBA24 03	0.3055	0.0063	0.0348	0.0268	0.0267	0.0009	0.0325	0.0348	0.0359	0.0335	0.0072	0.0054	0.0063	0.0054	0.0063	0.0036	0.0346	0.0054	0.0054	0.0326	0.0308	0.0009	0.0009	0.0000
CBA25 01	0.3102	0.0018	0.0358	0.0278	0.0256	0.0072	0.0313	0.0359	0.0370	0.0346	0.0045	0.0027	0.0018	0.0026	0.0018	0.0026	0.0357	0.0027	0.0027	0.0314	0.0318	0.0072	0.0072	0.0063
CBA25 02	0.3111	0.0027	0.0347	0.0266	0.0245	0.0063	0.0301	0.0347	0.0358	0.0334	0.0035	0.0018	0.0026	0.0018	0.0026	0.0018	0.0345	0.0018	0.0018	0.0303	0.0307	0.0063	0.0063	0.0054
CBA25 03	0.3112	0.0027	0.0347	0.0267	0.0245	0.0063	0.0301	0.0347	0.0358	0.0334	0.0035	0.0018	0.0026	0.0018	0.0026	0.0018	0.0345	0.0018	0.0018	0.0303	0.0285	0.0063	0.0063	0.0054
CBA25 04	0.3049	0.0027	0.0347	0.0267	0.0245	0.0063	0.0301	0.0347	0.0358	0.0334	0.0035	0.0018	0.0026	0.0018	0.0026	0.0018	0.0345	0.0018	0.0018	0.0303	0.0285	0.0063	0.0063	0.0054
CBA24	0.3103	0.0027	0.0346	0.0266	0.0244	0.0063	0.0301	0.0346	0.0357	0.0333	0.0035	0.0018	0.0026	0.0018	0.0026	0.0018	0.0344	0.0018	0.0018	0.0302	0.0306	0.0063	0.0063	0.0054
CBA00 113	0.3080	0.0018	0.0335	0.0255	0.0234	0.0054	0.0290	0.0335	0.0346	0.0322	0.0026	0.0009	0.0018	0.0009	0.0018	0.0009	0.0333	0.0009	0.0009	0.0291	0.0296	0.0054	0.0054	0.0045
CBP28	0.3006	0.0326	0.0044	0.0183	0.0183	0.0326	0.0082	0.0044	0.0053	0.0053	0.0291	0.0314	0.0303	0.0291	0.0325	0.0291	0.0062	0.0314	0.0314	0.0026	0.0234	0.0326	0.0326	0.0315
CBA28	0.3103	0.0027	0.0346	0.0266	0.0244	0.0063	0.0301	0.0346	0.0357	0.0333	0.0035	0.0018	0.0026	0.0018	0.0026	0.0018	0.0344	0.0018	0.0018	0.0302	0.0306	0.0063	0.0063	0.0054
CBA00 21 02	0.3083	0.0054	0.0335	0.0256	0.0234	0.0091	0.0290	0.0336	0.0347	0.0323	0.0009	0.0044	0.0054	0.0027	0.0054	0.0044	0.0333	0.0044	0.0044	0.0292	0.0296	0.0091	0.0091	0.0082
CBP30	0.3017	0.0308	0.0234	0.0201	0.0180	0.0307	0.0233	0.0234	0.0244	0.0222	0.0274	0.0296	0.0306	0.0274	0.0306	0.0274	0.0232	0.0296	0.0296	0.0256	0.0009	0.0308	0.0308	0.0297

CBA00 41 01	0.3071	0.0009	0.0347	0.0267	0.0245	0.0063	0.0301	0.0347	0.0358	0.0334	0.0035	0.0018	0.0009	0.0018	0.0009	0.0018	0.0345	0.0018	0.0018	0.0303	0.0307	0.0063	0.0063	0.0054
CBP31 01	0.2967	0.0244	0.0202	0.0081	0.0063	0.0244	0.0161	0.0202	0.0213	0.0191	0.0212	0.0233	0.0243	0.0212	0.0243	0.0212	0.0201	0.0233	0.0233	0.0183	0.0189	0.0244	0.0244	0.0233
CBP31 02	0.2967	0.0244	0.0202	0.0081	0.0063	0.0244	0.0161	0.0202	0.0213	0.0191	0.0212	0.0233	0.0243	0.0212	0.0243	0.0212	0.0201	0.0233	0.0233	0.0183	0.0189	0.0244	0.0244	0.0233
CBA31 41	0.3218	0.0291	0.0226	0.0121	0.0101	0.0291	0.0184	0.0226	0.0236	0.0214	0.0258	0.0279	0.0290	0.0258	0.0290	0.0257	0.0225	0.0279	0.0279	0.0206	0.0212	0.0291	0.0292	0.0280
CBP32 01	0.3045	0.0310	0.0223	0.0139	0.0119	0.0309	0.0181	0.0202	0.0212	0.0211	0.0254	0.0298	0.0308	0.0276	0.0308	0.0276	0.0222	0.0298	0.0298	0.0203	0.0230	0.0310	0.0310	0.0299
CBP32 02	0.3036	0.0299	0.0233	0.0148	0.0129	0.0321	0.0192	0.0213	0.0223	0.0222	0.0265	0.0309	0.0297	0.0287	0.0297	0.0287	0.0232	0.0309	0.0309	0.0214	0.0241	0.0321	0.0322	0.0310
CBP32 03	0.3113	0.0289	0.0245	0.0119	0.0100	0.0288	0.0203	0.0224	0.0235	0.0233	0.0255	0.0277	0.0288	0.0255	0.0288	0.0255	0.0244	0.0277	0.0277	0.0225	0.0231	0.0289	0.0289	0.0278
CBP32 04	0.3136	0.0300	0.0255	0.0129	0.0110	0.0299	0.0213	0.0235	0.0245	0.0244	0.0266	0.0288	0.0298	0.0266	0.0298	0.0266	0.0254	0.0288	0.0288	0.0236	0.0241	0.0300	0.0300	0.0288
CBP32 05	0.3002	0.0265	0.0192	0.0130	0.0121	0.0243	0.0151	0.0192	0.0202	0.0181	0.0232	0.0253	0.0264	0.0232	0.0264	0.0232	0.0191	0.0253	0.0253	0.0173	0.0181	0.0244	0.0244	0.0233
CBP32 06	0.2885	0.0287	0.0234	0.0170	0.0160	0.0265	0.0213	0.0234	0.0245	0.0223	0.0254	0.0275	0.0286	0.0254	0.0286	0.0254	0.0233	0.0275	0.0275	0.0235	0.0211	0.0265	0.0265	0.0254
CBP32 07	0.3076	0.0321	0.0233	0.0148	0.0129	0.0321	0.0192	0.0213	0.0223	0.0222	0.0265	0.0309	0.0320	0.0287	0.0320	0.0287	0.0232	0.0309	0.0309	0.0214	0.0241	0.0321	0.0321	0.0310
CBC32	0.3210	0.0311	0.0266	0.0138	0.0100	0.0332	0.0203	0.0245	0.0256	0.0254	0.0277	0.0298	0.0309	0.0277	0.0309	0.0298	0.0265	0.0298	0.0299	0.0225	0.0251	0.0333	0.0333	0.0321
CBP32 21	0.3159	0.0310	0.0245	0.0119	0.0100	0.0310	0.0202	0.0224	0.0234	0.0233	0.0276	0.0298	0.0309	0.0276	0.0309	0.0276	0.0244	0.0298	0.0298	0.0225	0.0230	0.0310	0.0311	0.0299
CBB00 21 01	0.2975	0.0289	0.0214	0.0151	0.0141	0.0288	0.0173	0.0215	0.0225	0.0203	0.0255	0.0276	0.0287	0.0255	0.0287	0.0255	0.0213	0.0276	0.0277	0.0195	0.0212	0.0289	0.0289	0.0277
CBB00 21 02	0.2945	0.0277	0.0204	0.0141	0.0131	0.0277	0.0162	0.0204	0.0214	0.0193	0.0244	0.0265	0.0276	0.0244	0.0276	0.0244	0.0203	0.0265	0.0265	0.0184	0.0202	0.0277	0.0277	0.0266
CBA40	0.3128	0.0280	0.0227	0.0130	0.0130	0.0280	0.0183	0.0227	0.0238	0.0216	0.0246	0.0268	0.0279	0.0246	0.0279	0.0246	0.0226	0.0268	0.0268	0.0228	0.0213	0.0280	0.0280	0.0269
CBA41	0.3013	0.0268	0.0216	0.0120	0.0120	0.0268	0.0172	0.0216	0.0226	0.0205	0.0235	0.0256	0.0267	0.0235	0.0267	0.0235	0.0215	0.0256	0.0256	0.0217	0.0201	0.0268	0.0268	0.0257
CBA42 01	0.2928	0.0288	0.0223	0.0062	0.0062	0.0288	0.0202	0.0203	0.0213	0.0212	0.0255	0.0276	0.0287	0.0255	0.0287	0.0254	0.0222	0.0276	0.0276	0.0225	0.0201	0.0288	0.0288	0.0277
CBA00 71	0.3092	0.0279	0.0226	0.0130	0.0130	0.0278	0.0162	0.0226	0.0237	0.0215	0.0245	0.0267	0.0277	0.0245	0.0277	0.0245	0.0225	0.0267	0.0267	0.0206	0.0212	0.0279	0.0279	0.0268
CBA00 32	0.3011	0.0267	0.0224	0.0081	0.0009	0.0288	0.0162	0.0224	0.0234	0.0212	0.0234	0.0255	0.0266	0.0234	0.0266	0.0255	0.0223	0.0255	0.0255	0.0184	0.0201	0.0289	0.0289	0.0278
CBA00 251	0.3069	0.0268	0.0216	0.0120	0.0120	0.0268	0.0172	0.0216	0.0226	0.0204	0.0235	0.0256	0.0267	0.0235	0.0267	0.0235	0.0215	0.0256	0.0256	0.0217	0.0201	0.0268	0.0268	0.0257
CBA42 02	0.3049	0.0045	0.0347	0.0267	0.0266	0.0027	0.0323	0.0347	0.0358	0.0334	0.0054	0.0035	0.0044	0.0035	0.0044	0.0018	0.0345	0.0035	0.0035	0.0325	0.0307	0.0027	0.0027	0.0018
CBA42 03	0.3138	0.0281	0.0228	0.0131	0.0131	0.0281	0.0184	0.0229	0.0239	0.0217	0.0248	0.0269	0.0280	0.0248	0.0280	0.0247	0.0227	0.0269	0.0269	0.0230	0.0214	0.0281	0.0282	0.0270
CBA00 21 03	0.3189	0.0316	0.0262	0.0161	0.0161	0.0316	0.0195	0.0262	0.0273	0.0250	0.0281	0.0304	0.0315	0.0281	0.0315	0.0281	0.0261	0.0304	0.0304	0.0242	0.0246	0.0316	0.0316	0.0305
CBA43 01	0.3118	0.0302	0.0249	0.0150	0.0150	0.0302	0.0183	0.0249	0.0260	0.0237	0.0268	0.0290	0.0301	0.0268	0.0301	0.0268	0.0248	0.0290	0.0290	0.0229	0.0234	0.0302	0.0302	0.0291
CBA43 02	0.2874	0.0256	0.0193	0.0035	0.0035	0.0256	0.0161	0.0193	0.0203	0.0182	0.0223	0.0245	0.0255	0.0223	0.0255	0.0223	0.0192	0.0245	0.0245	0.0194	0.0170	0.0256	0.0256	0.0245
CBA43 03	0.2930	0.0268	0.0204	0.0044	0.0045	0.0268	0.0172	0.0204	0.0214	0.0193	0.0235	0.0256	0.0267	0.0235	0.0267	0.0235	0.0203	0.0256	0.0256	0.0205	0.0181	0.0268	0.0268	0.0257
CBA00 41 02	0.2873	0.0256	0.0193	0.0035	0.0035	0.0256	0.0172	0.0193	0.0203	0.0182	0.0223	0.0245	0.0255	0.0223	0.0255	0.0223	0.0192	0.0245	0.0245	0.0194	0.0170	0.0256	0.0256	0.0245
CBA00 212	0.3059	0.0290	0.0237	0.0140	0.0139	0.0289	0.0173	0.0237	0.0248	0.0226	0.0256	0.0278	0.0288	0.0256	0.0288	0.0256	0.0236	0.0278	0.0278	0.0217	0.0222	0.0290	0.0290	0.0279
CBA00 31	0.3091	0.0301	0.0248	0.0150	0.0149	0.0301	0.0183	0.0248	0.0259	0.0236	0.0267	0.0289	0.0300	0.0267	0.0300	0.0267	0.0247	0.0289	0.0289	0.0228	0.0233	0.0301	0.0301	0.0290
CBA44 01	0.3129	0.0304	0.0250	0.0151	0.0151	0.0303	0.0184	0.0250	0.0261	0.0238	0.0269	0.0291	0.0302	0.0269	0.0302	0.0269	0.0249	0.0291	0.0291	0.0230	0.0235	0.0304	0.0304	0.0292
CBA44 02	0.3161	0.0315	0.0261	0.0161	0.0161	0.0315	0.0195	0.0261	0.0272	0.0249	0.0281	0.0303	0.0314	0.0281	0.0314	0.0280	0.0260	0.0303	0.0303	0.0241	0.0246	0.0315	0.0315	0.0304
CBA44 21	0.3097	0.0315	0.0261	0.0161	0.0161	0.0315	0.0195	0.0261	0.0272	0.0249	0.0281	0.0303	0.0314	0.0281	0.0314	0.0280	0.0260	0.0303	0.0303	0.0241	0.0246	0.0315	0.0315	0.0304
CBA45	0.3034	0.0339	0.0284	0.0182	0.0181	0.0338	0.0216	0.0284	0.0295	0.0272	0.0303	0.0326	0.0337	0.0303	0.0337	0.0303	0.0283	0.0326	0.0326	0.0264	0.0268	0.0339	0.0339	0.0327
CBA45 21	0.2966	0.0324	0.0270	0.0170	0.0170	0.0324	0.0204	0.0271	0.0281	0.0259	0.0290	0.0312	0.0323	0.0290	0.0323	0.0289	0.0269	0.0312	0.0312	0.0250	0.0255	0.0324	0.0325	0.0313
CBA00 101	0.3028	0.0301	0.0248	0.0150	0.0149	0.0301	0.0183	0.0248	0.0259	0.0236	0.0267	0.0289	0.0300	0.0267	0.0300	0.0267	0.0247	0.0289	0.0289	0.0228	0.0233	0.0301	0.0301	0.0290
CBP46	0.3011	0.0266	0.0193	0.0130	0.0121	0.0244	0.0152	0.0193	0.0203	0.0182	0.0233	0.0254	0.0265	0.0233	0.0265	0.0233	0.0192	0.0254	0.0254	0.0173	0.0180	0.0245	0.0245	0.0234

	CBA24 03	CBA25 01	CBA25 02	CBA25 03	CBA25 04	CBA24	CBA00113	CBP28	CBA28	CBA00 21 02	CBP30	CBA00 41 01	CBP31 01	CBP31 02	CBA31 41	CBP32 01	CBP32 02	CBP32 03	CBP32 04	CBP32 05	CBP32 06	CBP32 07	CBC32	CBP32 21
CBA24 03																								
CBA25 01	0.0063																							
CBA25 02	0.0054	0.0009																						
CBA25 03	0.0054	0.0027	0.0018																					
CBA25 04	0.0054	0.0027	0.0018	0.0018																				
CBA24	0.0054	0.0026	0.0018	0.0018	0.0018																			
CBA00 113	0.0045	0.0018	0.0009	0.0009	0.0009	0.0009																		
CBP28	0.0315	0.0325	0.0314	0.0314	0.0314	0.0313	0.0302																	
CBA28	0.0054	0.0026	0.0018	0.0018	0.0018	0.0018	0.0009	0.0313																
CBA00 21 02	0.0082	0.0054	0.0044	0.0044	0.0044	0.0044	0.0035	0.0302	0.0044															
CBP30	0.0297	0.0307	0.0296	0.0274	0.0274	0.0295	0.0285	0.0223	0.0295	0.0285														
CBA00 41 01	0.0054	0.0009	0.0018	0.0018	0.0018	0.0018	0.0009	0.0314	0.0018	0.0044	0.0296													
CBP31 01	0.0234	0.0244	0.0233	0.0233	0.0233	0.0232	0.0222	0.0152	0.0232	0.0222	0.0179	0.0233												
CBP31 02	0.0234	0.0244	0.0233	0.0233	0.0233	0.0232	0.0222	0.0152	0.0232	0.0222	0.0179	0.0233	0.0018											
CBA31 41	0.0280	0.0291	0.0279	0.0279	0.0279	0.0279	0.0268	0.0174	0.0279	0.0268	0.0201	0.0279	0.0073	0.0073										
CBP32 01	0.0299	0.0309	0.0298	0.0298	0.0298	0.0297	0.0287	0.0172	0.0297	0.0265	0.0219	0.0298	0.0091	0.0091	0.0111									
CBP32 02	0.0310	0.0298	0.0309	0.0309	0.0309	0.0308	0.0298	0.0182	0.0308	0.0276	0.0230	0.0287	0.0100	0.0100	0.0120	0.0009								
CBP32 03	0.0278	0.0288	0.0277	0.0277	0.0277	0.0276	0.0266	0.0193	0.0276	0.0266	0.0220	0.0277	0.0072	0.0072	0.0102	0.0110	0.0119							
CBP32 04	0.0289	0.0299	0.0288	0.0288	0.0288	0.0287	0.0276	0.0203	0.0287	0.0277	0.0230	0.0288	0.0081	0.0081	0.0111	0.0119	0.0129	0.0009						
CBP32 05	0.0233	0.0264	0.0253	0.0253	0.0253	0.0253	0.0242	0.0142	0.0253	0.0242	0.0171	0.0253	0.0092	0.0092	0.0112	0.0130	0.0140	0.0130	0.0140					
CBP32 06	0.0254	0.0287	0.0275	0.0275	0.0275	0.0275	0.0264	0.0203	0.0275	0.0265	0.0201	0.0275	0.0150	0.0150	0.0172	0.0190	0.0201	0.0171	0.0180	0.0109				
CBP32 07	0.0310	0.0320	0.0309	0.0309	0.0309	0.0308	0.0298	0.0182	0.0308	0.0276	0.0230	0.0309	0.0100	0.0100	0.0120	0.0009	0.0018	0.0119	0.0129	0.0140	0.0200			
CBC32	0.0322	0.0310	0.0298	0.0299	0.0299	0.0298	0.0287	0.0214	0.0298	0.0288	0.0241	0.0299	0.0090	0.0090	0.0121	0.0129	0.0139	0.0035	0.0044	0.0150	0.0191	0.0139		
CBP32 21	0.0299	0.0310	0.0298	0.0298	0.0298	0.0298	0.0287	0.0193	0.0298	0.0287	0.0220	0.0298	0.0072	0.0072	0.0102	0.0110	0.0119	0.0017	0.0026	0.0130	0.0170	0.0119	0.0017	
CBB00 21 01	0.0278	0.0288	0.0276	0.0277	0.0277	0.0276	0.0265	0.0163	0.0276	0.0266	0.0201	0.0277	0.0112	0.0112	0.0133	0.0140	0.0150	0.0151	0.0161	0.0091	0.0130	0.0150	0.0171	0.0151
CBB00 21 02	0.0266	0.0277	0.0265	0.0265	0.0265	0.0265	0.0254	0.0153	0.0265	0.0255	0.0191	0.0265	0.0102	0.0102	0.0123	0.0130	0.0140	0.0141	0.0151	0.0082	0.0120	0.0140	0.0161	0.0141
CBA40	0.0269	0.0279	0.0268	0.0268	0.0268	0.0267	0.0257	0.0196	0.0267	0.0257	0.0202	0.0268	0.0120	0.0120	0.0141	0.0159	0.0169	0.0160	0.0169	0.0141	0.0182	0.0169	0.0179	0.0159
CBA41	0.0257	0.0267	0.0256	0.0256	0.0256	0.0256	0.0245	0.0185	0.0256	0.0245	0.0191	0.0256	0.0110	0.0110	0.0131	0.0149	0.0159	0.0149	0.0159	0.0131	0.0171	0.0159	0.0169	0.0149
CBA42 01	0.0277	0.0287	0.0276	0.0276	0.0276	0.0276	0.0265	0.0193	0.0276	0.0265	0.0190	0.0276	0.0072	0.0072	0.0111	0.0109	0.0119	0.0091	0.0100	0.0130	0.0170	0.0119	0.0109	0.0091
CBA00 71	0.0268	0.0278	0.0267	0.0267	0.0267	0.0266	0.0256	0.0175	0.0266	0.0256	0.0201	0.0267	0.0101	0.0101	0.0121	0.0139	0.0149	0.0139	0.0149	0.0121	0.0181	0.0149	0.0159	0.0139
CBA00 32	0.0278	0.0266	0.0255	0.0255	0.0255	0.0255	0.0244	0.0173	0.0255	0.0245	0.0190	0.0255	0.0054	0.0054	0.0092	0.0110	0.0119	0.0091	0.0100	0.0111	0.0170	0.0119	0.0091	0.0091
CBA00 251	0.0257	0.0267	0.0256	0.0256	0.0256	0.0256	0.0245	0.0185	0.0256	0.0245	0.0191	0.0256	0.0110	0.0110	0.0131	0.0149	0.0159	0.0149	0.0159	0.0131	0.0171	0.0159	0.0169	0.0149
CBA42 02	0.0018	0.0044	0.0035	0.0035	0.0035	0.0035	0.0026	0.0314	0.0035	0.0063	0.0296	0.0035	0.0233	0.0233	0.0279	0.0298	0.0309	0.0277	0.0288	0.0232	0.0253	0.0309	0.0320	0.0298
CBA42 03	0.0270	0.0281	0.0269	0.0269	0.0269	0.0269	0.0258	0.0197	0.0269	0.0258	0.0203	0.0269	0.0121	0.0121	0.0142	0.0160	0.0170	0.0160	0.0170	0.0142	0.0183	0.0170	0.0180	0.0160
CBA00 21 03	0.0305	0.0315	0.0304	0.0304	0.0304	0.0303	0.0292	0.0209	0.0303	0.0292	0.0235	0.0304	0.0131	0.0131	0.0152	0.0171	0.0181	0.0171	0.0181	0.0153	0.0215	0.0181	0.0191	0.0171
CBA43 01	0.0291	0.0301	0.0290	0.0290	0.0290	0.0289	0.0279	0.0196	0.0289	0.0279	0.0223	0.0290	0.0120	0.0120	0.0141	0.0159	0.0170	0.0160	0.0170	0.0142	0.0203	0.0169	0.0180	0.0160
CBA43 02	0.0246	0.0256	0.0245	0.0245	0.0245	0.0244	0.0234	0.0162	0.0244	0.0234	0.0160	0.0245	0.0044	0.0044	0.0082	0.0100	0.0110	0.0081	0.0091	0.0101	0.0140	0.0110	0.0100	0.0081
CBA43 03	0.0257	0.0267	0.0256	0.0256	0.0256	0.0256	0.0245	0.0173	0.0256	0.0246	0.0171	0.0256	0.0054	0.0054	0.0092	0.0110	0.0120	0.0091	0.0100	0.0111	0.0151	0.0120	0.0110	0.0091
CBA00 41 02	0.0245	0.0255	0.0245	0.0245	0.0245	0.0244	0.0234	0.0162	0.0244	0.0234	0.0160	0.0245	0.0044	0.0044	0.0082	0.0100	0.0110	0.0081	0.0091	0.0101	0.0140	0.0110	0.0100	0.0081

CBA00 212	0.0279	0.0289	0.0278	0.0278	0.0278	0.0277	0.0267	0.0185	0.0277	0.0267	0.0212	0.0278	0.0110	0.0110	0.0131	0.0149	0.0159	0.0149	0.0159	0.0131	0.0192	0.0159	0.0169	0.0149
CBA00 31	0.0290	0.0300	0.0289	0.0289	0.0289	0.0288	0.0278	0.0196	0.0288	0.0278	0.0222	0.0289	0.0120	0.0120	0.0141	0.0159	0.0169	0.0159	0.0169	0.0141	0.0202	0.0169	0.0179	0.0159
CBA44 01	0.0292	0.0303	0.0291	0.0291	0.0291	0.0291	0.0280	0.0197	0.0291	0.0280	0.0224	0.0291	0.0121	0.0121	0.0142	0.0160	0.0170	0.0161	0.0170	0.0142	0.0204	0.0170	0.0181	0.0160
CBA44 02	0.0304	0.0314	0.0303	0.0303	0.0303	0.0302	0.0291	0.0208	0.0302	0.0292	0.0235	0.0303	0.0131	0.0131	0.0152	0.0170	0.0181	0.0171	0.0181	0.0152	0.0214	0.0181	0.0191	0.0171
CBA44 21	0.0304	0.0314	0.0303	0.0303	0.0303	0.0302	0.0291	0.0208	0.0302	0.0292	0.0235	0.0303	0.0131	0.0131	0.0152	0.0170	0.0181	0.0171	0.0181	0.0152	0.0214	0.0181	0.0191	0.0171
CBA45	0.0327	0.0338	0.0326	0.0326	0.0326	0.0325	0.0314	0.0230	0.0325	0.0315	0.0257	0.0326	0.0151	0.0151	0.0173	0.0191	0.0202	0.0192	0.0202	0.0173	0.0236	0.0201	0.0212	0.0191
CBA45 21	0.0313	0.0323	0.0312	0.0312	0.0312	0.0311	0.0300	0.0217	0.0311	0.0301	0.0244	0.0312	0.0140	0.0140	0.0161	0.0179	0.0190	0.0180	0.0190	0.0162	0.0224	0.0190	0.0200	0.0180
CBA00 101	0.0290	0.0300	0.0289	0.0289	0.0289	0.0288	0.0278	0.0196	0.0288	0.0278	0.0222	0.0289	0.0120	0.0120	0.0141	0.0159	0.0169	0.0159	0.0169	0.0141	0.0202	0.0169	0.0179	0.0159
CBP46	0.0234	0.0265	0.0254	0.0254	0.0254	0.0254	0.0243	0.0143	0.0254	0.0244	0.0170	0.0254	0.0092	0.0092	0.0113	0.0131	0.0141	0.0131	0.0141	0.0009	0.0110	0.0141	0.0151	0.0131

	CBB00 21 01	CBB00 21 02	CBA40	CBA41	CBA42 01	CBA00 71	CBA00 32	CBA00 251	CBA42 02	CBA42 03	CBA00 21 03	CBA43 01	CBA43 02	CBA43 03	CBA00 41 02	CBA00 212	CBA00 31	CBA44 01	CBA44 02	CBA44 21	CBA45	CBA45 21	CBA00 101	CBP46
CBB00 2101																								
CBB00 2102	0.0009																							
CBA40	0.0163	0.0152																						
CBA41	0.0152	0.0142	0.0009																					
CBA42 01	0.0151	0.0141	0.0140	0.0129																				
CBA00 71	0.0142	0.0132	0.0018	0.0009	0.0139																			
CBA00 32	0.0131	0.0122	0.0140	0.0130	0.0072	0.0120																		
CBA00 251	0.0152	0.0142	0.0009	0.0000	0.0129	0.0009	0.0130																	
CBA42 02	0.0277	0.0265	0.0268	0.0256	0.0276	0.0267	0.0277	0.0256																
CBA42 03	0.0163	0.0153	0.0018	0.0009	0.0140	0.0018	0.0140	0.0009	0.0269															
CBA00 2103	0.0175	0.0164	0.0045	0.0036	0.0171	0.0027	0.0151	0.0036	0.0304	0.0026														
CBA43 01	0.0163	0.0153	0.0036	0.0026	0.0159	0.0018	0.0140	0.0026	0.0290	0.0036	0.0009													
CBA43 02	0.0122	0.0112	0.0101	0.0091	0.0026	0.0100	0.0044	0.0091	0.0245	0.0101	0.0131	0.0120												
CBA43 03	0.0132	0.0122	0.0111	0.0101	0.0035	0.0110	0.0054	0.0101	0.0256	0.0111	0.0141	0.0130	0.0009											
CBA00 4102	0.0122	0.0112	0.0111	0.0101	0.0026	0.0110	0.0044	0.0101	0.0245	0.0111	0.0141	0.0130	0.0000	0.0009										
CBA00 212	0.0152	0.0142	0.0026	0.0018	0.0149	0.0009	0.0130	0.0018	0.0278	0.0027	0.0018	0.0009	0.0110	0.0120	0.0120									
CBA00 31	0.0162	0.0152	0.0035	0.0026	0.0159	0.0018	0.0140	0.0026	0.0289	0.0036	0.0027	0.0018	0.0120	0.0130	0.0130	0.0009								
CBA44 01	0.0164	0.0153	0.0036	0.0027	0.0160	0.0018	0.0141	0.0027	0.0291	0.0018	0.0009	0.0018	0.0121	0.0131	0.0131	0.0009	0.0018							
CBA44 02	0.0174	0.0164	0.0045	0.0036	0.0170	0.0027	0.0151	0.0036	0.0303	0.0026	0.0018	0.0027	0.0130	0.0141	0.0141	0.0018	0.0009	0.0009						
CBA44 21	0.0174	0.0164	0.0045	0.0036	0.0170	0.0027	0.0151	0.0036	0.0303	0.0026	0.0018	0.0027	0.0130	0.0141	0.0141	0.0018	0.0027	0.0009	0.0018					
CBA45	0.0195	0.0185	0.0063	0.0054	0.0191	0.0045	0.0171	0.0054	0.0326	0.0044	0.0036	0.0045	0.0150	0.0161	0.0161	0.0036	0.0045	0.0026	0.0035	0.0018				
CBA45 21	0.0183	0.0173	0.0054	0.0044	0.0179	0.0035	0.0160	0.0044	0.0312	0.0054	0.0045	0.0036	0.0139	0.0150	0.0150	0.0026	0.0035	0.0036	0.0045	0.0027	0.0009			
CBA00 101	0.0162	0.0152	0.0035	0.0026	0.0159	0.0018	0.0140	0.0026	0.0289	0.0036	0.0027	0.0018	0.0120	0.0130	0.0130	0.0009	0.0018	0.0018	0.0027	0.0009	0.0027	0.0018		
CBP46	0.0092	0.0082	0.0142	0.0132	0.0131	0.0122	0.0112	0.0132	0.0233	0.0143	0.0154	0.0142	0.0102	0.0112	0.0102	0.0132	0.0142	0.0143	0.0153	0.0153	0.0174	0.0162	0.0142	

Appendix.4a. Cytochrome *b* haplotypes labeling after collapsing identical sequences in DAMBE software program. Number 0 is the out group (*Ctenosaura melanosterna*).

No	Sample Number(s)	Location	Label
0	1	Northern Honduras	LBCB.A.00
1	5	Yucatan (Eastern Mexico)	LBCB.A.05
2	47	Western El Salvador	LBCB.P.47
3	49	Southern Florida	LBCB.A.49
4	73	Northern Honduras	LBCB.A.73
5	123, 131	Yucatan (Eastern Mexico)	LBCB.A.00.2.1_01
6	210	Central Guatemala	LBCB.C.21
7	214	Southern Guatemala	LBCB.P.21_01
8	215	Southern Guatemala	LBCB.P.21_02
9	216	Southern Guatemala	LBCB.P.21_03
10	225	Yucatan (Eastern Mexico)	LBCB.A.22_01
11	226	Yucatan (Eastern Mexico)	LBCB.A.22_02
12	227	Campeche (Eastern México)	LBCB.A.22_03
13	228	Campeche (Eastern México)	LBCB.A.22_04
14	229	Yucatan (Eastern Mexico)	LBCB.A.22_05
15	230	Yucatan (Eastern Mexico)	LBCB.A.23_01
16	217, 232	Southern Guatemala, Campeche (Eastern Mexico)	LBCB.B.00.2.2
17	233	Yucatan (Eastern Mexico)	LBCB.A.23_02
18	239	Yucatan (Eastern Mexico)	LBCB.A.23_03
19	240	Southern Mexico	LBCB.P.24_01
20	241	Southern Mexico	LBCB.P.24_02
21	244	Tabasco (Eastern Mexico)	LBCB.A.24_01

22	245	Tabasco (Eastern Mexico)	LBCB.A.24_02
23	127, 234, 235, 236, 237, 242, 246, 247	Yucatan (Eastern Mexico)	LBCB.A.00.8.1
24	248	Yucatan (Eastern Mexico)	LBCB.A.24_03
25	250	Yucatan (Eastern Mexico)	LBCB.A.25_01
26	252	Yucatan (Eastern Mexico)	LBCB.A.25_02
27	257	Yucatan (Eastern Mexico)	LBCB.A.25_03
28	258	Yucatan (Eastern Mexico)	LBCB.A.25_04
29	262	Yucatan (Eastern Mexico)	LBCB.A.24(26)
30	72, 219, 221, 222, 223, 224, 249, 255, 256, 261, 265	Yucatán, Campeche, Quintana Roo (Eastern Mexico)	LBCB.A.00.11.3
31	287	Southern Mexico	LBCB.P.28
32	288	Yucatan (Eastern Mexico)	LBCB.A.28
33	158, 293	Yucatan (Eastern Mexico)	LBCB.A.00.2.1_02
34	305	Southern Mexico	LBCB.P.30
35	220, 259, 292, 313	Yucatan (Eastern Mexico)	LBCB.A.00.4.1_01
36	314	Western Nicaragua	LBCB.P.31_01
37	315	Western Nicaragua	LBCB.P.31_02
38	316, 317, 318, 319	Small Corn and Big Corn Islands (Eastern Nicaragua)	LBCB.A.31.4.1
39	320	Western Costa Rica	LBCB.P.32_01
40	321	Western Costa Rica	LBCB.P.32_02
41	323	Western Costa Rica	LBCB.P.32_03
42	324	Western Costa Rica	LBCB.P.32_04
43	325	Western Costa Rica	LBCB.P.32_05
44	326	Western Costa Rica	LBCB.P.32_06
45	327	Western Costa Rica	LBCB.P.32_07
46	328	Central Costa Rica	LBCB.C.32
47	322, 329	Western Costa Rica	LBCB.P.32.2.1

48	107, 389	Southern Panama, Utila Island (Northern Honduras)	LBCB.B.00.2.1_01
49	108, 109, 390	Southern Panama, Utila Island (Northern Honduras)	LBCB.B.00.2.1_02
50	402B	Utila Island (Northern Honduras)	LBCB.A.40
51	416	Utila Island (Northern Honduras)	LBCB.A.41
52	420a	Utila Island (Northern Honduras)	LBCB.A.42_01
53	393, 394, 401,404, 405, 408, 409, 421a	Utila Island (Northern Honduras)	LBCB.A.00.7(8).1
54	8, 419b, 421b	Northern Honduras, Utila Island (Northern Honduras)	LBCB.A.00.3.2
55	386, 387, 391, 392, 395, 396, 397, 398, 399, 400, 402A, 403, 406, 407, 410, 411, 412, 413, 414, 415, 417, 418b, 419a, 420b, 422	Utila Island (Northern Honduras)	LBCB.A.00.25.1
56	423	Utila Island (Northern Honduras)	LBCB.A.42_02
57	424	Utila Island (Northern Honduras)	LBCB.A.42_03
58	425, 432	Northern Honduras	LBCB.A.00.2.1_03
59	434	Northern Honduras	LBCB.A.43_01
60	439A	Northern Honduras	LBCB.A.43_02
61	439B	Northern Honduras	LBCB.A.43_03
62	436, 437, 438, 440	Northern Honduras	LBCB.A.00.4.1_02
63	373, 374, 375, 376, 377, 378, 379, 380, 381, 382, 383, 384, 385, 388, 426, 427, 428, 429, 433, 435, 441	Southern Florida, Northern Honduras	LBCB.A.00.21.2
64	430, 431, 442	Northern Honduras	LBCB.A.00.3.1
65	443	Northern Honduras	LBCB.A.44_01
66	444	Northern Honduras	LBCB.A.44_02
67	447, 448	Guanaja Island (Northern Honduras)	LBCB.A.44.2.1
68	450	Guanaja Island (Northern Honduras)	LBCB.A.45
69	445, 459	Guanaja Island (Northern Honduras)	LBCB.A.45.2.1
70	446, 449, 451, 452, 453, 454, 456, 458, 460, 461	Guanaja Island (Northern Honduras)	LBCB.A.00.10.1
71	463	Western Costa Rica	LBCB.P.46

Appendix.4b. Rhodopsin haplotypes labeling after collapsing identical sequences in DAMBE software program. Number 0 is the out group (*Ctenosaura melanosterna*).

No	Sample Number(s)	Location	Label
0	1	Northern Honduras	LBRD.A.00
1	49	Southern Florida	LBRD.A.49
2	72	Quintana Roo (Eastern Mexico)	LBRD.A.72
3	73	North Honduras	LBRD.A.73
4	108	Southern Panama	LBRD.A.10._01
5	109	Southern Panama	LBRD.A.10._02
6	210, 211, 212	Central Guatemala	LBRD.C.21.3.1
7	214	Southern Guatemala	LBRD.P.21
8	225, 236, 237, 246B, 251B	Tabasco, Campeche, Yucatan (Eastern México)	LBRD.A.00.5.3
9	287	Western Mexico	LBRD.P.28
10	216, 217, 240, 241, 305	Southern Guatemala, Western Mexico	LBRD.P.00.5.2
11	158, 219, 221, 222, 223, 224, 226, 227, 228, 229, 230, 231, 232, 233, 234, 235, 239, 243, 245, 247, 248, 249B, 250, 251A, 252, 253, 254B, 256, 257, 258, 259B, 261B, 262, 263, 264, 265, 290, 292, 293, 313	Tabasco, Campeche, Yucatan, Quintana Roo (Eastern Mexico)	LBRD.A.00.40.3
12	315	Southern Nicaragua	LBRD.P.31_01
13	319B	Big Corn Island, Eastern Nicaragua	LBRD.A.31
14	321A	Western Costa Rica	LBRD.P(A).32_01
15	321B	Western Costa Rica	LBRD.P.32_02
16	322B	Western Costa Rica	LBRD.P.32_03
17	323A	Western Costa Rica	LBRD.P.32_04
18	317B, 323B	Small Corn Island (Eastern Nicaragua), Western Costa Rica	LBRD.B.00.2.2

19	324A	Western Costa Rica	LBRD.P.32_05
20	254A, 259A, 261A, 324B	Yucatan, Quintana Roo (Eastern Mexico), Western Costa Rica	LBRD.B.00.4.3
21	325	Western Costa Rica	LBRD.P.32_06
22	326B	Western Costa Rica	LBRD.P.32_07
23	322A,327B	Western Costa Rica	LBRD.P.32.2.1
24	328A	Central Costa Rica	LBRD.C.32_01
25	328B	Central Costa Rica	LBRD.C.32_02
26	249A, 329A	Yucatan (Eastern Mexico), Western Costa Rica	LBRD.B.00.3.2
27	329B	Western Costa Rica	LBRD.P.32_08
28	402	Utila Island (Northern Honduras)	LBRD.A.40
29	428	North Honduras	LBRD.A.42_01
30	429B	North Honduras	LBRD.A.42_02
31	438B	North Honduras	LBRD.A.43
32	447B	Honduras Guanaja	LBRD.A.44
33	420b, 433, 439, 441, 446, 450	Northern Honduras, Utila Island (Northern Honduras), Guanaja Island (Northern Honduras)	LBRD.A.00.6.3
34	454	Guanaja Island (Northern Honduras)	LBRD.A.45_01
35	455B	Guanaja Island (Northern Honduras)	LBRD.A.45_02
36	47, 405, 427A, 429A, 447A, 448A, 455A, 458A	Western El Salvador, Northern Honduras, Utila Island (Northern Honduras), Guanaja Island (Northern Honduras)	LBRD.B.00.8.4
37	427B, 448B, 458B	Honduras Guanaja	LBRD.A.00.3.1
38	8, 123, 127, 131, 242, 244,246A, 314, 316, 317A, 318, 319A, 320, 326A, 327A, 386, 387, 389, 391, 392, 393, 396, 397, 400, 401, 403, 404, 406, 408, 410, 415, 417, 418b, 419a, 426, 437, 438A, 440, 451, 452, 453, 457, 459, 460, 462A	Vera Cruz, Yucatán (Eastern Mexico), Northern Honduras, Utila Island (Northern Honduras), Guanaja Island (Northern Honduras), Nicaragua, Small Corn and Big Corn Islands (Eastern Nicaragua), Western Costa Rica	LBRD.B.00.45.7
39	462B	Central Guatemala	LBRD.C.46
40	463	Western Costa Rica	LBRD.P.46